Spatiotemporal differences of early type I interferon response in acute and chronic viral infections

Valentina Casella

TESI DOCTORAL UPF / 2021

THESIS DIRECTORS

Dr. Andreas Meyerhans and Dr. Jordi Argilaguet

DEPARTMENT OF EXPERIMENTAL AND HEALTH SCIENCES

upf. Universitat Pompeu Fabra Barcelona

A te nonno,

E all’amore che mi hai trasmesso per il mare.

ACKNOWLEDGEMENTS

It was January 2017 when it all started. A new life, a new country, a new academic adventure. It was not easy, but all the challenges encountered are what made the whole experience so rewarding. And now, after 4 years, it's time to thank anyone who made this journey so memorable.

First of all, I want to thank you Andreas, for being a supportive mentor and a source of inspiration. Thanks for believing in me and helping me to grow, not just as a scientist, but also as a person. You showed me that great scientists first of all are good humans … and that a bit of craziness doesn't harm afterall (I might have taken it too literally though!!).

Jordi, what would have this journey been without you?! To me you were not only a supervisor … you have been a guide, a motivator (sometimes a psychoanalyst as well) but most of all a friend. Thanks for the brainstormings and for always caring. I will miss all this!

To JC, my tutor overseas, thanks for teaching me with dedication and for all the thought-provoking discussions and valuable advice on my project!

To all my labmates from the past and from the present. Mirs, thanks for all the help with the still incomprehensible informatic analysis XD and all the good times on the bench. Eva, thanks for being on this journey with me, despite being so different it was nice to complement each other. And then thanks to Kat, Mie, Celina, Selina, Ryu, Javier, Marta, Paula, Consol and everyone from Juana's lab.. No matter how much time we spent together, you all brought something great to my life…even if it was just a laugh, or a piece of cake :)

Thanks Eva, Oscar, Alex, Erica from the Flow Cytometry facility for all the guidance with the machines and the support along the way.

To the members of the Pythonissas team, proud winner of the PRBB beach volley tournament, year 2019 (category Disaster). Thanks for all the fun (and the beers), it was a pleasure to play with you.

A te Ma', grazie per tutta la pazienza che hai avuto durante questa infinita carriera accademica, e per il supporto che hai saputo dimostrarmi sempre. Grazie per 'cercare' di comprendere le mie decisioni più assurde, ma per me giuste …So che non è facile, ma ancora una volta.. porta pazienza!

E a te Pa', grazie per avermi lasciato la libertà di scegliere la mia strada. Per essere stato presente, nonostante gli ultimi anni non siano stati facili.
Spero di avervi resi orgogliosi.

To you Nas, these years not only gave me a PhD, but also one of the greatest friends I could ever ask for. Thanks for the emotional support and for being always there. I am truly happy to have you in my life. But now….. let's be serious and let's go surfing!

To you Daisy, my sister from another country. Thanks for helping me rediscover the artistic side of my brain, before the scientific one almost completely took over! You have been a huge inspiration and an amazing skate partner.

E poi ancora grazie…

A tutta la mia famiglia, per aspettarmi a braccia aperte ogni volta che torno a casa.
A te nonna, che mi conservi sempre un piatto di anolini fumante.
A voi amiche di una vita… Eri, Chia, Fede, Nichi, Sabri… che nonostante la distanza non mi avete mai abbandonata.

Vale

Barcelona, 15th February 2021

ABSTRACT

Type I interferons (IFN-I) play a critical role in shaping the antiviral immune response early after an infection. However, the dynamics by which different immune cell subsets regulate the IFN-I response during the early stages of acute and chronic infections is not completely understood. Here we used the Lymphocytic Choriomeningitis Virus (LCMV)-infection mouse model system to characterize the dynamics of the IFN-I response in acute and chronic infections. Time-resolved spleen-transcriptomes revealed that during an acute infection, IFN-I showed two waves of expression at days 2 and 5 post-infection, while in chronically infected mice a single wave of IFN-I genes was induced at day 1. We identified metallophilic marginal zone macrophages as an important source of the second wave of IFN-I only during acute infection. Moreover, we characterized a polyfunctional role for the second wave of IFN-I, which was required to induce pro-inflammatory macrophages and virus-specific CD8 T cells. In contrast, during chronic infection, the early depletion of metallophilic marginal zone macrophages mediated by CD8+ cells, resulted in a lack of IFN-I production and the pro-inflammatory response was not induced. Importantly, we also linked the second wave of IFN-I with the development of lymphoid tissue fibrosis during acute LCMV infection. Together our data demonstrate that the spatiotemporal regulation of IFN-I production in the early stages of infection is crucial for the induction of IFN-I dependent sequential events that lead to viral infection resolution. Further studies are ongoing to decipher the regulatory mechanisms underlying the characterized events, thus revealing universal concepts related to infection fate decisions that are also relevant for persistent human infections such as HIV or HCV.

RESUMEN

Los interferones de tipo I (IFN-I) desempeñan un papel fundamental en el desarrollo de la respuesta inmunitaria antiviral al comienzo de una infección. Sin embargo, todavía no se comprende completamente la dinámica por la cual diferentes tipos de células inmunes regulan la respuesta de IFN-I durante las primeras etapas de infecciones virales agudas y crónicas. En el presente estudio utilizamos como modelo de infección ratones infectados por el virus de la coriomeningitis linfocítica (LCMV) con el objetivo de caracterizar la dinámica de la respuesta de IFN-I en infecciones agudas y crónicas. El análisis de los transcriptomas de los bazos de animales infectados reveló que durante una infección aguda, el IFN-I muestra dos olas de expresión en los días 2 y 5 después de la infección, mientras que durante una infección crónica se induce un solo pico de expresión de genes de IFN-I el día 1. Análisis subsiguientes permitieron demonstrar que los macrófagos CD169+ de la zona marginal del bazo son responsables de la segunda ola de expression de IFN-I durante la infección aguda. Demostramos también que este IFN-I más tardío tienen un papel polifuncional basado en la inducción macrófagos proinflamatorios y células T CD8 específicas de virus. Por el contrario, durante la infección crónica, la temprana desaparición de los macrófagos CD169+ mediada por las células CD8+, resulta en una falta de producción de IFN-I y la consiguiente respuesta proinflamatoria. Por último, la segunda ola de IFN-I durante una infección aguda tiene como consecuencia el desarrollo de fibrosis en tejido linfoide. En resumen, los resultados demuestran que la regulación espaciotemporal en la producción de IFN-I en las primeras etapas de la infección es crucial para la inducción de eventos secuenciales dependientes de IFN-I que conducen a la resolución de la infección viral. Nuevos estudios están en marcha con el objetivo de caracterizar los mecanismos reguladores subyacentes a los eventos descritos, de modo que podamos entender mejor los mecanismos subyacentes a la toma de decisiones por elhuésped en relación al destino de una infección, conceptos que serán también aplicables a infecciones humanas persistentes como las del VIH o del VHC.

PROLOGUE

The outcome of a viral infection is determined by the dynamic interplay between the expanding virus and the concomitantly induced immune response. Viral infections can be categorized as either acute or persistent depending on temporal virus-host relationships. In humans, acute infections are usually resolved within a few weeks. In contrast, chronic infections are not resolved and, instead, develop when innate and adaptive immune responses are not sufficient to eliminate the invading virus. Once a chronic infection is established, the medical challenge becomes to either eliminate the virus or keep it sufficiently controlled to minimize its pathogenic consequences.

A multitude of viral and host factors are known to influence acute or persistent infection outcomes. Among these, IFN-I represents the first line of the host defense against viral infections and plays a critical role in shaping the antiviral immune response. Most cells, once infected, can produce IFN-I. However, during the course of the infection, IFN-I expression is orchestrated by different cellular sources. IFN-I exerts its functions by binding to its receptor and inducing the expression of interferon-stimulated genes (ISGs) which restrict viral replication and activate an antiviral state within cells. Moreover IFN-I interaction with both innate and adaptive immune cells is crucial for promoting antigen presentation and virus-specific immunity.

Importantly, numerous studies have reported unexpected roles of IFN-I signaling during both acute and persistent viral infections. In the early acute phase of SARS-CoV2 infection, a dysregulation either in timing and/or magnitude of IFN-I expression can exacerbate the inflammatory response and contribute to the severity of COVID19. During chronic viral infections like HIV, the prolonged IFN-I signaling promotes immune suppression, lymphoid tissue disruption and T cell dysfunction. Together these studies show that the actions of IFN-I can dramatically differ depending on the time of its presence. Today, the dynamics by which different immune cell subsets regulate the IFN-I response are not completely understood. For this reason, deciphering the mechanism behind the regulation of IFN-I responses early after pathogen encounter, and its consequences for the infection fate may impact new immunotherapeutic cure strategies against both acute and chronic viral infections.

TABLE OF CONTENTS

INTRODUCTION

1. Virus infection fates

1.1 Viral Infections today: still a major global issue (from SARS-CoV-2 pandemic to HIV)

2020 was the year that raised global awareness on the incredible burden that viruses still represent for our society. The extreme heterogeneity in disease presentation and immune responses arising from SARS-CoV-2 infection highlight how much we still do not know about host-virus interactions. However, emergent viruses such as SARS-CoV-2 are not the only challenge we are facing during the 21th century. Chronic viral infections still represent a significant global health burden. For example, human immunodeficiency virus types 1 and 2 (HIV-1 and HIV-2) are the causative agents of acquired immune deficiency syndrome (AIDS), which results in an estimated 1.5 million deaths worldwide annually. Hepatitis C virus (HCV) and hepatitis B virus (HBV) are major causes of viral hepatitis. Moreover, HCV is the major risk factor for the development of hepatocellular carcinoma, the fifth most common cancer in the world. Notably, these persistent viral infections cause drastic and sustained alterations in the host immune system. This often results in altered susceptibility to secondary infections, cancers, and inflammatory disorders *(Zuniga et al., 2015, Annu Rev Virol).* Taken all this into account, today we are caught in a battle between old enemies and constantly emerging ones. Our weapon is to develop vaccines strategies and drugs that will help to eradicate them. In order to do so, we need to implement our understanding of the battlefield, namely the virus-host interaction in its complexity.

1.2 Acute vs chronic viral infections

Viral infections can be fundamentally categorized as acute or chronic according to their temporal relationships with their hosts *(Virgin et al., 2009, Cell)*. Acute infections in humans are usually resolved within a few weeks. By contrast, chronic infections are not resolved and, instead, develop when innate and adaptive immune responses are not sufficient to eliminate the invading virus during the primary infection phase. Viruses of both categories continue to threaten human health. Notable examples are the regular recurrences of Influenza virus strains that cause acute infections with partly critical

illness or death every year (*Fukuyama & Kawaoka, 2011, Curr Opin Immunol; Oldstone et al., 2013, Virology*) and chronic infections with the Human Immunodeficiency Virus (HIV) or the Hepatitis B and C viruses (HBV, HCV) that cause a tremendous disease burden with more than 500 million people infected worldwide. These viruses can establish persistence in their hosts with different probabilities and pathogenic consequences. Whilst nearly all HIV infections lead to virus persistence, 50-80% of HCV and only about 5% of HBV infections in adults are persistent. The level of persistence of HBV-infected newborns is massively increased to about 95% indicating that the state of the immune system is an important component in determining infection fate *(Feinberg & Ahmed, 2012, Nat Immunol; Rehermann & Nascimbeni, 2005, Nat Rev Immunol).*

Acute infections are characterized by a vigorous expansion of virus-specific B and T cells with antiviral activity which lead to virus clearance. Infection resolution is rapidly followed by a reset of the immune system to an uninfected but memory-armed state that includes quiescent memory B and T cells, as well as plasma cells that continuously produce antibodies (*Virgin et al., 2009, Cell*). In contrast, chronic viral infections are characterized by the down-regulation of immune effector mechanisms to avoid immunopathology. Indeed, the simultaneous presence of a widespread virus infection and strong cytotoxic effector cell responses can induce massive cell and tissue destruction and may directly threaten the life of the infected host (*Rouse et. al, 2010, Nat Rev*). One of the most remarkable immunological features of chronic infections is T cell exhaustion, defined as the deletion and functional impairment of virus-specific T cells (*Moskophidis et al., 1993, Nature* ; *Barber et al., 2006, Nature*; *Ng et al., 2013, Cell Host & Microbe; Okoye et al., 2017, Front Immunol*). Exhausted T (Tex) cells are characterized by a prolonged and high expression of inhibitory receptors such as PD1 and Tim3, an altered metabolism and a unique transcriptional program when compared with functional effector T cells and memory T cells (*Crawford & Wherry, 2009, Curr Opin Immunol; Wherry et al., 2007, Immunity; Crawford et al., 2014, Immunity*). Recent work from *Beltra et al*., defined a four-stage developmental hierarchy for Tex cells and described the key interplay of TCF1, T-bet, and Tox in coordinating these subsetes transitions (*Beltra et al., 2020, Immunity)*. Concomitant with T cell exhaustion, other regulatory elements also participate in the downregulation of the antiviral effector responses during chronic infections. Relevant factors are IL10, regulatory T cells and myeloid derived suppressor cells (MDSCs) (*Norris et al. 2013, Immunity; Brooks et al.,*

2006, Nat Med). A consequence of this immunological adaptation is the establishment of a dynamic equilibrium between virus expansion and virus-specific adaptive responses that may be maintained stably for years without major pathological consequences or disrupted in a way that rapidly leads to overt disease.

1.3 Factors influencing infection outcome

The failure of host immune responses to contain a virus that eventually results in the establishment of a chronic infection is the consequence of a myriad of viral (strain, tropism, titre, mutations, escape from immune recognition, etc.) and host (genetic background, age, immune status, etc.) factors, as well as the dynamics of the virus-host interactions occurring in the early stages of the viral infection *(Li et al., 2009; J Immunol)*.

1.3.2. Viral factors

All viruses have evolved a multitude of strategies to modulate and escape the host immune response. Some rely on the role of individual viral genes that modify infected cells or the immune system itself. Such strategies include inhibition of humoral responses, interference with interferons, inhibition and modulation of cytokines and chemokines, inhibition of apoptosis that may facilitate virus dissemination, evasion of cytotoxic T lymphocytes (CTL) and NK responses, and modulation of MHC expression *(Alcami et al., 2000, Trends Microbiol)*. Tropism, exposure dose and route of infection are also relevant variables. It is likely that the majority of persons who remain uninfected during flu outbreaks could in part be explained by minimal exposure. Indeed, infection of mice with minimal doses of Influenza are controlled subclinically by innate defenses, without the induction of an adaptive immune response. In contrast, massive doses can overwhelm immune defenses and cause severe disease and rapid death (*Sumbria et al., 2019, Front Microbiol*). The route of viral exposure is also a critical factor influencing infection outcome. For example, with HIV, infection risks are higher through rectal versus vaginal routes *(Sumbria, 2019, Front Micro; Rouse et. al, 2010, Nat Rev)*.

1.3.2. Host factors

Several host factors are involved in the fate decision between an acute or chronic infection. The age of the individual significantly influences the outcome of viral infections. The immature immune system of newborn, and immunosenescence in elderly people, make them more susceptible to suffer the most severe consequences of an infection compared to healthy adults (*Rouse et. al, 2010, Nat Rev; Sumbria, 2019, Front Microbiol).* Host genetic factors also influence infection outcome. For example, a particular genotype of the chemokine receptor gene CCR5 is associated with greater resistance to HIV infection, and a higher susceptibility to West Nile virus (*Glass et al., 2006, J Exp Med),* and loss of function mutations in genes of the IFN-I pathway account for a few percent of cases that develop severe COVID19 disease (*Beck et al., 2020, Science*). In addition to host genetics, there is evidence that the composition of the gut microbiome can markedly affect how the host responds to exogenous viral pathogens *(Zhang et al., 2019, Signal Transduction and Targeted Therapy)*.

1.4 Dynamics of virus-host interaction

The location, timing, and magnitude of the immune response relative to the viral replication speed and spread are also major determinants of infection fate *(Li et al., 2009; Journal of Imm)*. Mathematical models have been extensively used in the last decades in the study of the immune response. They provide rigorous means of thinking about and describing the immune system and its interactions with viruses. To this end a combination of analytical studies of the simplified versions of the model and numerical simulations have been conducted to elucidate the role of key infection parameters such as dose, virus diffusion coefficient, and delay in the establishment of the antiviral immune response (*Bocharov et al., 2016, PLoS ONE*).

During an infection, virus loads over time show a bell-shaped curve behaviour with varying maximum titres and widths depending on the infected tissue. This bell-shaped behavior reflects virus expansion in available target cells and virus restriction from concomitantly induced immune responses. It is generally accepted that the outcome of a virus infection results from the “numbers game” characterized by the kinetics of virus growth in target cells, its spread across sensitive tissue and the strength of the antiviral

immune responses (*Bocharov et al., 2020, Front Cell Infect Microbiol*). Analysis by Bocharov et al. suggests that viral spreading in tissues can proceed as a travelling wave, spatially periodic or irregular oscillations, and a combination of those *(Bocharov et al., 2015, J Immunol Res; Bocharov et al., 2016, PLoS ONE)*. The possibility that the infection spreads as waves differing in their amplitude suggests the existence of spatiotemporal mechanisms of disease pathogenesis. This means that the immune response and the infection kinetics should be highly coordinated to ensure a proper clearance of the infection. Deciphering the many interaction dynamics that occur between the virus and host cells over the course of an infection is paramount to understanding mechanisms of pathogenesis and developing novel immunotherapeutic antiviral strategies.

2. Type I Interferon responses

2.1 IFN-I: the first line antiviral defense

Interferon (IFN) genes encode for widely expressed cytokines that possess strong antiviral and immunomodulatory properties. They represent one of the body's primary defense systems against viral infections. In order to accomplish this incredible feat, IFN signaling has evolved to generate an astonishing diversity and redundancy. There are three distinct IFN families. The type I IFN (IFN-I) family is a multi-gene cytokine family that encodes 13 partially homologous IFNα subtypes in humans (14 in mice), a single IFNβ and other poorly characterized gene products (IFNε, IFNτ, IFNκ, IFNω, IFNδ and IFNζ). The type II IFN family consists of a single gene product, IFNγ, that is predominantly produced by T cells and natural killer (NK) cells. IFNγ acts on a broad range of cell types expressing the IFNγ receptor (IFNγR). The type III IFN family comprises IFNλ1, IFNλ2, IFNλ3 and IFNλ4, which have similar functions to cytokines of the IFN-I family but limited activity, as the expression of their receptor is restricted to epithelial cell surfaces (*McNab et al., 2015, Nat Rev*). Although the discovery of IFN dates back to half a century ago (*Isaacs & Lindenmann, 1957, Proc R Soc Lond B Biol Sci; Isaacs et al., 1957, Proc R Soc Lond B Biol Sci), novel aspects of these cytokines are constantly being re*ported and updated. Outstanding work over the past 50 years

contributed to the present view of IFN-I as the first line of antiviral defense and a critical link between innate and adaptive immunity (*Pitha, 2007, Curr Top Microbiol Immunol*). The signalling pathways that lead to the induction of IFN-I differ depending on the stimulus and the responding cell types (Figure 1; *McNab et al., 2015, Nat Rev*). Almost all cells in the body can produce IFN-I, and this usually occurs in response to the stimulation of receptors known as pattern recognition receptors (PRRs) by microbial products.

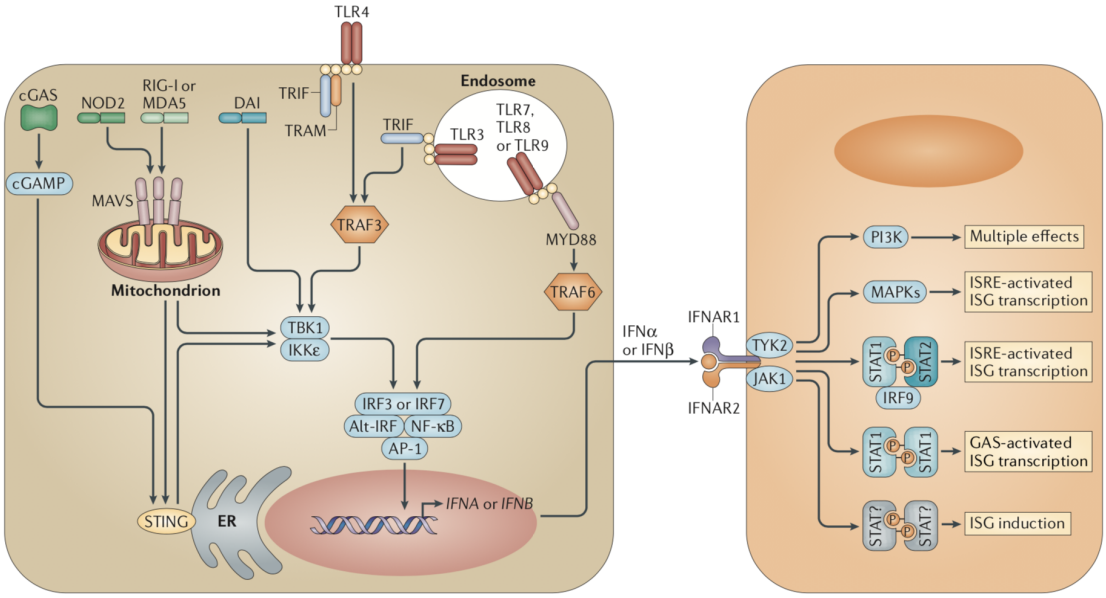

Figure 1. IFN-I induction and receptor signaling. Recognition of microbial products by a range of cell-surface and intracellular PRRs can lead to induction of the genes encoding type I interferons, which is mediated by several distinct signalling pathways. IFN-I, upon binding its receptor (IFNAR), induces multiple downstream signalling pathways which eventually lead to a diverse range of biological effects (from *McNab et al., 2015, Nat Rev*).

These receptors are located on the cell surface, in the cytosol or in endosomal compartments. The RNA helicases retinoic acid-inducible gene I (RIG-I) and melanoma differentiation-associated gene 5 (MDA5) are the main cytosolic receptors that are responsible for the recognition of RNA. Viral DNA motifs in the cytosol can be recognized by receptors such as DNA-dependent activator of IRFs (DAI) and cytosolic GAMP synthase (cGAS). In addition to these cytosolic receptors, several Toll-like receptors (TLRs) located in the cell surface or in endosomal compartments activate pathways that lead to IFN-I production after recognition of LPS (TLR4), double-stranded RNA (TLR3), single-stranded RNA (TLR7 and TLR8) and unmethylated CpG DNA (TLR9).

Diverse pathways downstream of these receptors transduce signals that converge on a

few key molecules, such as the IFN-regulatory factor (IRF) family of transcription factors, that activate the transcription of genes encoding IFNα/β. In most cases, IRF3 and IRF7 are the fundamental IRFs that are required. The IFNB and IFNA4 genes are induced in an initial wave of transcription that relies on IRF3. This initial IFN burst triggers the transcription of IRF7, which then mediates a positive feedback loop, leading to the induction of a second wave of gene transcription, including additional IFNα-encoding genes (*McNab et al., 2015, Nat Rev*). All IFN-I proteins are best known for their ability to induce an antiviral state in both virus-infected cells and uninfected, bystander cells, by inducing a programme of gene transcription that interferes with multiple stages of the viral replication cycle through various mechanisms. In order to do so, IFN-I proteins bind and signal through a common heterodimeric receptor, known as the IFNα/β receptor (IFNAR), which is expressed by nearly all cell types. This receptor consists of two subunits, IFNAR1 and IFNAR2, that are constitutively associated with Janus kinase 1 (JAK1) and non-receptor tyrosine kinase 2 (TYK2). Activation of JAK1 and TYK2 results in the tyrosine phosphorylation and activation of several signal transducers and activators of transcription (STAT) family members. In the canonical pathway of IFN-I induction, the activation of STAT1 and STAT2 leads to the recruitment of IRF9 and the formation of a STAT1–STAT2–IRF9 complex, which is known as the IFN-stimulated gene factor 3 (ISGF3) complex. This complex then migrates to the nucleus and binds to IFN-stimulated response elements (ISREs) in the promoters of ISGs to initiate gene transcription. Binding of IFN-I to its receptor can also signal through STAT1 homodimers, mitogen-activated protein kinases (MAPKs) and the phosphoinositide 3-kinase (PI3K) pathway, thereby leading to diverse effects on the cell. In this manner, IFN-I signaling induces the expression of several hundreds of ISGs, a large number of which function to induce an antiviral state within the cell (*Gonzalez-Navajas et al., 2012, Nat Rev; McNab et al., 2015, Nat Rev*).

2.2 Cellular sources of IFN-I

Although most cells can produce IFN-I proteins, the cellular sources can vary during different viral infections, depending on several factors like the route of infection and virus tropism. For example, during skin, mucosal and non-lymphoid organ infections IFN-I proteins are mainly produced by epithelial cells, parenchymal cells, fibroblasts, resident macrophages and dendritic cells (DCs). In this scenario, a virus-infected cell releases IFN-I proteins causing nearby cells to heighten their antiviral defenses and

recruit innate immune cells, such as macrophages and DCs. These innate cells after being infected, sense pathogen components using various intracellular PRRs, finally inducing IFN-I production (Figure 2). In contrast, in systemic infections affecting lymphoid tissues, IFN-I secretion is first mediated by marginal zone metallophilic macrophages, plasmacytoid DCs (pDCs) and monocytes (*Swiecki et al., 2011, Curr Opin Virol)*. In addition, the different cell subsets also differ in the type of IFN-I proteins produced. While non-immune cells such as fibroblasts and epithelial cells predominantly produce IFNβ, immune cells can produce both IFNα and IFNβ. In particular, pDCs are known to secrete large quantities of IFNα early during a viral infection (Figure 2)(*Ivashkiv et al., 2014, Nat Rev)*. pDCs utilize a unique mechanism for IFN-I gene expression, involving retarded internalization of viruses into endocytic vesicles where they stimulate TLR7/9 thereby activating the MyD88-IRF7 pathway (*Trinchieri, 2012, Cell Host & Microbe*). This means that their IFN-I gene expression is independent of whether they are productively infected or not. Owing to their ability to produce high levels of IFN-I proteins per cell, pDCs are usually considered to be the main IFN-I–producing cells during viral infection. However, their relevance during a viral infection varies depending on the pathogen and the dose and route of infection. For example, in the context of the murine LCMV infection model (see section 4), within the amplitude and duration of IFN-I response, pDCs contribute only to the IFN-I response detected 16–24 h postinfection *(Wang et al., 2012, Cell Host & Microbe; Trinchieri, 2012, Cell Host & Microbe; Ali et al., 2019, Front Immunol)*. However, already at day 2 post-LCMV infection pDC frequencies are markedly reduced, and the bulk of IFN-I is produced through the TLR-independent-MDA-5 signaling pathway by conventional dendritic cells (cDCs) and macrophages. Importantly, although cDCs and macrophages produce less IFN-I than pDCs on a per-cell basis, they exceed pDCs in number, therefore being important in regulating the virus-triggered IFN-I response *(Hervas-Stubbs et al., 2014, J Immunol)*. Thus, instead of a single specialized cell type, it is rather the orchestrated IFN-I gene expression by multiple cellular sources that ensures protective anti-infectious immune responses *(Ali et al., 2019, Front Immunol).* However, the functional differences of IFN-I proteins from different cell subsets as well as their relative contribution to infection control are not properly understood.

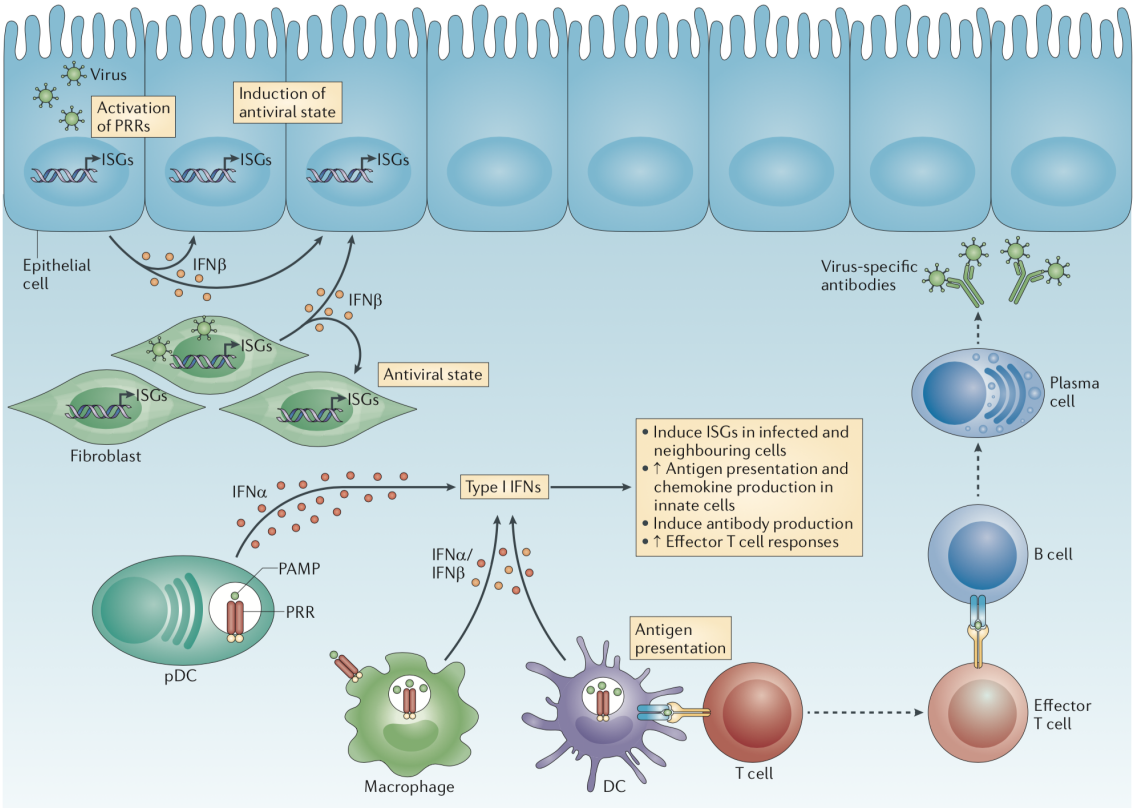

Figure 2. Sources of IFN-I and IFN-I-mediated immune-stimulation. On pathogen detection, infected cells produce IFN-I. Non-immune cells, such as fibroblasts and epithelial cells, predominantly produce IFNβ. In infected and neighbouring cells, IFN-I induce the expression of ISGs, the products of which initiate an intracellular antimicrobial programme that limits the spread of infectious agents. Innate immune cells, such as macrophages and DCs, produce type I IFNs after sensing pathogen components using various pattern-recognition receptors (PRRs). In particular, pDCs produce large quantities of IFNα. Innate immune cells also respond to IFN-I by enhancing antigen presentation and the production of immune response mediators, such as cytokines and chemokines. Adaptive immunity is also affected by IFN-I: for example, IFN-I can augment antibody production by B cells and amplify the effector function of T cells (from *Ivashkiv et al., 2014, Nat Rev).*

2.2.1 The splenic marginal zone as the frontline of an infection

Back to 1996, *Seiler et. al* demonstrated the crucial role of cells localized in the splenic marginal zone (MZ) for the clearance of LCMV infection in mice (*Seiler et al., 1997, Eur J Immunol)*. Later studies proved that an intact splenic MZ is instrumental for IFN-I production during LCMV infection and therefore the establishment of an efficient adaptive antiviral response (*Louten et al., 2006, J Immunol*). The MZ is a complex anatomic compartment of the spleen that separates the white pulp from the red pulp. Within the murine MZ, two main macrophage subsets arranged around the marginal sinus can be distinguished according to their tissue location and phenotypic

characteristics: (i) the metallophilic marginal zone macrophages (MMMΦs), and (ii) the marginal zone macrophages (MZMΦs). MMMΦs typically express in their surface CD169 (Siglec-1, Sialoadhesin) and MOMA-1. MZMΦs instead are defined by the expression of C-type lectin SIGN-related 1 (SIGNR1) and a type I scavenger receptor called Macrophage Receptor with Collagenous structure (MARCO) (Figure 3). Although MZMΦs are typically referred to as a single population of cells, closer examination shows that they are in fact heterogeneous, and that in addition to cells co-expressing both SIGNR1 and MARCO, the outer rim of the MZ also contains a subset of macrophages that express the MARCO receptor but lacks SIGNR1. The relationship between these two cell subsets is not well understood, and it is possible that they reflect different activation states of cells with a common origin *(Grabowska et al., 2018, Front Immunol; Pirgova et al., 2020, PNAS).* MZMΦs and MMMΦs play a similar role in LCMV infection, and their localization in the interface between the bloodstream and lymphocyte-rich zones makes them important bridges between innate and adaptive immunity. While both macrophage populations mediate pathogen recognition and elimination from the circulation, MMMΦs also collaborate in both B- and T-cell activation by the direct or indirect transferring of antigen, respectively *(Borges de Silva et al., 2015, Front Immunol; Honke et al. 2011 Nat Immunol).* Importantly, MMMΦs have recently been shown to release high amounts of IFN-I after acute LCMV infection. Selective depletion of these cells in CD169-diphtheria toxin receptor (DTR) transgenic mice resulted in reduced IFN-I levels at days 3-5 post-infection and persistent viral titers *(Shaabani et a., 2016, Cell death & disease)*.

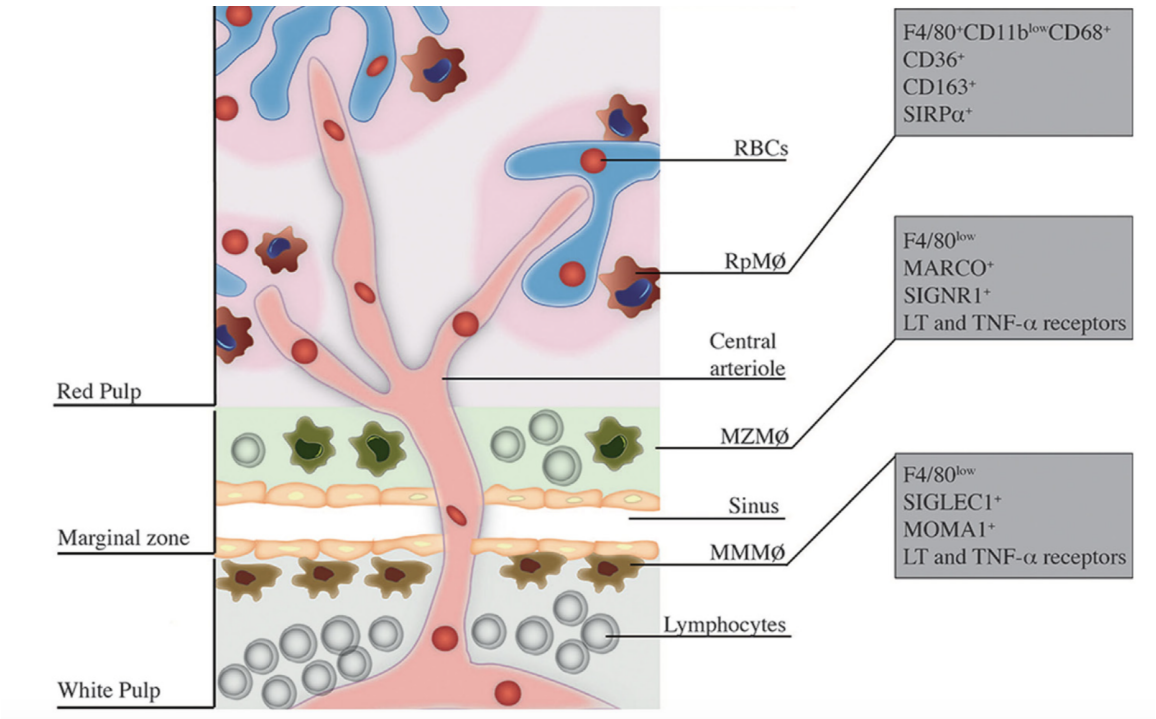

Figure 3. Localization and phenotype of splenic macrophage subsets. Red pulp macrophages (RpMΦs; in red) are typically found within cords on the red pulp, allowing direct contact with red blood cells (RBCs) and other blood cells/particles passing through venous sinuses. They are defined by the concomitant expression of F4/80, CD11b (at low levels), and CD68. Marginal zone macrophages (MZMΦs; in green) are found in the marginal zone (MZ) outer layer, they are also in direct contact with blood-borne particles. These cells express the surface molecules MARCO and SIGNR1 and other receptors that help in the uptake of blood-borne pathogens. Finally, the metallophilic marginal zone macrophages (MMMΦs; in brown) reside within the inner layer of the MZ, in contact with the white pulp. They are also specialized in blood-borne particle uptake and express the surface markers SIGLEC-1 (or CD169) and MOMA-1 *(*adapted from *Borges de Silva et al., 2015, Front Immunol).*

2.3 Regulation of innate and adaptive immunity by the IFN-I response

Besides the direct antiviral role of IFN-I proteins described above, the IFN-I response is generally regarded as a key bridging mechanism between innate and adaptive immune responses. It modulates innate immune responses in a balanced manner that promotes antigen presentation and natural killer cell functions while restraining pro-inflammatory pathways and cytokine production, and activates the adaptive immune system promoting the development of high-affinity antigen-specific T and B cell responses and

immunological memory (Figures 2 and 4)*(Ivashkiv et al., 2014, Nat Rev; Swiecki et al., 2011, Curr Opin Virol)*. Therefore, the early IFN-I response during a viral infection is a critical factor that determines the infection outcome by influencing most components of the host immune response.

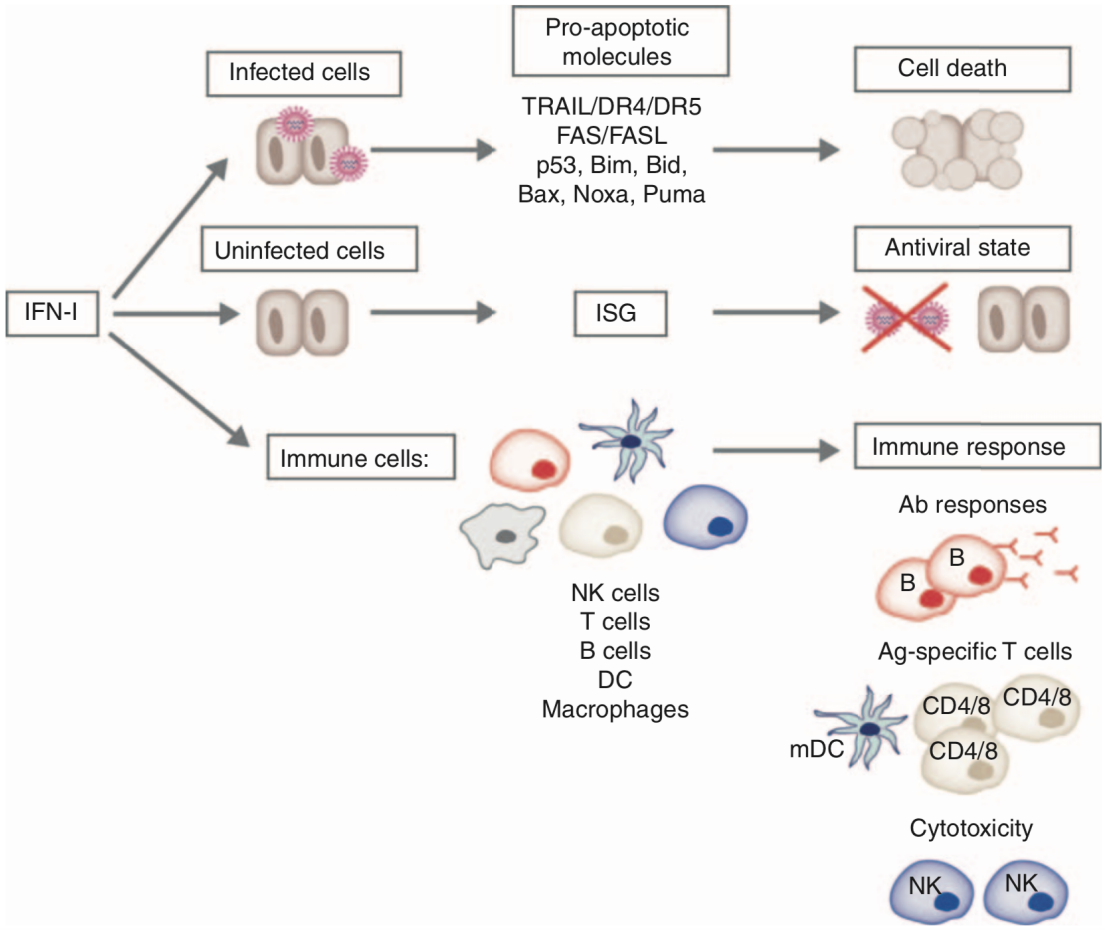

Figure 4. Effects of IFN-I at the cellular level. IFN-I promotes the death of virus-infected cells through the induction of pro-apoptotic molecules involved in the extrinsic (TRAIL/DR4/DR5 or Fas/FasL) and intrinsic (p53, Bim, Bid, Bax, Noxa and Puma) apoptosis pathways. In addition, IFN-I acts on uninfected cells by inducing ISGs that restrict viral replication and confer an antiviral state. IFN-I has also immunostimulatory effects on both innate and adaptive immune cells, by inducing the maturation, expansion and effector functions of NK cells, T and B cells. DCs and macrophages are also profoundly influenced by IFN-I (from *Swiecki et al., 2011, Curr Opin Virol).*

2.3.1 Regulation of innate immune responses

IFN-I proteins exert their effects on innate immune cells either directly through IFNAR triggering, or indirectly by the induction of chemokines and cytokines, which further recruit and regulate immune cells. Direct IFN-I stimulation promotes antigen presentation and cell maturation in antigen presenting cells (APCs) through the upregulation of MHCI and MHCII, and their respective co-stimulatory molecules such as CD80 and CD86. This process enhances APCs ability to stimulate T cell differentiation, expansion, and killing of virus-infected cells (*Hervas-Stubbs et al., 2011, Clin Cancer Res)*. Function and differentiation of monocyte/macrophages are highly affected by IFNAR signaling. Specifically, IFN-I signaling supports the differentiation of monocytes into DC with high capacity for antigen presentation, stimulates macrophage antibody-dependent cytotoxicity, and positively or negatively regulates macrophage production of various cytokines (e.g., TNF, IL1, IL6, IL8, IL12, and IL18). In addition, autocrine IFN-I signaling is required for the enhancement of macrophage phagocytosis and oxidative bursts through the generation of nitric oxide synthase 2. IFN-I proteins have multiple effects on DCs, affecting their differentiation, maturation, and migration. IFN-I signaling on DCs induces their activation and the secretion of proinflammatory cytokines that lead to activation of the adaptive immune response (*McNab et al., 2015, Nat Rev; Hervas-Stubbs et al., 2011, Clin Cancer Res)*. Furthermore, by inducing the upregulation of chemokine receptor expression, IFN-I signaling promotes the ability of DCs to migrate to lymph nodes and cross-present antigens. IFN-I signaling is also required for pDCs to migrate from the marginal zone into the T-cell area of the secondary lymphoid organs. Finally, NK cell functionionality is also modulated by IFN-I signaling, enhancing their cytolytic capacity and cytokine production, thereby turning these cells into potent killers of virus-infected cells, and promoting their accumulation and survival (Figure 5) (*Teijaro et al., 2016, Adv Immunol; Saprunenko et al., 2019, Viruses*).

2.3.2 Regulation of T cell responses

As previously mentioned, the IFN-I response directly affects the functionality of innate immune cells, thus indirectly influencing T cell immunity (*Hervas-Stubbs et al., 2011, Clin Cancer Res)*. In contrast, the IFN-I induced antiviral response that aims to reduce viral loads in infected cells might result in a decrease of viral antigens required to

induce an adaptive immune response by APCs. This paradox was resolved by *Honke et al.* in an elegant study using the murine VSV infection model. They demonstrated that in metallophilic macrophages IFN-I signaling is inhibited by high expression levels of the IFNAR-inhibitor Usp18 which results in enforced viral replication in these cells, thereby allowing sufficient viral antigen accumulation for the effective activation of virus-specific adaptive immunity (*Honke et al., 2011, Nat Immunol).* Another example of how macrophages can indirectly influence adaptive immunity through IFN-I signaling was recently published by *Barbet et al.*. In this study they demonstrate that IL-1b produced by IFN-I activated macrophages promotes T follicular helper (Tfh) cell activation and differentiation, thus promoting an efficient antibody response (*Barbet et al., 2018, Immunity*). Finally, NK cells are another innate immune cell subset that influences adaptive immunity through their activation by IFN-I signaling. Indeed, NK cells can either directly kill effector T cells, or indirectly regulate T cell function by modulation of APC numbers and/or function. Importantly, IFN-I activates the cytotoxic activity of NK cells, while simultaneously acting directly on T cells to protect them against NK cell-mediated attack *(Crouse et al., 2015, Nat Rev Immunol; Crouse et al., 2014, Immunity)*.

Direct IFN-I signaling on antiviral CD8 T cells acts as a signal 3 cytokine which promotes survival and effector cell differentiation (Figure 5). However, the timing of CD8 T cell exposure to IFN-I significantly influences the differentiation and magnitude of this response. When TCR stimulation coincides with, or shortly precedes, IFNAR signalling, the role of IFN-I as a signal 3 cytokine predominates. Conversely, if IFNAR signalling precedes TCR engagement, it induces anti-proliferative and pro-apoptotic programmes on CD8 T cells, thus preventing the expansion of non-relevant T cell clones *(Crouse et al., 2015, Nat Rev Immunol)*. IFN-I signaling during viral infection can also signal to regulatory T cells and subsequently alter their suppressive functions, allowing for optimal antiviral T cell responses during the ongoing viral infection *(Gangaplara et al., 2018, PLoS Pathogen; Teijaro et al., 2016, Adv Immunol).*

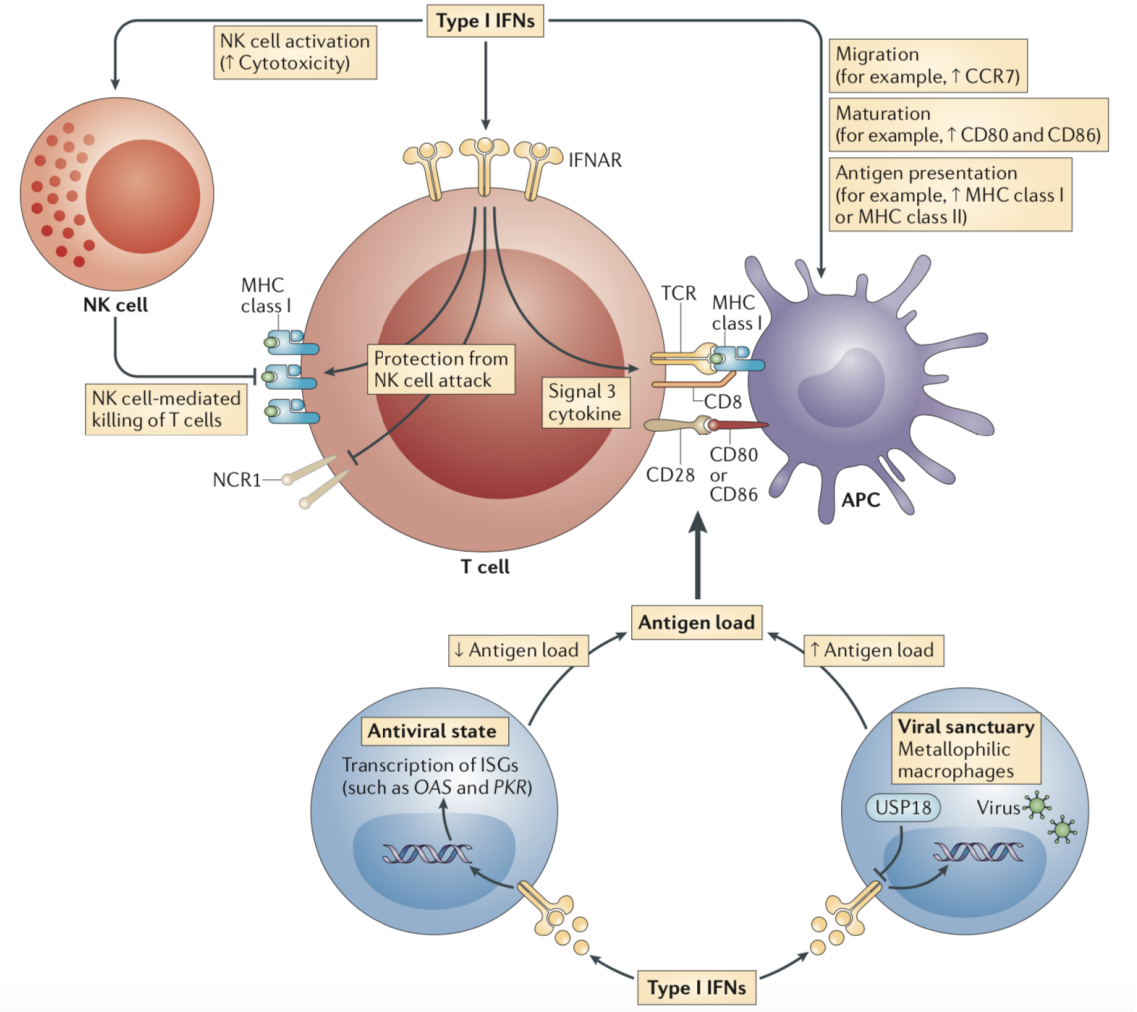

Figure 5. Representation of the direct and the indirect influence of IFN-I on T cells. IFN-I indirectly regulates T cell immunity by promoting dendritic cell maturation, migration and antigen presentation, and by regulating viral replication, thereby modulating the amount of antigen that is presented to T cells. Viral replication is restricted in all cells except metallophilic macrophages in the spleen, in which inhibition of IFN-I signalling ensures sufficient amounts of antigen for T cell priming. IFN-I directly affects T cell activation, proliferation and survival by acting as a signal 3 cytokine during T cell priming, and by protecting clonally expanding T cells against natural killer (NK) cell-mediated attack. IFN-I-mediated activation of NK cells enhances their cytotoxicity, which contributes to early control of viral infection *(*from *Crouse et al., 2015, Nat Rev Immunol).*

2.3.3 IFN-I-mediated immunosuppression in chronic infections

During the early stages of a viral chronic infection, IFN-I genes are powerfully and systemically induced. However, this initial response is rapidly attenuated, although low IFN-I and ISGs levels still persist in multiple cells and tissues. Several mechanisms

may contribute to the attenuation of IFN-I response in the post-acute stages including a direct suppression of innate pathways by viral products as well as host immunomodulatory mechanisms to avoid the detrimental effects of a persistent IFN-I exposure (*Snell et.al, 2017, Trends Immunol)*. In 2013 two important studies showed the fundamental role of IFN-I signaling during chronic LCMV infection. *Wilson et a*l. and *Teijaro et al.*, demonstrated that persistent IFN-I signaling elicits immunosuppressive effects on T cell responses via upregulation of the inhibitory factors IL-10 and PD-L1, promotes chronic immune activation, lymphoid tissue disorganization and consequent virus persistence (Figure 6).

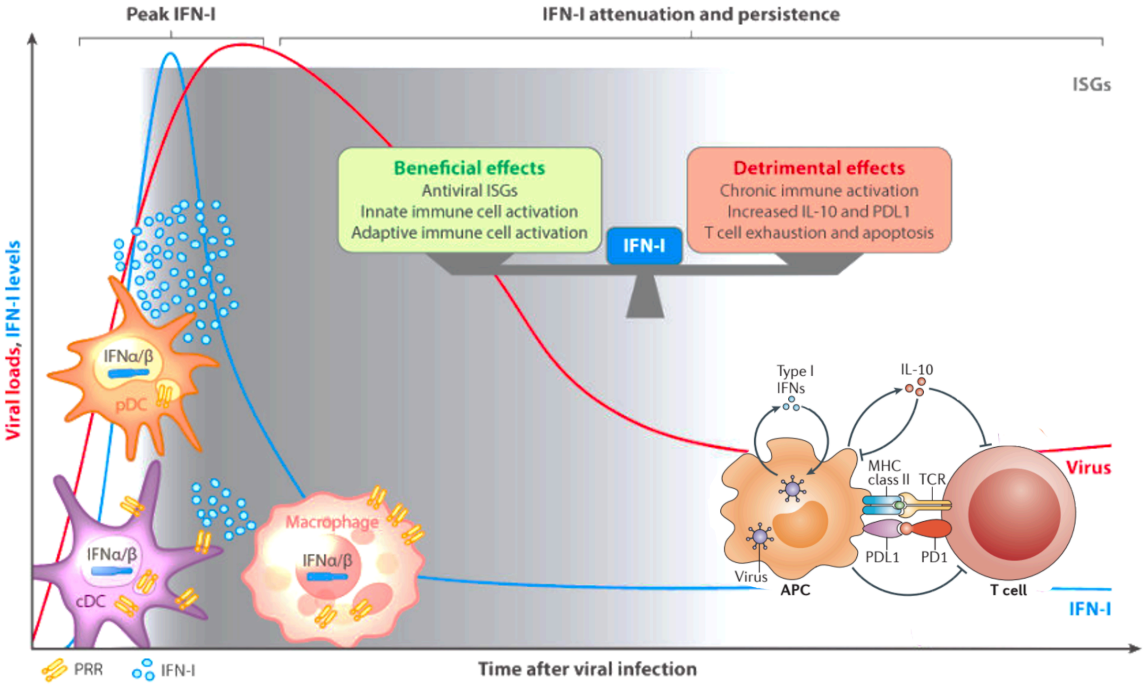

Figure 6. IFN-I dynamics and opposing effects during chronic infection. Following the initial IFN-I peak after infection, systemic IFN-I becomes undetectable at later stages, despite maintained viral loads. While early IFN-I production mediates antiviral functions, during chronic infections, the balance of the response shifts to greater immunomodulatory effects. During chronic viral infection, IFN-I induces the production of immunosuppressive cytokines such as interleukin-10 (IL-10) and induces APCs to express ligands (such as programmed cell death 1 ligand 1 (PDL1)) for T cell-inhibitory receptors (such as PD1, the PDL1 receptor). These factors lead to the suppression of T cell function and failure to clear infection (Adapted from *McNab et al., 2015, Nat Rev & Zuniga et al., 2015, Ann Rev Virol).*

Importantly, blockade of IFNAR signaling before and after the establishment of persistent virus infection restored proper immune functions and resulted in enhanced virus clearance (*Wilson et. al, 2013, Science; Teijaro et al., 2013, Science*). Further

studies demonstrated that the IFN-I-mediated pathological effects are mediated by IFNβ but not IFNα *(Ng et al., 2015, Cell Host & Microbe)*. In summary, when viral infections cannot be cleared, sustained IFN-I signalling takes a predominantly immunosuppressive role to limit host toxicity and tissue pathology during persistent infection *(Snell et al., 2015, Curr Opinion Imm; Crouse et al., 2015, Nat Rev Immunol).*

2.3.4 Time-dependent functions of IFN-I

As described above, IFN-I functionality shifts from an early antiviral to a late immunosuppressive role over the course of a chronic infection (*Saprunenko et al., 2019, Viruses*). Importantly, the administration of recombinant IFN-I during the early phase of chronic LCMV infection prevents CD8 T cell exhaustion and the establishment of chronic infection (*Wang et al., 2012, Cell Host & Microbe).* On the contrary, in the late phase of chronic LCMV infection IFN-I signaling has mainly detrimental effects and its therapeutic blockage dampens the immunosuppressive program and facilitates viral clearance (*Wilson et al., 2013, Science; Teijaro et al.,2013, Science)*. Similarly, IFNAR blockage in a humanized murine model of HIV infection also leads to a reversion of exhaustion, reduction of immune activation and decreased HIV plasma viral loads *(Cheng et al, 2017, J Clin Invest; Zhen et al, 2017, J Clin Invest)*. Consistent with these observations, a study using the SIV-infection model in monkeys showed that early administration of IFNα2 protected against infection, whereas prolonged administration resulted in IFN-I desensitization and accelerated disease progression (*Sandler et al., 2014, Nature*). Additionally, IFN-I sensing during the first 24 hours post-LCMV infection in mice, drives CD4 T cells polarization toward Tfh rather than T helper 1 (Th1) phenotype, thereby differentially influencing the subsequent adaptive immune response *(De Giovanni et al., 2019, Nat Immunol).*

Thus, there is a specific time window of effectiveness for IFN-I production and/or administration, out of which its effects can dramatically change (*Wang et al., 2012, Cell Host Microbe*). As an example, recent studies showed that an impaired or delayed IFN-I response during SARS-CoV-2 infection correlates with the severity of COVID-19. This is further supported by clinical data showing favorable clinical responses and reduced mortality after early IFN-I administration in virus-exposed individuals *(Bocharov et al., 2020, Front Cell Infect Microbiol).*

3. Lymphoid tissue fibrosis during viral infections

Fibrosis is an essential component of tissue repair and its aim is to deposit connective tissue in order to preserve tissue architecture after a damaging event. However, if the tissue injury is severe or repetitive, or if the wound-healing response itself becomes dysregulated, the normal tissue repair process can evolve into a progressively irreversible fibrotic response. This condition reflects a pathologic state and is characterized by the excessive accumulation of fibrous connective tissue (such as collagen and fibronectin) in the inflamed or damaged tissue which finally results in scarring, impairment of tissue function and organ damage *(Suthahar et al., 2017, Curr Heart Failure Reports; Rosenbloom et al., 2013, Biochimica et Biophysica Acta).*

Depending on the context, the mechanisms responsible for fibrosis induction can differ. A dysregulation in innate and adaptive immune responses is known to be one of the major triggers *(Suthahar, 2017, Curr Heart Failure Reports)*. During a viral infection, an immune dysregulation can determine an imbalanced proinflammatory response which finally results in tissue pathology. For example, recent studies showed that many severe COVID19 patients had an impaired IFN-I response, which was associated with the induction of a “cytokine-storm” *(Hadjadj et al., 2020, Science)*. Linked to this exacerbated inflammatory response, lung fibrosis emerged as a secondary event related to the progression of the pathology *(Garcia-Revilla et al., 2020, Front Immunol)*. Once recruited to the site of inflammation, immune cells such as lymphocytes and macrophages, release growth factors and cytokines that, by promoting fibroblasts production of extracellular matrix (ECM), leads to the development of fibrotic tissue *(Rosenbloom et al., 2013, Biochimica et Biophysica Acta)* (Figure 6). Specifically, macrophages are known to secrete massive amounts of transforming growth factor beta (TGFβ) that directly contributes to fibrosis, but they can also contribute to tissue damage by secreting reactive oxygen and nitrogen species which further exacerbate the inflammatory response *(Wynn et al., 2013, Nat Med)*.

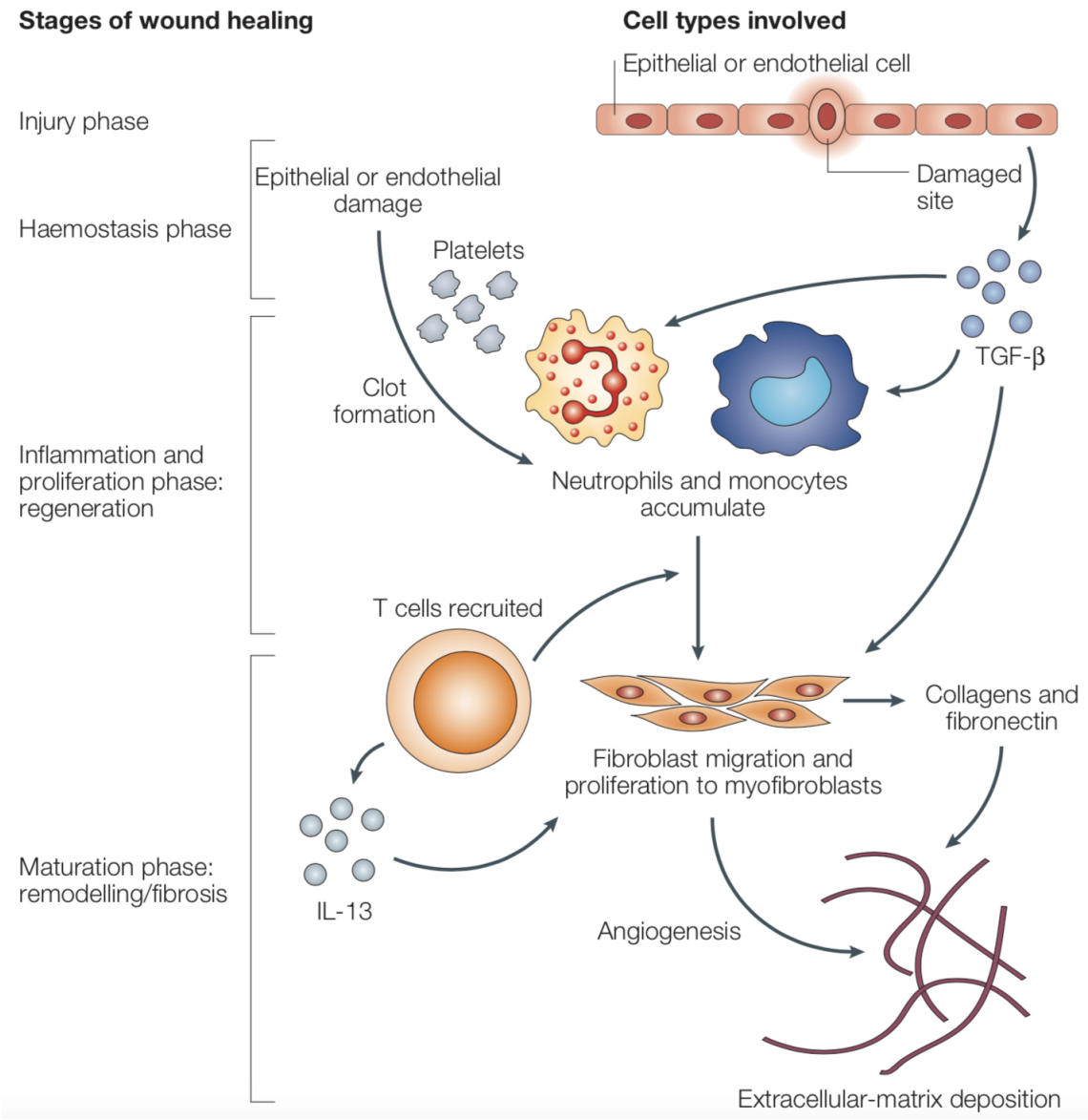

Figure 6. Induction of fibrosis. Following tissue injury, damaged epithelial and/or endothelial cells release inflammatory mediators that initiate an antifibrinolytic–coagulation cascade and secrete growth factors such as TGFβ that stimulate the proliferation and recruitment of leukocytes. Activated macrophages and neutrophils 'clean-up' dead cells and produce chemokines that recruit and activate T cells. Fibroblasts are subsequently recruited and activated to regenerate the damaged tissue via deposition of extracellular-matrix components. When repeated injury occurs, chronic inflammation and repair can cause an excessive accumulation of extracellular-matrix components that lead to the formation of a permanent fibrotic scar (from *Wynn, 2004, Nat Rev Immunol*).

Current studies have suggested multifaceted functions of immune cells in fibrotic diseases, possibly due to dynamic changes in the microenvironment during disease development. Indeed, various T cell subsets appear to have differential pro- or anti-

fibrotic roles depending on the specific context. For example, IFNγ production by Th1 cells is generally considered to be anti-fibrotic via suppression of fibroblast-induced collagen synthesis. However, Th1-mediated IFNγ-dependent induction of TGFβ in cardiac fibroblasts is a driver of cardiac fibrosis *(Zhang et al., 2020, Front Immunol)*. Moreover, most immune cell types are heterogeneous with functional plasticity modulated by both systemic and microenvironmental factors. Thus, the cellular identities and local niches are of key significance for their functions in fibrosis *(Huang et al., 2020, Int J Mol Sci).*

The development of fibrosis in lymphoid organs such as spleen and lymph nodes, represent an important issue. Indeed, the LT structure provides a conduit system for lymphocyte migration, delivery of soluble antigens and cytokines, and produces growth factors critical for T cell survival and proliferation *(Brown et al., 2015, J Immunol)*. Given these functions, fibrosis-mediated disruption of the LT structure alters immune cell motility and T cell–APC interaction dynamics thus impairing the generation of a robust host-immune response to infectious agents *(Schacker et al., 2006, Clin Vacc Immunol)* and following therapeutic strategies such as vaccination *(Kityo et al., 2018, J Clin Invest).* For example, several studies have demonstrated that chronic HIV infection results in progressive LT fibrosis, and these fibrotic changes correlate with a reduction in the size of the total population of CD4+ T cells. Importantly, this represents an obstacle during the recovery with ART therapy (*Schacker et al., 2006, Clin Vacc Immunol*). Previous results from our laboratory identified fibrosis induction in the spleen of LCMV acute- but not chronic-infected mice. Interestingly, acute-infected mice developed spleen fibrosis that was maintained even when the virus was already well controlled while in chronic infection, fibrosis was almost absent *(Argilaguet et al., 2019, Genome Res).* However, the mechanisms behind this tissue pathology were not elucidated.

4. Lymphocytic choriomeningitis virus: a mouse model to study antiviral immunology

4.1 The virus

LCMV is a non-cytopathic virus and a member of the Arenaviridae family. It causes a persistent infection in the mouse, its natural host, but it can also infect a wide range of other animals, including humans. Although there is no quantitative data on the relative threats of the different LCMV virus strains for humans, it can cause a variety of syndromes that go from a mild respiratory infection to encephalitis or meningitis. Death from LCMV infection is rare, and patients usually recover without any sequelae *(Farmer & Janeway, 1942, Medicine)*. Since its discovery in the early 1930s, infection of mice with several LCMV strains has been a widely used tool in scientific laboratories for examining mechanisms of viral persistence and basic concepts of virus-induced immunity and immunopathology (*Wilson & Brooks, 2010, Immunol Res*).

LCMV is an enveloped RNA virus with a bisegmented negative single-stranded RNA genome. Its life cycle is restricted to the cytoplasm of the infected cell. Each of the RNA genome segments, designated as large (L, 7.3kb) and small (S, 3.5kb), uses an ambisense coding strategy to produce two viral gene products, in opposite orientation, and separated by a non-coding intergenic region that folds into a stable hairpin structure (*De la Torre, 2009, Ann N Y Acad*). The S RNA encodes the nucleoprotein (NP), the most abundant protein, and the viral glycoprotein precursor (GPC). The NP is the main structural element and plays an essential role in viral RNA synthesis. NP has been also associated with a IFN-I counteracting activity (*Martínez-Sobrido et al., 2007, J Virol*). The GPC is post-translationally cleaved into GP1 and GP2, and GP1/2 together make the spike of the virion. The L RNA segment encodes for the viral RNA-dependent RNA polymerase (RdRp, also referred to as L polymerase), and a small RING finger protein Z that localizes in the plasma membrane. The Z protein is a structural component of the virion that interacts with host proteins, inhibits RNA synthesis by the RdRp, and is the main driver of LCMV budding (*De la Torre, 2009, Ann N Y Acad*).

α-dystroglycan (α-DG) is the main cellular receptor protein for LCMV and the majority

of arenaviruses. α-DG is a highly conserved, ubiquitous cell surface molecule that links the extracellular matrix with the cytoskeleton (*Cao, 1998, Science; Kunz et al., 2003, Virology; De la Torre, 2009, Ann N Y Acad*). Within immune cell populations, α-DG is mainly expressed on DCs (*Oldstone & Campbell, 2011, Virology*). Virus strains and variants that bind α-DG with high affinity are associated with virus replication in the white pulp of the spleen with preferential replication in DCs (*Oldstone & Campbell, 2011, Virology*). After interaction of α-DG with the viral GP1, LCMV virions are endocytosed. The subsequent fusion between the viral and cell membranes is triggered by the acidic environment found in the late endosome and GP2 (*Gallaher et al., 2001, BMC Microbiology*). Upon release of viral genomic RNA, protein synthesis and genomic RNA replication starts. Formation and budding of arenavirus infectious progeny requires assembly of the viral ribonucleoproteins (RNPs) and the cellular membranes enriched with viral GPs. Finally, there is the assembly and cell release of the infectious virions (*Kunz et al., 2002, Curr Top Microb Immunol; Perez & de la Torre, 2003, J Virol*).

4.2 LCMV as a crucial tool for understanding viral immunology

The concept of persistent viral infection evolved from an observation that Traub made in 1936, in which neither mice infected with LCMV in the utero nor shortly after birth died or eliminated the virus (Traub 1936a; Traub 1936b). In that time, three different LCMV isolates originated: the Armstrong strain isolated from monkeys, the Traub strain isolated from a laboratory colony of persistently infected mice, and the WE strain, isolated from a human after exposure to persistently infected mice. Many different variants of these strains exist, but the most used are Clone13 which derives from the Armstrong strain, and Docile, a derivative of the WE strain (*Welsh & Seedhom, 2008, Curr Prot Microbiol*). LCMV infection fate varies dramatically depending on the virus strain, age and genetic background of mice, route of infection, as well as the dose used for infection (*Spiropoulou et al., 2002, J Virol; Zinkernagel et al., 2002, Curr Top Microb Immunol*). In fact, one of the key features of the LCMV system is the ability to compare two different immune responses: acute and persistent infections (*Klenerman & Hill, 2005, Nat Immunol; Wilson & Brooks, 2010, Immunol Res*). For example, the viral strains Armstrong and Clone13 have genomes that only differ by two amino acids, a K to Q substitution at position 1079 and a F to L substitution at position 260. Interestingly, these two differences in the viral ‘polymerase’ and ‘glycoprotein’ genes, respectively,

accounts for the biological phenotype of acute versus persistent infection. In particular, the latter substitution alters receptor tropism, enabling Clone13 to infect CD11c+ DCs more efficiently than the Armstrong strain (*Matloubian et al., 1994, J Viro*l). Viral targeting of CD11c+ DCs is associated with defective antigen presentation and costimulation, and results in impaired T cell responses and ultimately, viral persistence (*Bergthaler et al., 2010, PNAS*).

In addition to genetic differences, also the route and the dose of administration have a significant impact on clinical manifestation following infection. While infection of mice with the Armstrong strain via the intraperitoneal (i.p.) route results in an acute infection, the intracranial route of infection causes a lethal neurological disease mediated by a cytotoxic CD8+ T cell response. By contrast, the Clone13 strain is used to establish a chronic infection in mice through the intravenous (i.v) administration route. Regarding the impact of viral dose on infection outcome, a relevant example is represented by the LCMV strain Docile ($LCMV_{DOC}$). A low dose of this strain induces a robust virus-specific T cell response that results in viral clearance within 8-10 days post-infection (p.i). In contrast, infection with high doses of $LCMV_{DOC}$ results in T cell exhaustion and viral persistence (*Cornberg et al., 2013, Front Imm*; *Saprunenko et al., 2019, Viruses*).

Since Traub's discovery, the use of LCMV infection of mice as a model system had vast implications throughout immunology and medicine, allowing to characterize the immune response during acute and persistent viral infections. First, the MHC-restricted function of cytotoxic T lymphocytes was demonstrated by Rolf Zinkernagel and Peter Doherty, for which they were awarded the Nobel Prize in 1996 (*Zinkernagel and Doherty, 1975, Nature*). Second, the mechanism of CTL-mediated lysis of virus-infected target cells was shown to be mediated via perforin secretion (*Kägi et al., 1994; Masson and Tschopp, 1985, J Biol Chem*). Third, the concept of "memory" of adaptive immune responses where T cells remember their cognate antigen after initial antigen encounter was developed (*Murali-Krishna et al., 1998, Immunity*). Fourth, the key role of NK cells as important regulators of CD4 T-cell-mediated support for antiviral CD8 T cells was shown (*Waggoner et al., 2011, Nature*). Fifth, the role of organized secondary lymphoid organs in the induction of naive T and B cells, and subsequent virus control was established (*Karrer et al., 1997, J Exp Med*). Sixth, the concept of immunopathology was developed in which the damage of the tissue and organs is associated with or directly caused by the immune response and not as a direct result of

the pathogen burden or toxicity from the infected cell. Mediators of immunopathology include CTL, macrophages, neutrophils and interferons (*Cole et al., 1972, Nature; Kim et al., 2009, Nature; Rivière et al., 1977, PNAS*). Seventh, the state of dysfunction of effector T cells, a phenomenon known as “immune exhaustion” (see section 1.2) was established (*Welsh & Seedhom, 2008, Curr Prot Microbiol*). Eighth, the role of host immunoregulatory proteins such as PD1 in directly inhibiting antiviral immune functionality and maintaining the immunosuppressive state was shown (*Barber et al., 2006, Nature ; Okoye et al., 2017, Front Immunol; Waggoner et al., 2011, Nature*). Thus, the LCMV mouse model system has proven to be an excellent platform for immunological studies.

4.3 Similarities between LCMV and HIV immunology

LCMV and HIV are inherently different viruses regarding genetic composition, replicative strategies and mechanisms of infection. Despite that, they both elicit comparable antiviral responses at least under certain LCMV infection conditions. For this reason, some of the immune features described in LCMV were then extended to the understanding of persistent HIV infections in humans (*Klenerman & Hill, 2005, Nat Immunol*). Some examples are: (i) exhausted CD8+ T cell responses in persistent LCMV infection are comparable to the exhausted CD8+ T cell responses found in HIV infection, specifically the failure to proliferate and produce cytokines in responses to viral antigen (*Klenerman & Hill, 2005, Nat Immunol*); (ii) PD1 expression on virus-specific CD8+ T cells are increased in LCMV and HIV infections, correlating with T cell exhaustion (*Barber et al., 2006, Nature*). PDL1 blockade results in an increase of CD8+ T cell functionality in both viral infections *(Blackburn et al., 2008, PNAS; Day et al., 2006, Nature; Petrovas et al., 2006, J Exp Med*); (iii) IL-10 plays an immunomodulatory role during persistent LCMV and HIV infection. Blockade of this cytokine enhances virus-specific T cell responses in both persistent infections (*Clerici et al., 1994, J Clin Invest; Landay et al., 1996, J Infect Dis*); (iv) CD4+ T cells are required to sustain virus-specific CD8+ CTL during chronic LCMV infection (*Battegay et al., 1994, J Virol; Matloubian et al., 1994, J Virol*); (v) The role of IL-2 as a regulator of effector and memory CTL generation has been pinpointed (*Pipkin et al., 2010, Immunity)*. IL-2 expression is suppressed by both CD4+ and CD8+ T cells in persistent LCMV and HIV infection, diminishing the expansion and generation of lasting memory CD8+ T cells (*Aiuti & Mezzaroma, 2006, AIDS Rev*); and finally (vi) IL-21 production by CD4+ T cells

is necessary for the maintenance of CD8+ T cell effector responses during persistent LCMV infection (*Frohlich et al., 2009, Science; Yi et al., 2009, Science*) as well as in HIV infection (*Yue et al., 201, J Immunol*). Thus, LCMV has been proven to be a valuable experimental tool to address meaningful mechanistic correlations between the mouse system and what one observes in human HIV infection.

OBJECTIVES

The fate of a viral infection is the result of a dynamic interplay between infecting viruses and induced host responses. Type I IFN (IFN-I) proteins are major players in shaping the antiviral immune response, and the timing of IFN-I response appears to have a crucial impact on the outcome of the infection. However, the differential dynamics by which different immune cell subsets regulate the IFN-I response during the early stage of acute and chronic infections is not completely understood.

The main objective of this thesis was to uncover the spatiotemporal events influencing IFN-I dynamics/responses during early acute and chronic infections.

The specific objectives were:

1. To characterize by whole-tissue RNAseq the differential dynamics of the IFN-I response during early acute and chronic LCMV infection of mice.

2. To spatially and temporally characterize the cell subsets contributing to IFN-I production in acute and chronic LCMV infection.

3. To analyze the implications of the differential dynamics of IFN-I responses for the infection outcome.

MATERIAL & METHODS

1. Media, buffer and solutions

Lysing solution

0.15 M NH_4Cl (Merck), 10 mM $KHCO_3$ (Sigma-Aldrich), 0.1 mM Na_2EDTA (Sigma-Aldrich). pH 7,2-7,4.

FACS buffer

Phosphate buffered saline (PBS) (Gibco), 5% FCS, 0,5% Bovine serum albumin (Sigma- Aldrich), 0,07% sodium azide (Sigma-Aldrich).

FACS Fix buffer

Deionized water, 1% paraformaldehyde (Sigma-Aldrich), 150 mM NaCl (Sigma-Aldrich), pH7,4.

Complete RPMI

RPMI 1649 with L-glutamine (Sigma-Aldrich), 10% heat inactivated fetal calf serum (FCS) (Sigma-Aldrich), 1 U/mL penicillin, 1 µg/mL streptavidin, 0,05 mM β-Mercaptoethanol, 1mM sodium pyruvate (Sigma-Aldrich).

Perm Wash buffer

Phosphate buffered saline (PBS) (Gibco), 1% fetal bovine serum (FCS), 0,1% NaN_3 (Sigma-Aldrich), 0,1% Saponine.

MACS Buffer

Phosphate buffered saline (PBS) (Gibco), 0,5% Bovine serum albumin (Sigma-Aldrich), 2 mM EDTA (Sigma, E5134), pH 7.2.

0.1M Tris Buffer

Deionized water, 1 M Tris powder (Mw=121.1 g/mol), pH 7.

Standard Block Buffer

0.1 M Tris buffer, 1% Bovine serum albumin (Sigma-Aldrich), 0.3% Triton 100X (Sigma-Aldrich).

2. Mice and LCMV infection

Experiments were performed with C57BL/6 and CD169 diphteria toxin receptor (DTR) transgenic male and female mice (6-12 weeks of age) maintained in a specific pathogen-free facility at the Parc de Recerca Biomèdica de Barcelona. Experimental procedures were conducted according to the guidelines from the Generalitat de Catalunya and approved by the ethical committee for animal experimentation at the Parc de Recerca Biomèdica de Barcelona (CEEA-PRBB, Spain). CD45.2 mice were purchased from Charles River Laboratories and CD169DTR transgenic mice, generated in the Tanaka laboratory, were a kind gift from Andres Hidalgo, Madrid.

LCMV strain Docile ($LCMV_{DOC}$) was used for mouse infections. The virus was grown, stored and quantified according to previously published methods (*Argilaguet et al., 2019, Genome Research)*. Mice were infected by intraperitoneal (i.p.) injection of either $2x10^2$ or $2x10^6$ plaque-forming units (pfu) of $LCMV_{DOC}$ to respectively induce an acute or a chronic infection.

3. *In vivo* treatments with antibodies and inhibitory peptides

To block the IFN-I signaling at the desired timepoint, C57BL/6J mice were intraperitoneally inoculated with 500 µg of anti-IFNAR (aIFNAR) antibody (clone MAR1-5A3; Leinco Technologies) or 500 µg of a mouse IgG1 isotype control (clone MOPC21; Bio X Cell) on days 3 and 4.5 post-infection. anti-PDL1 (aPDL1) antibody (clone 10F.9G2; Bio X Cell) was administered i.p. in three or five shots of 200 µg every three days. In particular, early aPDL1-treated mice were given three shots at days 11, 14 and 17 p.i., late aPDL1-treated mice group 1 were given three shots at days 22, 25 and 28 p.i. and late aPDL1-treated mice group 2 were given five shots at days 19, 22, 25, 28 and 31 p.i.. In order to block the proinflammatory response at day 6 p.i., NBP2 (IKK-Gamma NEMO Binding Domain (NBD) inhibitor peptide; Novus Biologicals) was injected i.p. at days 3, 4 and 5 p.i., at the dose of 1 mg/kg; control mice were injected with a control peptide at the same time-points and doses.

4. *In vivo* cell depletion

In order to deplete CD169+ macrophages, diphtheria toxin (DT; Sigma-Aldrich) was i.p. injected into CD169DTR transgenic mice (30 µg per kg body weight) at day 3 post acute infection. Upon DT administration, CD169+ macrophages are efficiently ablated at day 5 p.i.. Physiological serum was used as a control vehicle. CD8 T cell depletion in acute and chronic LCMV infection was performed by i.p. administration of anti-CD8α antibody (clone 2.43; Bio X Cell) respectively at days -1 and 2 p.i. and at days 7 and 10 p.i..

5. Quantification of virus in tissue

Viral titers from spleens of infected mice were determined by focus-forming assay *(Battegay et al., 1991, J Virol Methods*). One third of the spleen was collected in cryotubes the day of necropsy and stored at -80°C until their use. For the assay, frozen spleens were smashed, resuspended in DMEM (Invitrogen), and used to make 6 serial dilutions. Next, 200 µL/well of all the dilutions were plated in a 24 well plate (Sigma-Aldrich) containing 400,000 cells/well and were incubated for 5 hours at 37°C. After verifying that the cells had formed a monolayer, a 1:1 mixture of 3% methocel (Sigma-Aldrich) and 2X DMEM (Invitrogen) was added into each well and incubated for 48 hours at 37°C .

For LCMV antigen staining to count plaque forming units, cells were fixed with 37% formaldehyde (Sigma-Aldrich), washed twice with PBS (Gibco), and incubated for 20 minutes with 1% TritonX solution (Sigma-Aldrich). In order to prevent nonspecific bindings, cells were incubated 1 hour at RT with PBS containing 10% FCS. After that, cells were incubated for 1 hour with VL4-rat anti-LCMV mouse antibody and 1 hour with anti-rat IgG HRP secondary antibody (Jackson ImmunoResearch). To visualize the plaques, DAB Peroxidase Substrate kit (Vector Laboratories) was used.

6. Total RNA extraction, cDNA synthesis and quantitative real-time PCR

Total RNA was extracted from whole spleens (15-20 mg) with Qiagen RNeasy Mini Kit and from sorted cells (5-50x10^5 cells per sample) with Qiagen RNeasy Micro Kit. Quality and concentration of RNA were determined by an Agilent Bioanalyzer. Good quality RNA (50 ng) from whole spleens was reverse-transcribed to cDNA using SuperScript III Reverse Transcriptase (ThermoFisher). Quantitative real-time PCR was performed on these cDNA samples in a total volume of 10 µL that includes 20 ng of cDNA, forward and reverse primers at a concentration of 0.3 µM, and 5 µL of SYBR select master mix (ThermoFisher). Each reaction was performed in triplicate in a 384 well plate (Sigma-Aldrich) using a Quantstudio 12K flex (ThermoFisher) applying the following parameters: 2 min 50°C, 95°C 10 min, 40 cycles of 15 sec at 95°C and 60 sec at 60°C.

Good quality RNA from sorted cells, having RNA Integrity number (RIN) greater than 8, was directly used to perform quantitative real-time PCR using a one-step Quantitect SYBR green kit (Qiagen). The reaction was performed in a total volume of 10 µL that includes 0.1-1 ng of cDNA, forward and reverse primers at a concentration of 0.4 µM, 0.1 µL of Quantitect mix RT, and 5 µL of 2X Quantitect SYBR mix. Each reaction was performed in triplicate in a Lightcycler 384 well plate (Roche) using a Lightcycler 480 II (Roche) applying the following programs: retrotranscription 30 min 50°C; HotStarTaq DNA Polymerase activation 15 min 95°C; 40 cycles of: denaturation 15 sec 94°C, annealing 30 sec 54°C, extension 30 sec 50°C; cooling 10 min 30°C. Primers for all genes were designed using the program Primer Express 3.0 (Applied Biosystems). Primer selection parameters were as follows: primer size between 10 and 40 nucleotides; primer melting temperature from 55°C to 60°C; GC content between 50% and 60%; self and 3' complementarity lower than 4, and product size between 150 and 250 nucleotides. Gene expression was normalized to that of *Gapdh* and compared for the study groups. Primers were ordered from Biomers. Sequences for the primers used are listed in Table M1.

Table M1. Primers sequence

Gene	Strand	Sequence
Ifnb1	Forward	5'-TGTCCTCAACTGCTCTCCAC-3'
	Reverse	5'-CCACCACTCATTCTGAGGCA-3'
Mx1	Forward	5'-AGGATGGCACCTCTCAGGAT-3'
	Reverse	5'-CTGATGGGTGGTGGGCTAAA-3'
Usp18	Forward	5'-GAGATGTTTCGTCCAGCCCA-3'
	Reverse	5'-GGTTGGCAGAACCTGACTGA-3'

7. Splenocyte isolation

Spleen samples from mice were collected in complete RPMI media. When analyzing cytokine production, the media was additionally supplemented with brefeldin A (10 µg/ml), a protein transport inhibitor. After collection on ice, spleens were processed into a single-cell suspension and filtered through a 40 µm nylon cell strainer (Falcon) to remove clumps of cells. Splenocytes were then resuspended in ammonium chloride for 5 minutes at room temperature (RT) to lyse red blood cells, washed twice, and resuspended either in complete RPMI for stimulation or cell sorting, or in FACS buffer for flow cytometry staining.

8. Cell staining and flow cytometry

8.1 Splenocyte stimulation

For intracellular detection of IFNɣ, splenocytes were plated at 1,5-2x10^6 cells/well in 96 wells round-bottom plates (Sigma-Aldrich) and incubated with gp33 (1 µg/ml) LCMV peptides for two hours at 37°C. Next, 10 µL of brefeldin A (10 µg/ml) was added to each well and cells were further incubated for three hours. After these incubations, cells were ready to proceed with surface and intracellular staining, as described in the following section.

8.2 Cell staining

Splenocytes were plated at 1,5-2x10^6 cells/well in 96 wells round-bottom plates (Sigma-Aldrich), washed with PBS and stained with a viability stain for 20 minutes at 4ºC in order to exclude dead cells from the analysis. Depending on the panel we used

three different viability stains: Live/Dead fixable violet dye (Vivid) (Invitrogen) or Fixable viability stain 620 (BD biosciences) or Fixable viability stain 780 (BD biosciences). After washing splenocytes twice with FACS buffer, cells were pelleted and incubated for 20 minutes on ice in a total volume of 50 µL with Fc block (BD Biosciences) to block non-antigen-specific binding of immunoglobulins to Fc receptors. After blocking, cells were washed twice with FACS buffer and stained with 50 µL of fluorochrome-labelled monoclonal antibodies against: CCR2, CD4, CD8a, CD45R, CD11c, CD11b, CD169, CXCR5, CX3CR1, MHCII, NK1.1, Ly6G, Ly6C, PD1, SiglecF, SIGNR-1 and Tim3. After surface antibody staining, cells were washed twice with FACS buffer and fixed with FACS fix. To perform intracellular staining, cells were fixed using 2% formaldehyde diluted in cold PBS for 20 min and then permeabilized for 20 minutes with 100 µL of Perm wash buffer. Once permeabilized, cells were washed twice with Perm wash buffer, pelleted and then incubated for 20 minutes on ice with 50 µL of fluorochrome-labelled monoclonal antibodies mix against IFNɣ, IL-1b or Bcl6. Last, cells were washed with Perm wash and resuspended in FACS fix.

Stained cells were acquired in a flow cytometer within two hours after staining. During all the steps and until acquisition, cells were kept away from light at 4°C. Flow cytometry data were collected on a Spectral Analyzer SP6800 (SONY) or an Aurora Spectral Analyzer (Cytek) and analyzed with FlowJo software (Tree Star). Fluorescence minus one (FMOs) were done for CD169, SIGNR-1, CXCR5, PD1, Tim3 and Bcl6 to set the gates. The data were analyzed using FlowJo 10.1 software. Flow cytometry panels are listed in Table M2.

Table M2. Flow cytometry panels. (BD: BD Biosciences; dil: dilution; Cat. Nº: catalog number)

Il1b in Macrophages

Antigen	Fluorochrome	Company	Cat. Nº	Clone	Volume
Live/Dead	FVS780	BD	565388	-	dil 1:1000
CD45R	PECF594	BD	562313	RA3-6B2	0,15µL
NK1.1	PECF594	BD	562864	PK136	0,3µL
Ly6G	PECF594	BD	562700	1A8	0,625µL
Cd11c	PerCP-Cy5.5	BD	560584	HL3	5µL
Cd11b	PE/Cy5	Thermofisher	15-0112-82	M1/70	0,0625µL
SiglecF	BV421	BD	565934	E50-2440 (RUO)	0,3125µL
Il1b	PE	Thermofisher	12-7114-82	NJTEN3	0,075µL

Macrophages immunophenotyping

Antigen	Fluorochrome	Company	Cat. Nº	Clone	Volume
Live/Dead	FVS780	BD	565388	-	dil 1:1000
CD45R	PECF594	BD	562313	RA3-6B2	0,15µL
NK1.1	PECF594	BD	562864	PK136	0,3µL
Ly6G	PECF594	BD	562700	1A8	0,625µL
Cd11c	PerCP-Cy5.5	BD	560584	HL3	5µL
Cd11b	PE	BD	553311	M1/70	0,625µL
SiglecF	BV421	BD	565934	E50-2440 (RUO)	0,3125µL
Ly6C	PE/Cy7	Biolegend	128018	HK1.4	0,15µL
CCR2	BV605	BD	747969	475301	0,5µL
CX3CR1	APC	Biolegend	149007	SA011F11	0,3µL
Il1b	FITC	Thermo Fisher	11-7114-80	NJTEN3	0,25µL

Marginal zone macrophages

Antigen	Fluorochrome	Company	Cat. Nº	Clone	Volume
Live/Dead	FVS780	BD	565388	-	dil 1:1000
CD45R	PECF594	BD	562313	RA3-6B2	0,15µL
NK1.1	PECF594	BD	562864	PK136	0,3µL
Ly6G	PECF594	BD	562700	1A8	0,625µL
Cd11c	PerCP-Cy5.5	BD	560584	HL3	5µL
Cd11b	PE/Cy5	Thermo Fisher	15-0112-82	M1/70	0,0625µL
SiglecF	BV421	BD	565934	E50-2440 (RUO)	0,3125µL
SIGNR-1	PE	R&D systems	FAB1836P	-	10µL
CD169	AF647	Biolegend	142407	3D6.112	1µL

LCMV-specific CD8 T cells

Antigen	Fluorochrome	Company	Cat. Nº	Clone	Volume
Live/Dead	Vivid	Invitrogen	L34955	-	dil 1:5000
CD4	PerCP/Cy5.5	BD	550954	RM4-5	0,15µL
CD8a	PE/Cy7	BD	552877	53-67	0,3µL
IFNɣ	FITC	BD	554411	XMG1.2	0,03µL

Follicular helper T cells

Antigen	Fluorochrome	Company	Cat. Nº	Clone	Volume
Live/Dead	FVS620	BD	564996	-	dil 1:1000
CD45R	PECF594	BD	562313	RA3-6B2	0,15µL
NK1.1	PECF594	BD	562864	PK136	0,3µL
CD4	PE	BD	553048	RM4-5	0,01µL
CXCR5	APC	Thermo Fisher	17-7185-82	SPRCL5	0,625µL
PD1	FITC	Thermo Fisher	11-9985-81	J43	1,25µL
BCL6	PE/Cy7	BD	563582	K112-91	2,5µL

Macrophage/neutrophil sorting

Antigen	Fluorochrome	Company	Cat. Nº	Clone	Volume
Live/Dead	FVS620	BD	564996	-	dil 1:1000
CD45R	PECF594	BD	562313	RA3-6B2	0,15µL
NK1.1	PECF594	BD	562864	PK136	0,3µL
Cd11c	PerCP-Cy5.5	BD	560584	HL3	5µL
Cd11b	PE/Cy7	BD	552850	M1/71	1,25µL
Ly-6G	PE	BD	551461	1A8	0,625µL
Ly-6C	FITC	BD	561085	AL-21	0,625µL

CD169+ biotin-labelled macrophage sorting

Antigen	Fluorochrome	Company	Cat. Nº	Clone	Volume
Biotinilated CD169	Streptavidin-PE	Thermo Fisher	12-4317-87	-	1µL
CD11b	PE/Cy7	BD	552850	M1/71	1,25µL

pDC/cDC sorting

Antigen	Fluorochrome	Company	Cat. Nº	Clone	Volume
Live/Dead	DAPI		564996	-	dil 1:10000
CD19	Pacific Blue	Biolegend	115526	6D5	0,125µL
CD3	Pacific Blue	Biolegend	100213	17A2	0,5µL
NK1.1	Pacific Blue	Biolegend	108721	PK136	0,5µL
CD45R	PECF594	BD	562313	RA3-6B2	0,15µL
Cd11c	PerCP-Cy5.5	BD	560584	HL3	5µL
MHCII	AF647	BD	562367	M5/114	0,625µL
SiglecH	PE	Thermo Fisher	12-0333-82	eBio440c	0,625µL

8.3 Cell sorting

8.3.1 Fluorescence-activated cell sorting

For sorting of monocytes/macrophages and cDCs, cells were seeded in polypropylene round bottom test tubes (Falcon) at $50x10^6$ cells/tube, rinsed with FACS buffer and incubated for 20 minutes on ice in a total volume of 100 µL with Fc block (BD Biosciences) to block non-antigen-specific binding of immunoglobulins to Fc receptors. Cells were then washed twice with FACS buffer and stained with 100 µL of fluorochrome-labelled monoclonal antibodies against: CD45R, CD11c, CD11b, NK1.1, Ly6G, Ly6C and SiglecF for monocyes/macrophages and with CD45R, CD11c, MHCII, SiglecH for cDCs. After surface antibody staining, cells were washed twice with FACS buffer and resuspend with complete RPMI. Flow cytometry panels are listed in Table M2. Stained monocytes/macrophages and cDCs were sorted in a FACSAria II Sorter

(BD Biosciences) right after staining. Sorted cells were collected in RLT buffer (Qiagen) and kept on ice during and after sorting. Sort purity was > 95% for all populations.

8.3.2 Magnetic-activated cell sorting (MACS)

To sort CD169+ macrophages from spleens, mice were injected with a biotin-anti-CD169 antibody (36 µg; Abcam) and 10 minutes later spleens were digested using Liberase-DNAse mix (0,16 mg/ml; 0,2 mg/ml). CD169+ cells were stained with anti-biotin microbeads (Miltenyi) for 30 min and purified by magnetic-activated cell sorting using LS columns (Miltenyi). CD169+ cells were additionally sorted by flow cytometry after staining with streptavidin-phycoerythrin (Thermo Fisher) and Cd11b. Sorted cells were collected in RLT buffer (Qiagen) and kept on ice. Sorting purity was > 95% for all populations.

9. Immunohistochemistry

Spleen samples for immunohistochemistry were embedded in paraffin after an overnight fixation with 4% buffered formaldehyde. For semi quantification of fibrosis, 3 µm thick spleen sections were stained with Masson's Trichrome staining, which stains collagen fibers in blue. A set of values was defined from 0 to 10: a score of 0 represents normality (a certain amount of blue stained collagen is to be observed in the splenic capsule and trabeculae); a score of 10 would correspond to a spleen in which the parenchyma has totally been replaced by connective tissue.

10. Immunofluorescence

Freshly removed spleens were fixed for 24h using Cytofix buffer (BD), washed twice in PBS and dehydrated for 12h in 30% sucrose at 4°C. Next, samples were OCT-embedded (Tissue-TEK) in cryomolds and stored at -80°C for at least two months before proceeding with sectioning. Serial tissue sections of 10 µm in thickness were obtained using Leica Cryostat and mounted on Superfrost Plus slides (Fisher Scientific) and frozen at -20ºC. Spleen sections were rehydrated in 0.1M Tris buffer and blocked for 2h in standard blocking buffer. After washing with 0.1M Tris buffer, the sections were incubated overnight at 4°C with primary and/or conjugated antibodies. Splenic

marginal zone macrophage populations, CD169+ and MARCO+ macrophages, were visualized respectively by staining with CD169 AF647 (MOMA-1; clone 3D6.112; Biolegend) and MARCO (rat anti-mouse; clone ED31; Bio Rad). B cells and T cells were identified using antibodies against B220 (rat anti-mouse clone RA3-6B2; Biolegend) and CD3 (hamster anti-mouse clone 145-2C11; Biolegend). For unconjugated primary antibodies, species-specific secondary antibody coupled to Alexa Fluor 488 (goat anti-hamster; Biolegend), or Alexa Fluor 555 (goat anti-rat; Thermofisher) fluorochromes were incubated for 8 h at 4°C. Sections were washed, DAPI-stained (4',6'-diamino-2-phenylindoledihydrochloride; Sigma) to visualize nuclei and finally mounted using Vectashield mounting media (Vector laboratories). Images were captured using a Leica SP5 Upright Confocal microscope and analyzed using ImageJ software.

11. Bioinformatic analysis

11.1 RNA-seq library preparation and sequencing

Total RNA from samples was isolated and submitted for sequencing to the Genomics Unit of the Centre for Genomic Regulation (CGR, PRBB). Sequencing libraries were obtained after removing ribosomal RNA by a Ribo-Zero kit (Illumina). cDNA was synthesized and tagged by addition of barcoded Truseq adapters. Libraries were quantified using the KAPA Library Quantification Kit (KapaBiosystems) prior to amplification with Illumina's cBot. Four libraries were pooled and sequenced (single strand, 50 nts) on an Illumina HiSeq2000 sequencer to obtain 50-60 million reads per sample.

11.2 RNA-seq bioinformatic analysis

This bioinformatic analysis was carried out by Anna Esteve-Codina and kindly provided. It was performed as follows: Reads mapping against the Mus musculus reference genome (GRCm38) was done using the GEMtools RNA-seq pipeline (http://gemtools.github.io/docs/rna_pipeline.html), and were quantified with Flux Capacitor (http://sammeth.net/confluence/display/FLUX/Home) with the Mus musculus gencode annotation M2 version (https://www.gencodegenes.org/). Normalization was performed with the edgeR TMM method (*Robinson & Oshlack, 2010, Genome*

Biology). Pairwise Pearson's correlation coefficients (PCC) were calculated for comparison among transcriptomes of spleens from uninfected (n=2, day 0), acute (n=2 per time point) or chronic (n=2 per time point) infected mice. Hierarchical clustering across all samples was based on pairwise Pearson's correlation coefficients among RNA-seq libraries. Differential expression analysis was performed with the 'robust' version of the edgeR R package (*Zhou et al., 2014, Nucleic Acid Research*). Genes with a false discovery rate (FDR)<5% were considered significant. Differentially expressed genes in acute and chronic time series (n=13971) were used to construct a coexpression network with the WGCNA R package for each dataset (*Langfelder & Horvath, 2008, BMC Bioinformatics*). First, a signed weighted adjacency matrix was calculated with the 'blockwiseModules' function using these parameters: power=30, TOMtype="signed", minModuleSize=15, mergeCutHeight=0.25, reassignThreshold=0, networkType="signed", numericLabels=TRUE, pamRespectsDendro=FALSE, nThreads=7, maxBlockSize=17000. The power law of 30 was selected to meet the scale-free topology assumption with the pickSoftThreshold function. Then, genes were clustered into network modules using average linkage hierarchical clustering and the topological overlap measure (TOM) as proximity. Each of the identified modules was summarized by its module eigengene (the first principal component), which represents the weighted average expression profile of all module genes (*Langfelder & Horvath, 2008, BMC Bioinformatics*). To identify intramodular hub genes inside a given module, the intramodular connectivity was calculated for each gene (Kin) and ViSANT (http://visant.bu.edu/) was employed for network visualizations (TOM>0.3). Module preservation and module overlapping were calculated with functions 'modulePreservation' and 'userListEnrichment', respectively. Viral loads, CD4 and CD8 levels were correlated with the module eigengenes with Pearson correlation. Gene ontology (GO) enrichment analysis was performed with DAVID (http://david.ncifcrf.gov/)(*Huang et al., 2009, Nat Protoc*).

12. Statistical analysis

Two-tailed t-test and ANOVA analyses were performed using GraphPad Prism 6.0 (San Diego, CA, USA). p-values (p) below 0.05 were considered significant and were indicated by asterisks as follows: *$p \leq 0.05$; **$p \leq 0.01$; ***$p \leq 0.001$; ****$p \leq 0.0001$. Non-significant differences were indicated as "ns".

RESULTS

1. Differential kinetics of type I IFN genes during acute and chronic LCMV infections

The temporal events underlying early type I IFN (IFN-I) responses during acute and chronic infections are poorly understood. Although several of the individual components that contribute to these responses have been described, a systemic global view is still lacking. To gain insight into the differential IFN-I dynamics during acute and chronic infections, we characterized the early transcriptome changes in spleens from mice infected with $LCMV_{DOC}$. We constructed a RNAseq-based data set built upon our previous work where we characterized time-resolved splenic transcriptomes during acute and chronic LCMV infections by gene coexpression network analysis *(Argilaguet et al., 2019, Genome Res)* (see Material and Methods). C57BL/6 mice were infected with a low-dose (2×10^2 plaque-forming units; acute infection) or a high-dose (2×10^6 plaque-forming units; chronic infection) of $LCMV_{DOC}$. Spleen-derived total messenger RNA (mRNA) transcriptomes were determined longitudinally by RNAseq every 24 hours from day 0 to 7, and at days 9 and 31 post-infection (p.i.). Taking non-infected mice as a reference point, we identified 15919 differentially expressed genes in both acute and chronic infections, among which 2825 are interferon-regulated genes (IRGs)(Figure 1A). During chronic infection, the number of total and interferon-regulated differentially expressed genes remain constant over time, reaching the maximum levels already at d1 p.i.. In contrast, transcriptomic changes in acute LCMV infected mice showed a biphasic dynamic characterized by an initial peak at d2 p.i., followed by a gradual increase reaching the same level as in chronic infections by d7 p.i. (Figure 1A). To further characterize the behaviour of IRGs in acute and chronic infections, we analyzed their coexpression patterns in a gene correlation matrix (Figure 1B). While during acute infection IRGs showed very well defined clusters of coexpressed genes, during chronic infection they displayed a more heterogeneous pattern indicating a differential regulation of the IFN-I response.

To better understand the differences observed, we used the 15919 differentially expressed genes as input to construct two signed coexpression networks via the weighted gene coexpression network analysis software (WGCNA) (*Zhang & Horvath, 2005, Stat Appl Genet Mol Biol*). This methodology allows to cluster genes with similar patterns of expression based on the topological overlap measure, subsequently defining modules of highly coexpressed genes (Figure S1A) (*Argilaguet et al., 2019, Genome Research*).

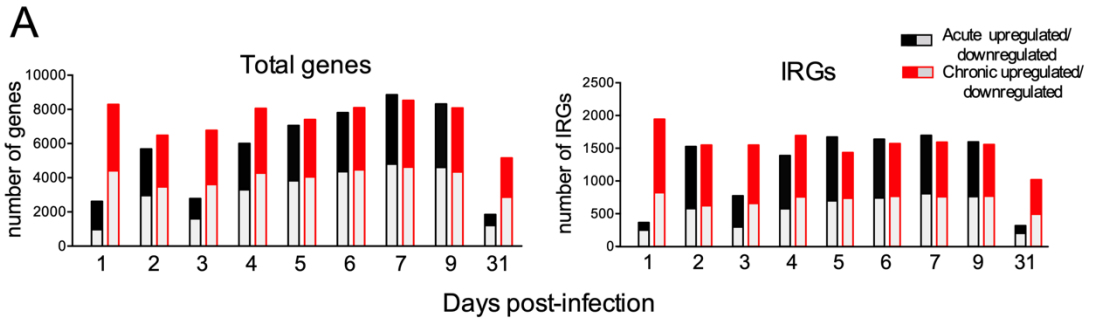
A
Total genes
IRGs
Acute upregulated/ downregulated
Chronic upregulated/ downregulated
number of genes
number of IRGs
Days post-infection

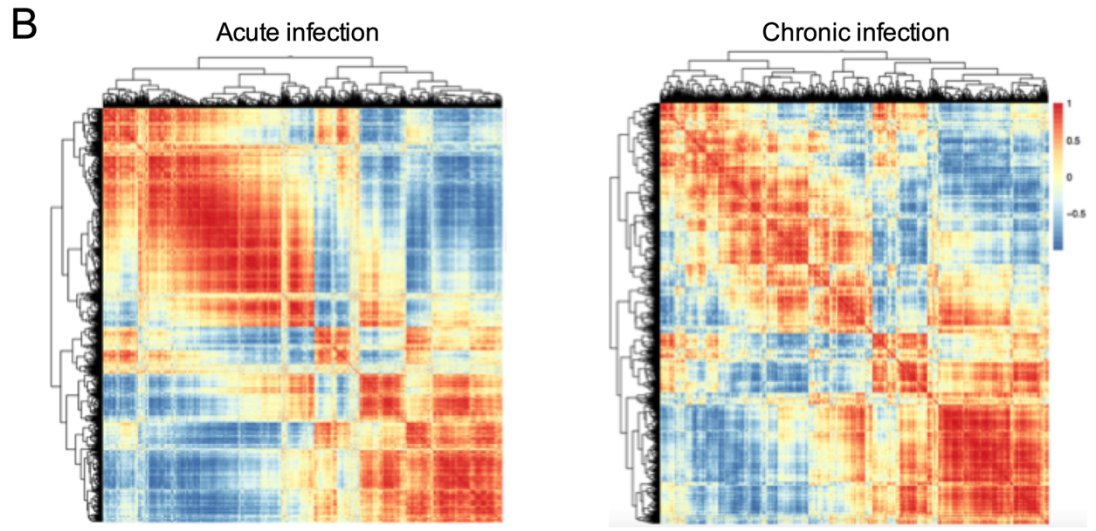
B
Acute infection
Chronic infection

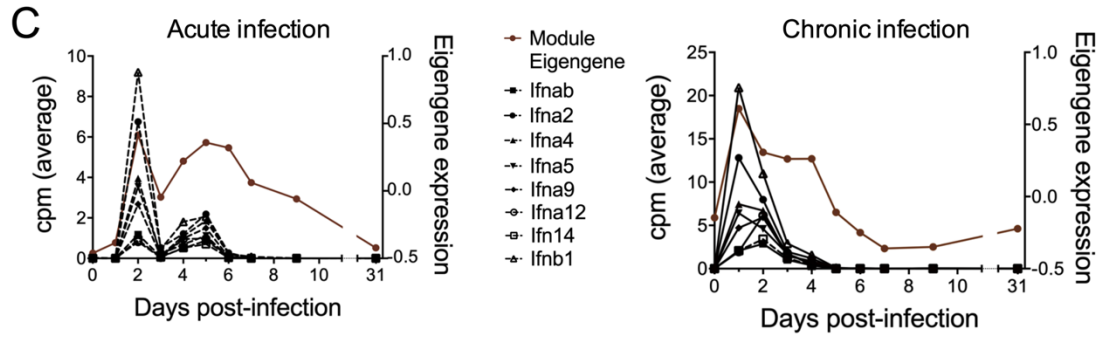
C
Acute infection
Chronic infection
Module Eigengene
Ifnab
Ifna2
Ifna4
Ifna5
Ifna9
Ifna12
Ifn14
Ifnb1
cpm (average)
Eigengene expression
Days post-infection

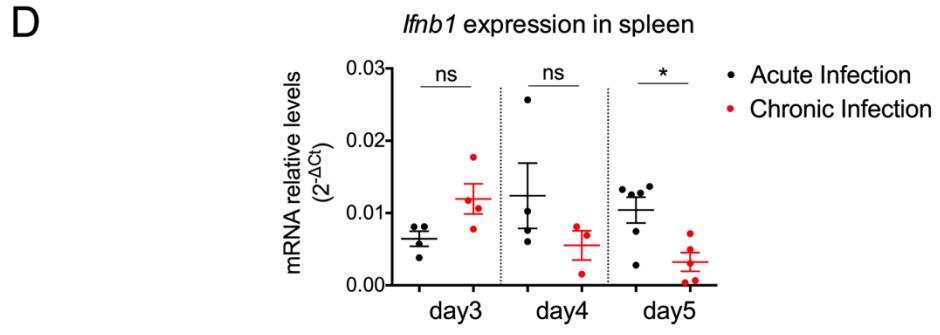
D
Ifnb1 expression in spleen
mRNA relative levels (2-ΔCt)
ns
ns
*
Acute Infection
Chronic Infection
day3
day4
day5

Figure 1. Differential type I IFN response in acute and chronic LCMV infection. (A) Number of upregulated and downregulated total differentially expressed genes and IRGs in spleens at the indicated time points during acute and chronic LCMV infections. The transcriptome of naive mice is used as reference. (B) Pearson's pairwise correlation matrix showing IRGs expression patterns in acute and chronic infections. The color scale indicates the degree of correlation. (C) Eigengene expression profiles from acute-brown and chronic-brown modules are represented together with expression kinetics of IFN-I genes contained in the same modules. (D) qPCR of *Ifnb1* from spleens of acute- and chronic-infected mice at the indicated time points. The relative gene expression level was normalized to Gapdh. For each group and time point the mean ± SEM of n=3 to 6 mice is shown. * $p \leq 0.05$; (unpaired two-tailed t test).

We identified 20 and 21 modules from acute and chronic infections, respectively (Figure S1B). Gene Ontology (GO) analysis allowed the identification of 2 modules (acute-brown and chronic-brown) in which the term "cellular response to interferon-beta" was enriched (Figure S2). Indeed, these two modules contained *Ifnb1* and seven *Ifna* genes (Figure 1C) together with several IRGs (Figure S3) (Table S1). Importantly, analysis of the module eigengenes and of individual IFN-I genes showed a different expression kinetics in acute and chronic infections. Acutely infected mice showed two IFN-I gene expression peaks at d2 and d5 post-infection, while chronically-infected mice had only a single peak at d1 post-infection (Figure 1C). These results were further validated with a higher number of animals by quantifying expression levels of *Ifnb1* in spleens by qPCR at days 3, 4 and 5 p.i. (Figure 1D). Altogether, these results revealed an early differential IFN-I regulation in acute and chronic LCMV infection that may contribute to the regulation of the virus infection fate.

2. CD169+ marginal zone macrophages produce the second peak of type I IFN genes during acute LCMV infection

pDCs are the main producers of IFN-I early during LCMV infection, while at later time points, IFN-I is produced by other cells subsets such as macrophages and cDCs (*Wang et al., 2012, Cell Host & Microbe; Zuniga et al., 2015, Annu Rev Virol*). Thus we next investigated if these cell subsets are responsible for the expression of the second peak of IFN-I during acute LCMV infection. Quantitative PCR (qPCR) on RNA extracted from sorted cells at day 5 p.i. showed that macrophages but not DC from acutely infected mice expressed higher levels of *Ifnb1* than uninfected controls. In chronically infected mice, the two cell subsets had basal *Ifnb1* levels (Figure 2A).

Interestingly, although the IFN-I response during chronic infection was limited to the initial peak at d1-2 p.i., (Figure 1C), *Mx1* expression levels in macrophages from d5 p.i. were higher than in acute infection (Figure 2B). Remarkably, this enhanced interferon-mediated response was accompanied by reduced levels of the IFN-I signaling inhibitor *Usp18* (Figure 2B), indicating that this negative regulatory feed-back mechanism was lacking in macrophages during chronic infection.

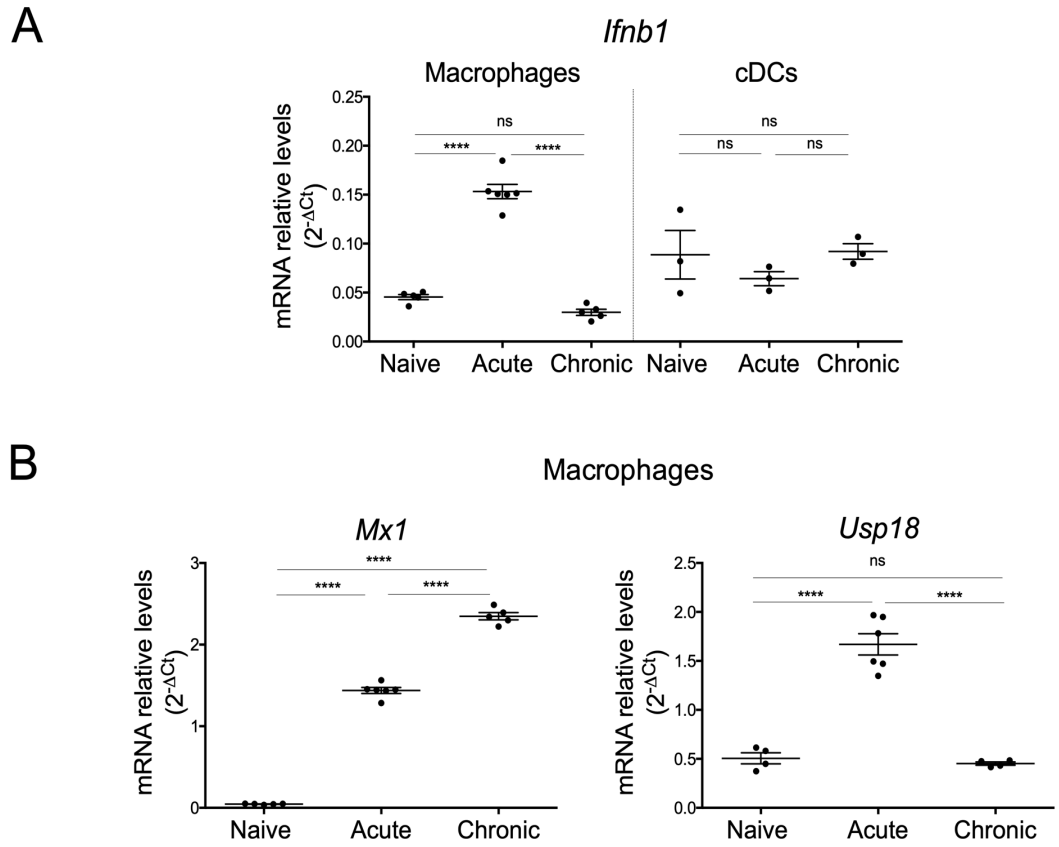

Figure 2. Analysis of *Ifnb1*, *Usp18* and *Mx1* expression at day 5 post acute and chronic LCMV infections. QPCR was performed using RNA extracted from sorted splenocytes of naive or infected mice. The relative gene expression level was normalized to Gapdh. Data shown are mean of n=3 to 6 mice; significance is determined via one-way ANOVA; * $p \leq 0.05$; ** $p \leq 0.01$; *** $p \leq 0.001$; **** $p \leq 0.0001$.

Since CD169+ macrophages from the splenic marginal zone play an important role in prolonging the IFN-I response during acute LCMV-WE infection *(Shaabani, 2016, Cell death & disease)*, we next evaluated if they are responsible for the production of the second wave of IFN-I. Indeed, CD169+ macrophages expressed higher levels of *Ifnb1*, *Mx1* and *Usp18* in acute than in chronic infected animals (Figure 3A and S4AC). Since

chronic infection is characterized by a rapid accumulation of virus loads during the first days of infection *(Argilaguet et al., 2019, Genome Res)*, we hypothesized that lack of IFN-I-producing CD169+ macrophages during chronic infection could be explained by an earlier killing of infected marginal zone cells by cytotoxic cells (Scandella et al. 2008). Indeed, RNAseq-derived expression kinetics of *Siglec1 (Cd169)* and *Marco* that characterize the two macrophage subpopulations in the marginal zone clearly showed an early downregulation during chronic infection (Figure S4A), and flow cytometry staining revealed a significant reduction in CD169+ macrophages at day 5 post-chronic infection when compared to acutely infected mice (Figure 3B). Moreover, immunofluorescence analysis of spleens from acutely and chronically infected mice showed differential disruption dynamics of the splenic architecture during LCMV infection, with an earlier loss of marginal zone in chronic infection (Figure 3C). This disruption was linked to differential virus distribution at early time points. LCMV nucleoprotein was already found in the marginal zone of chronically infected mice at day 3p.i., two days earlier than in acute infection (Figure S4C). Importantly, loss of CD169+ metallophilic marginal zone macrophages and lymphoid tissue structure were partially avoided by anti-CD8α antibody treatment at days -1 and 2 p.i. (Figure 3B and C), indicating that rapid killing of infected macrophages by antiviral CD8+ cells impedes a second wave of IFN-I production during chronic infection. All these results demonstrate that the early IFN-I response dynamics is determined by spatiotemporal changes induced in lymphoid tissue by kinetics of virus expansion and the consequent antiviral cytotoxic cell response.

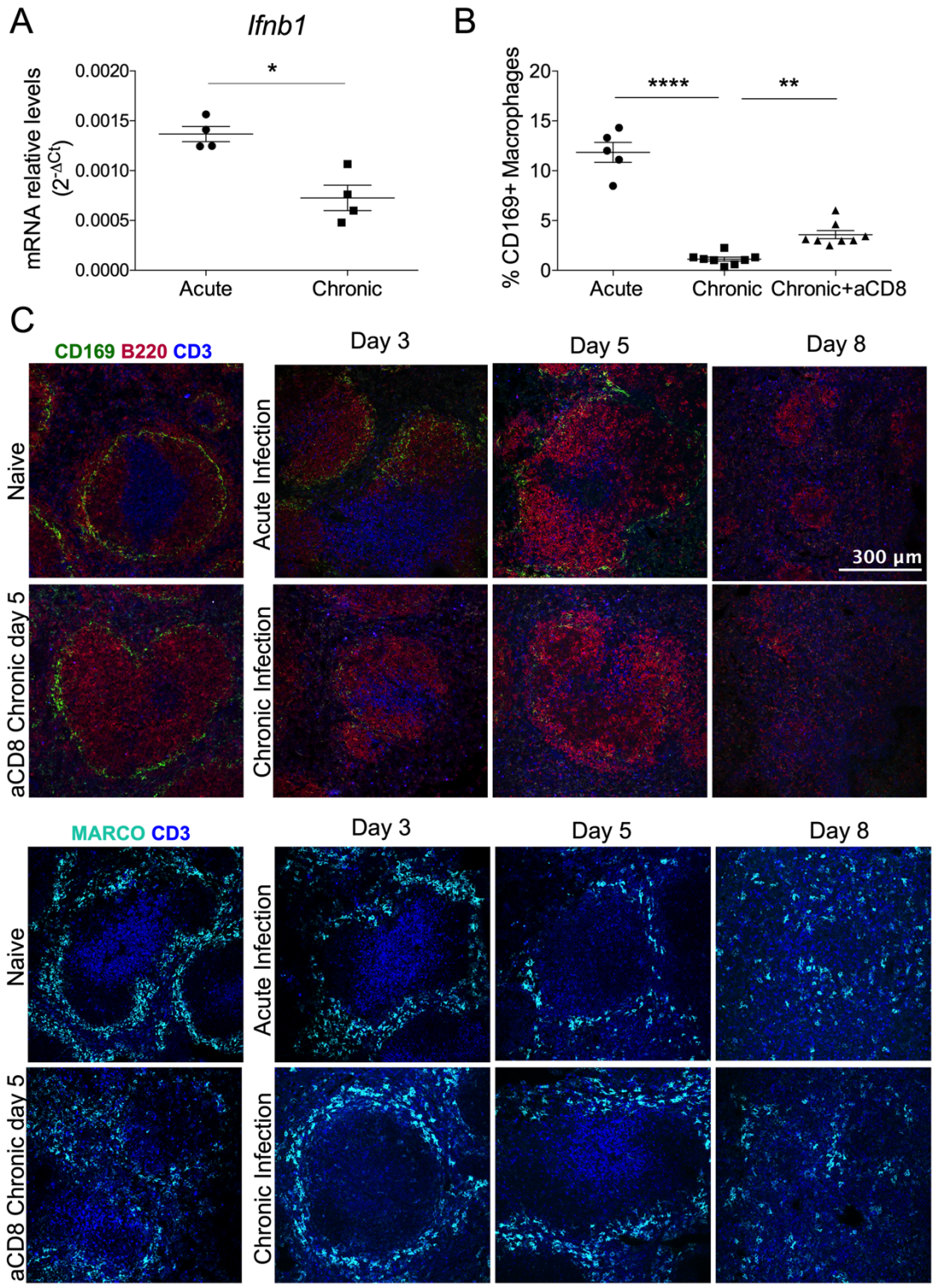

Figure 3. Temporal changes of the splenic marginal zone in acute versus chronic LCMV infection. Mice were acutely (10^2 pfu) or chronically (10^6 pfu) infected with $LCMV_{DOC}$. Chronically-infected mice were treated with 200µg of anti-CD8α or isotype control at days -1 and 2 post-infection. (A) *Ifnb1* expression was analyzed by qPCR using RNA extracted from MACS-sorted splenic CD169+ macrophages from infected mice at day 5 p.i.. To obtain CD169+ macrophages animals were injected *in vivo* with a biotin-labelled anti-CD169 antibody. After sacrifice, cells were purified from spleens by magnetic separation using anti-biotin microbeads

and stained with Streptavidin-Phycoerythrin for sorting by FACSAria. (B) CD169+ macrophages were quantified in spleens from day 5 post-infection. (C) Immunofluorescence was performed on cytofix-fixed OCT-embedded spleens from different timepoints (d3, d5 and d8) post-acute and -chronic infection and at day 5 post-chronic infection, after CD8+ cell depletion. Spleen sections were stained for CD169 (CD169+ Macrophages; green), CD3 (T cells; blue), B220 (B cells; red), MARCO (MARCO+ Macrophages; cyan). One representative section of 3 mice per group is shown. Images were taken at 20X magnification, the scale bar indicates 300 µm. Data shown are mean (± SEM) of n=5 to 8 mice (significance is determined via one-way ANOVA or unpaired two-tailed t test); * $p \leq 0.05$; ** $p \leq 0.01$; *** $p \leq 0.001$; **** $p \leq 0.0001$.

3. The second peak of type I IFN in acutely infected mice is required to induce inflammatory macrophages and virus-specific CD8 T cells

Genes coexpressed within a WGCNA-derived module often belong to functionally related biological processes *(Langfelder & Horvath, 2008, BMC Bioinformatics)*. Thus, aiming to infer the potential functional implications of the second wave of INF-I in acute infection, we next analyzed those genes that are coexpressed with IFN-I genes in the acute-brown module. Interestingly, we found several genes related to inflammation, which in contrast were not coexpressed with IFN-I genes during chronic infection (Figure 4A). We have previously shown that inflammatory monocytes/macrophages are induced at day 6 after an acute LCMV infection, while during chronic infection these cells shift to an anti-inflammatory profile before T cell exhaustion becomes evident *(Argilaguet et al., 2019, Genome Research)*. All together, we speculated that the second wave of IFN-I expression could play a role in the induction of the previously identified pro-inflammatory response. Indeed, blockage of IFN-I signaling by treating mice with anti-type I IFN receptor monoclonal antibody (anti-IFNAR) at d3 and d4 post acute infection abolished the induction of IL1β-producing macrophages at day 6 p.i. (Figure 4B). Moreover, depletion of the IFN-I-producing CD169+ macrophages in CD169-DTR transgenic mice by administration of diphtheria toxin (DT) at d3 p.i. resulted in a significant reduction of IL1β+ macrophages (Figure 4B). The hierarchical production of IFNβ and IL1β resembles the one described by Barbet et al., who demonstrated that IFNβ-dependent production of IL1β by CX3CR1hi CCR2-Ly6C- monocytes is crucial for Tfh cells differentiation during the early stages of the innate immune response *(Barbet et al., 2018, Immunity)*. However, IL1β-producing macrophages from d6 post acute LCMV infection showed a different phenotype,

characterized by high expression of Ly6C and dim expression of CX3CR1 (Figure 4C). Moreover, both LIP-CLOD-mediated depletion of all macrophages and IFNAR blockage transiently decreased Tfh cell percentages in spleen at d8-9 post-acute infection. Tfh cells were restored at d15 (Figure 4C), suggesting a minor role of these acute infection-specific events in the induction of the humoral response.

Since IFNAR signaling in CD8 T cells is critical for the generation of effector and memory cells *(Kolumam et al., 2005, JEM)*, we next investigated how IFN-I produced by marginal zone macrophages and the subsequent induction of inflammatory macrophages influence the virus-specific CD8 T cell response. Both, IFNAR blockage in C57BL6/j WT mice and CD169+ macrophage depletion in CD169DTR mice resulted in increased virus titers (Figure 4D) and a dramatic drop of functional LCMV-specific CD8 T cells (Figure 4E) at days 9 and 15 p.i.. These effects were independent of the induction of inflammatory macrophages, since mice treated with the NF-κB inhibitor peptide NBP2 only resulted in a slight decrease of LCMV-specific IFNγ-producing CD8 T cells at d8 p.i. (Figure E), which did not lead to a significant change in virus loads (Figure D). Collectively, these results demonstrate the polyfunctional role of the second wave of IFN-I produced by CD169+ macrophages, which include regulatory events influencing both innate and adaptive immune responses.

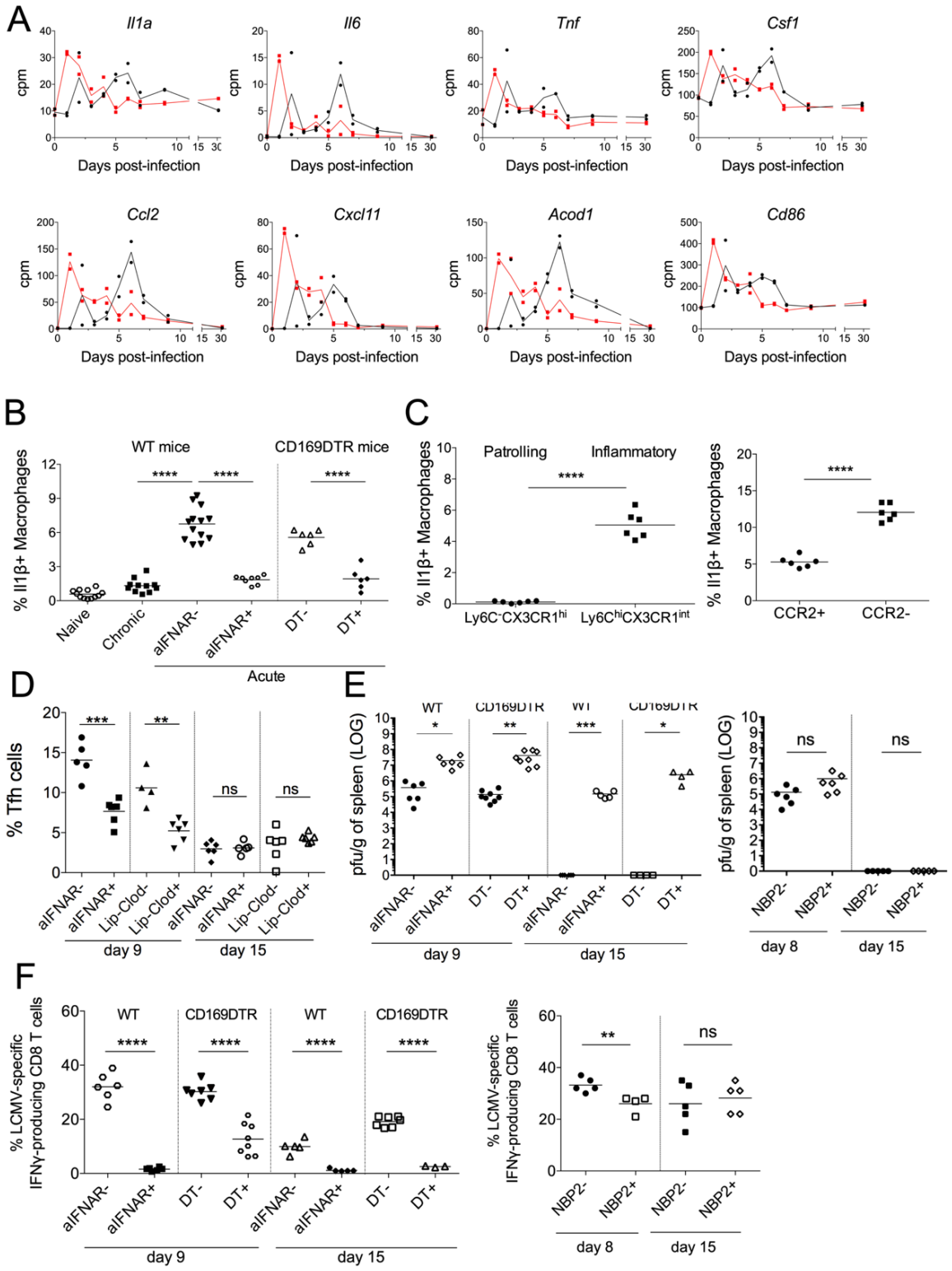

Figure 4. Characterization of type I IFN-dependent inflammatory macrophage and CD8 T cell responses. (A) RNAseq-derived normalized expression kinetics of genes related to pro-inflammatory macrophages in spleens from acute and chronic infected mice. (B) Percentage of IL1β-producing macrophages at d6 post acute or chronic infection in C57BL6/j WT mice treated (aIFNAR+) or untreated (aIFNAR-) with anti-IFNAR antibody, and in CD169DTR mice after treated (DT+) or untreated (DT-) with diphtheria toxin (DT). (C) Immunophenotyping of IL1β-

producing macrophages by flow cytometry. (D) Percentage of Tfh cells at days 9 and 15 post acute infection in C57BL6/j WT mice treated (aIFNAR+) or untreated (aIFNAR-) with anti-IFNAR antibody. (E-F) Viral loads (E) and frequency of GP33-specific IFNγ-producing CD8+ T cells (F) in C57BL6/j WT mice treated (aIFNAR+) or untreated (aIFNAR-) with anti-IFNAR antibody, and in CD169DTR mice after treated (DT+) or untreated (DT-) with diphtheria toxin (DT) at the indicated time points post acute infection. (G) Viral loads and frequency of GP33-specific IFNγ-producing CD8+ T cells in C57BL6/j WT mice treated or untreated with NBP2 peptide at the indicated time points post acute infection. For each group, the mean of n=4 to 13 mice, representative of three independent experiments, is shown. * $p \leq 0.05$; ** $p \leq 0.01$; *** $p \leq 0.001$; **** $p \leq 0.0001$; (unpaired two-tailed t test).

4. Early IFN-I kinetics determines the appearance of fibrosis in lymphatic tissue

We have previously described that acutely infected mice develop spleen fibrosis that is maintained even when the virus is already well controlled (*Argilaguet et al., 2019, Genome Res*) Since macrophage-derived inflammatory mediators have been shown to contribute to the formation of fibrosis *(Wynn et al., 2016, Immunity)*, and CTL-mediated killing of virus-infected cells is accompanied by varying extents of immunopathology *(Bocharov, 2003, JTB)*, we investigated the role of the second wave of IFN-I and the subsequent immunological events described above in the development of fibrosis during acute LCMV infection. Importantly, blockage of IFNAR signaling during the second wave of the IFN-I response totally prevented the appearance of fibrosis in spleens at d15 p.i., and similar results were obtained in mice depleted of CD8 T cells (Figure A and C). In clear contrast, mice treated with NBP2 peptide did not prevent fibrosis (Figure A), thus indicating that the generation of fibrotic tissue in spleens from acutely infected mice is a consequence of the IFN-I-dependent antiviral CD8 T cell response that is required to resolve the infection. Finally, we next wondered if immunotherapy-mediated restoration of CD8 T cell functionality in chronically infected mice would lead to an increase of fibrosis as a consequence of the increased killing of infected cells. To address this question, chronic LCMV-infected mice were treated with either 3 or 5 doses of anti-PD-L1 antibody at different time-points, and lymphoid tissue fibrosis was analyzed at days 30, 35 and 42 p.i. Anti-PDL1-treated mice displayed no signs of increased spleen pathology compared to littermate controls regardless of the regimen used (Figure 5B and 5D). Collectively, our results strongly suggest that the excessive immunopathology observed in acute LCMV-infected mice is CD8 T cell-mediated in an IFN-I-dependent manner. The reactivation of the exhausted CD8 T cell

response in chronic LCMV-infected mice seemed not strong enough to mediate the respective tissue damage.

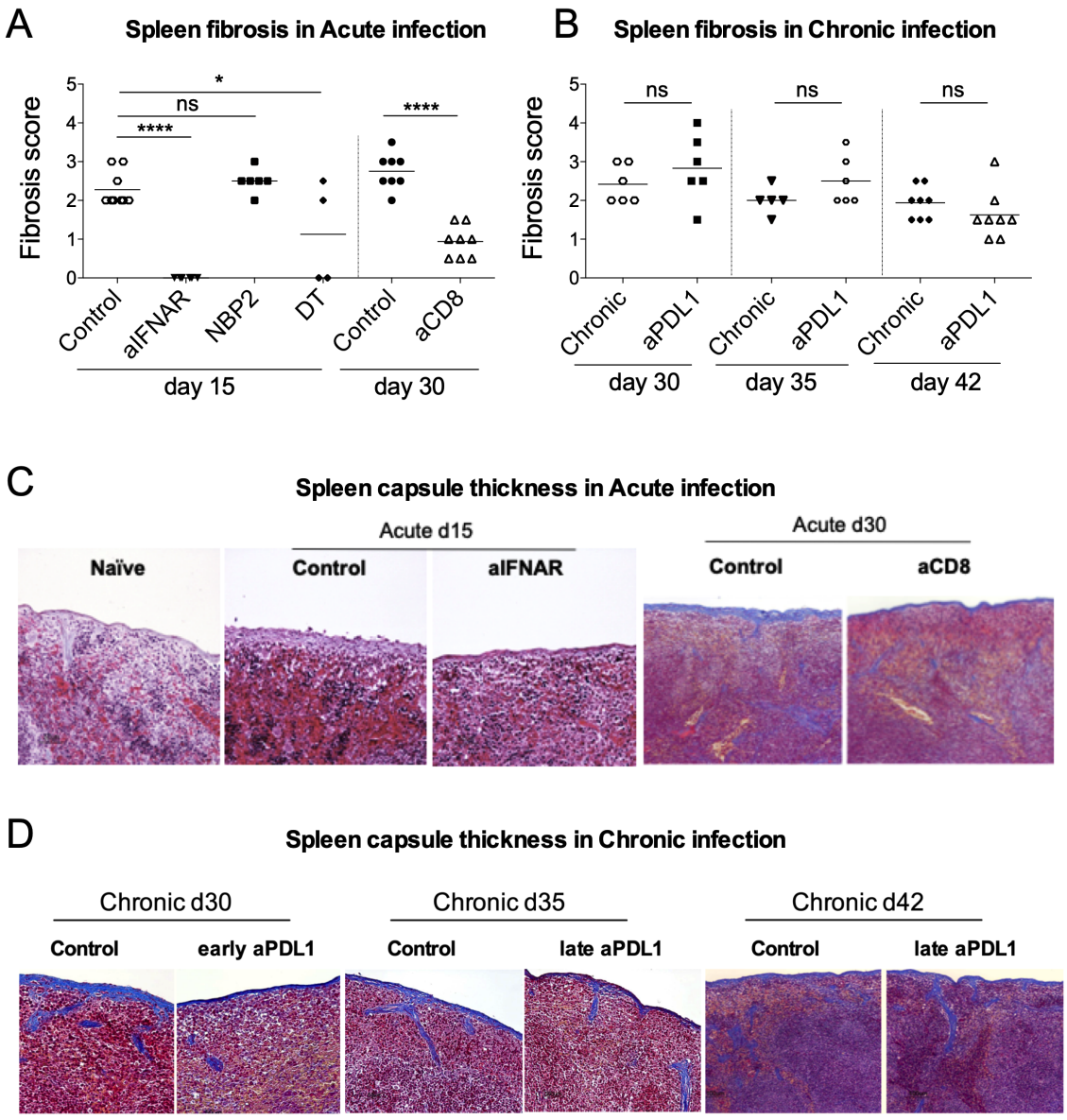

Figure 5. CTL-mediated IFN-I-dependent spleen fibrosis is not worsened by anti-PDL1 antibody treatment. (A) C57/BL6 and CD169DTR mice were acutely infected with 10^2 pfu of $LCMV_{DOC}$. Infected C57/BL6 mice were treated with 500 µg of anti-IFNAR or NBP2 or control peptide at days 3 and 4, or 200 µg of anti-CD8α antibody at days 7 and 10 post-infection. Infected CD169DTR mice were treated with 30 ng/kg of DT at day 3 post-infection. Spleen fibrosis was evaluated at days 15 and 30 post-infection. (B) Mice were chronically infected with 10^2 pfu of $LCMV_{DOC}$ and divided into three groups. They were then treated with 200 µg of anti-PDL1 at days 11, 14 and 17 (group 1), at days 22, 25 and 28 (group 2), and at days 19, 22, 25, 28 and 31 (group 3) post-infection, respectively. Spleen fibrosis was evaluated at days 30 (group 1), 35 (group 2) and 42 (group 3) post-infection. (C-D) Representative images of Masson's trichrome staining showing thickness of the splenic capsule. Data shown are the mean of n=4 to 8 mice. * $p \leq 0.05$; ** $p \leq 0.01$; *** $p \leq 0.001$ (unpaired two-tailed t test)

SUPPLEMENTAL FIGURES

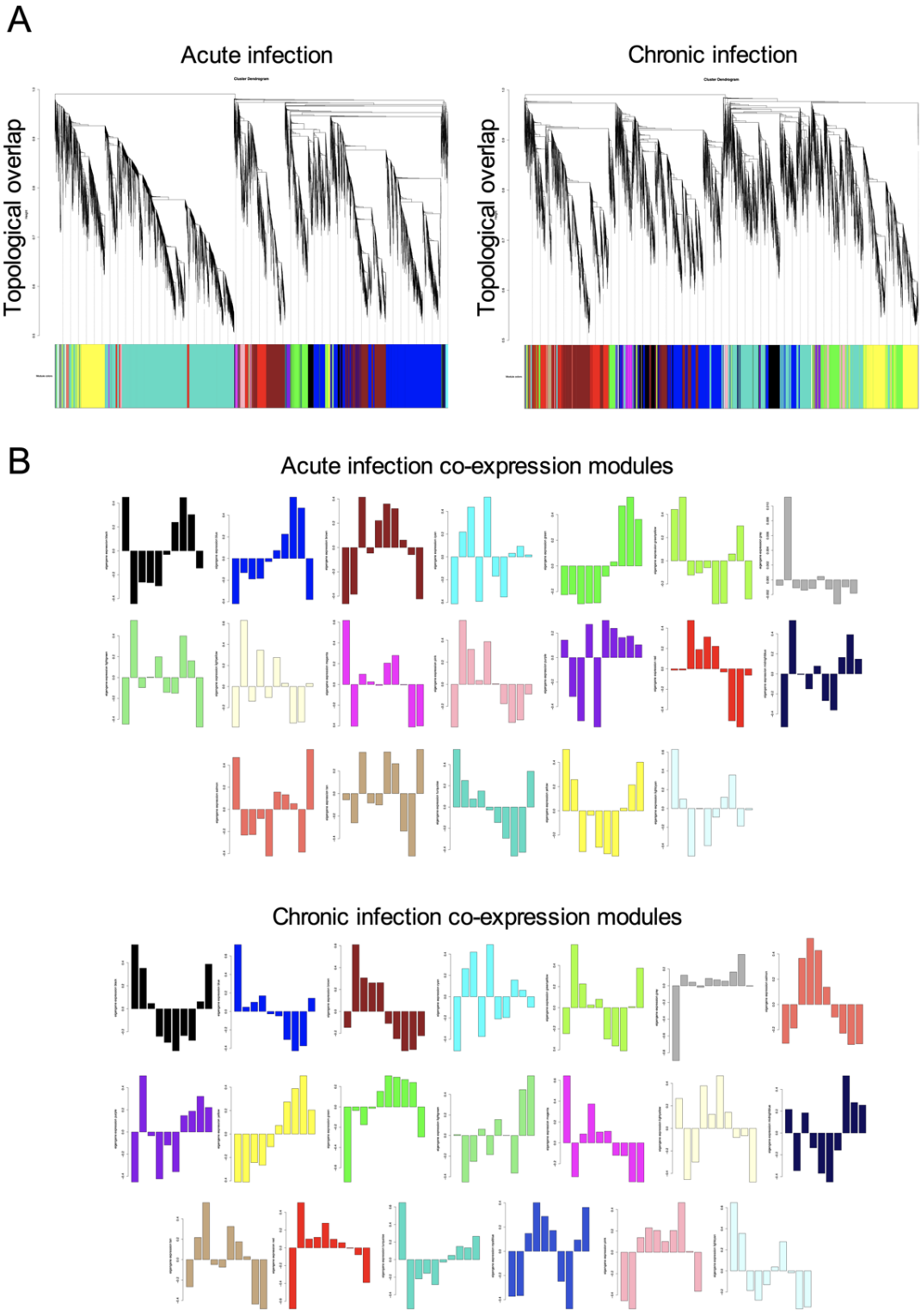

Supplemental Figure S1. WGCNA and identification of modules of co-regulated genes from acute and chronic LCMV infections. (A) Hierarchical clustering dendrogram for all differentially expressed genes (lines) obtained by WGCNA. The branches correspond to modules of highly coexpressed groups of genes. Colors below the dendrogram indicate the module to which each gene was assigned. (B) Module eigengene expression patterns obtained from acute and chronic infections. Each bar within a module represents relative expression at a defined time point.

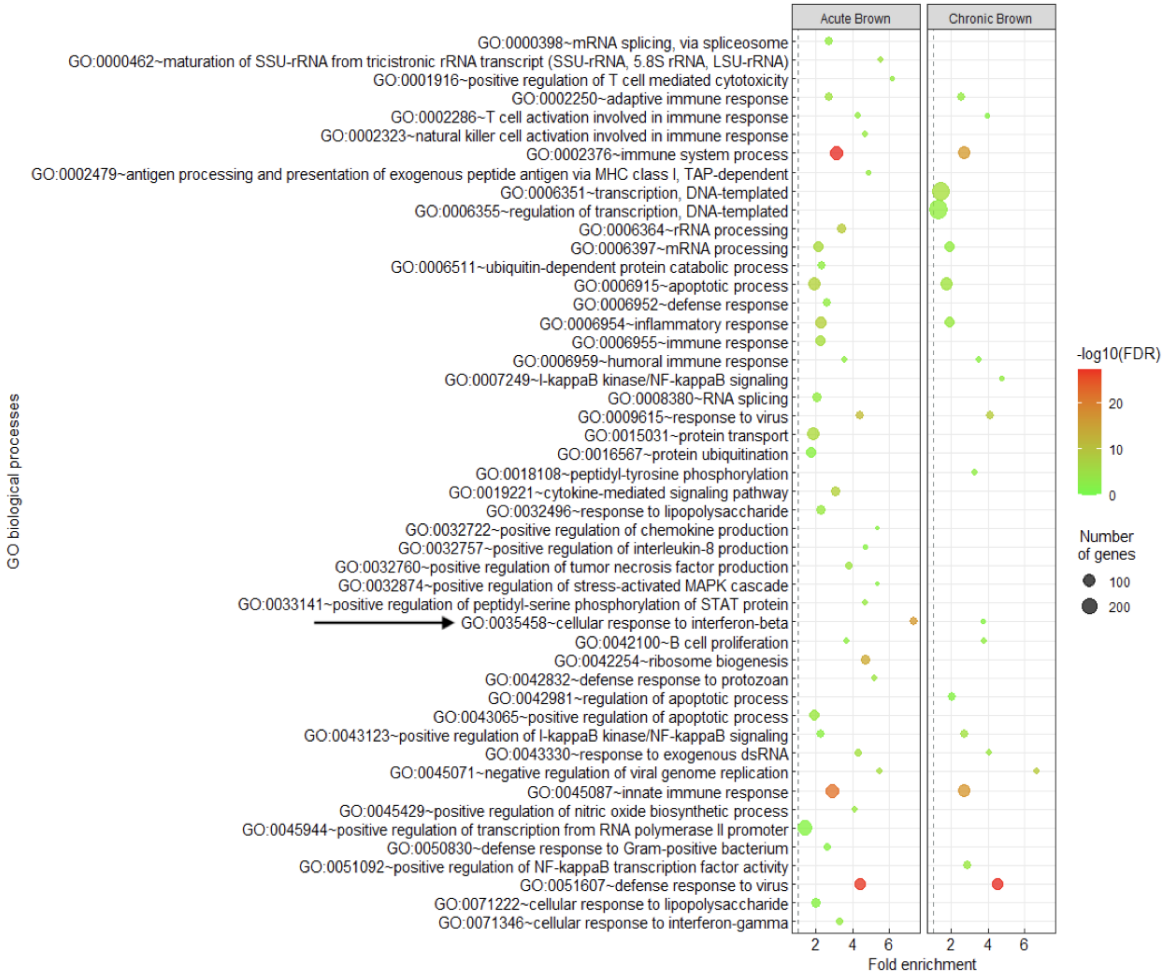

Supplemental Figure S2. Enriched GO terms (obtained from DAVID) for genes of acute-brown and chronic-brown modules. The arrow shows the GO term “cellular response to interferon-beta”.

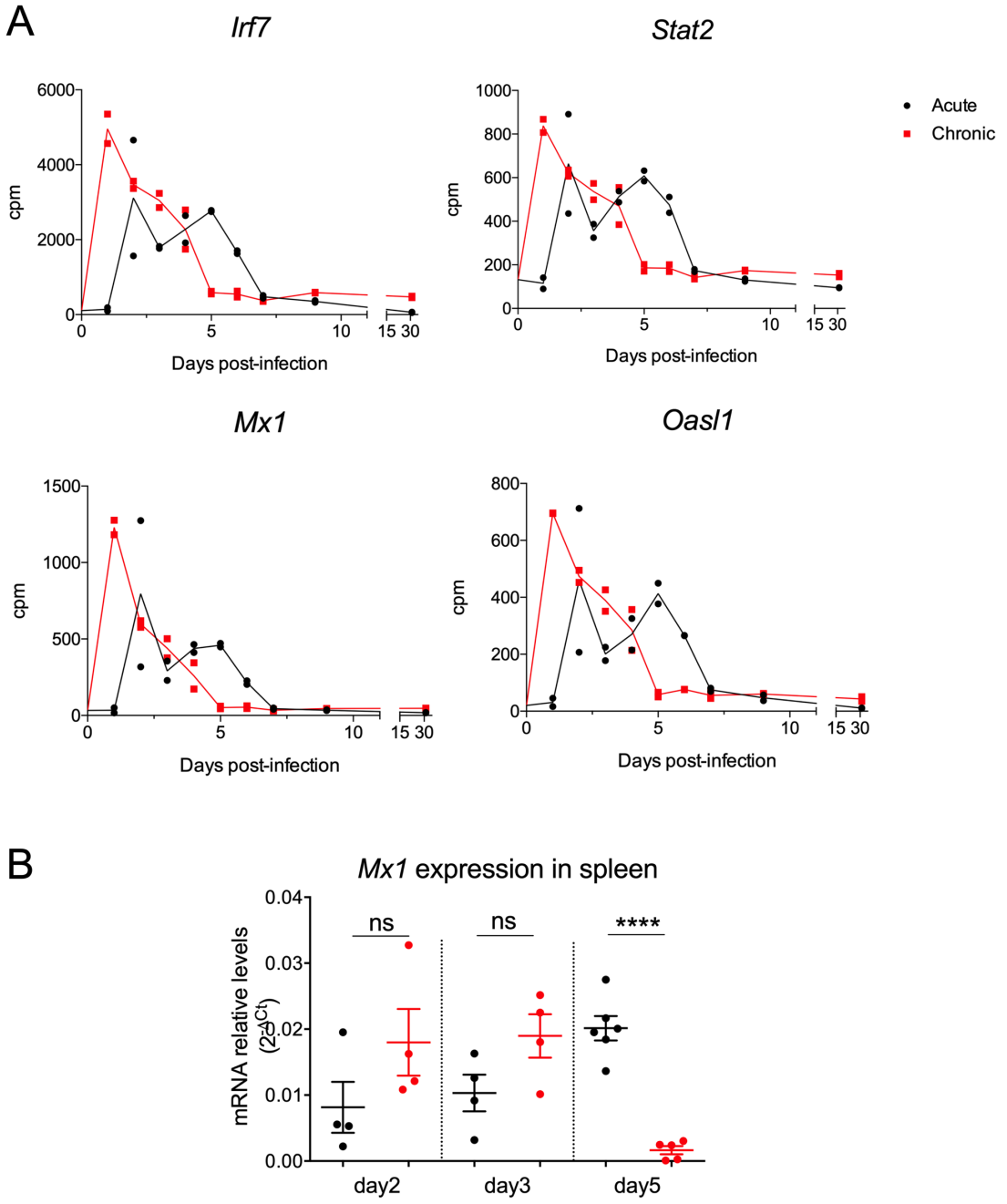

Supplemental Figure S3. (A) Expression kinetics of selected IRGs contained in brown acute and brown chronic modules. (B) qPCR of Mx1 from spleens of acute- and chronic-infected mice at the indicated time points. Relative gene expression levels were normalized to Gapdh. For each group and time point the mean ± SEM of n=4 to 6 mice is shown. * $p \leq 0.05$; ** $p \leq 0.01$; *** $p \leq 0.001$; **** $p \leq 0.0001$ (unpaired two-tailed t test).

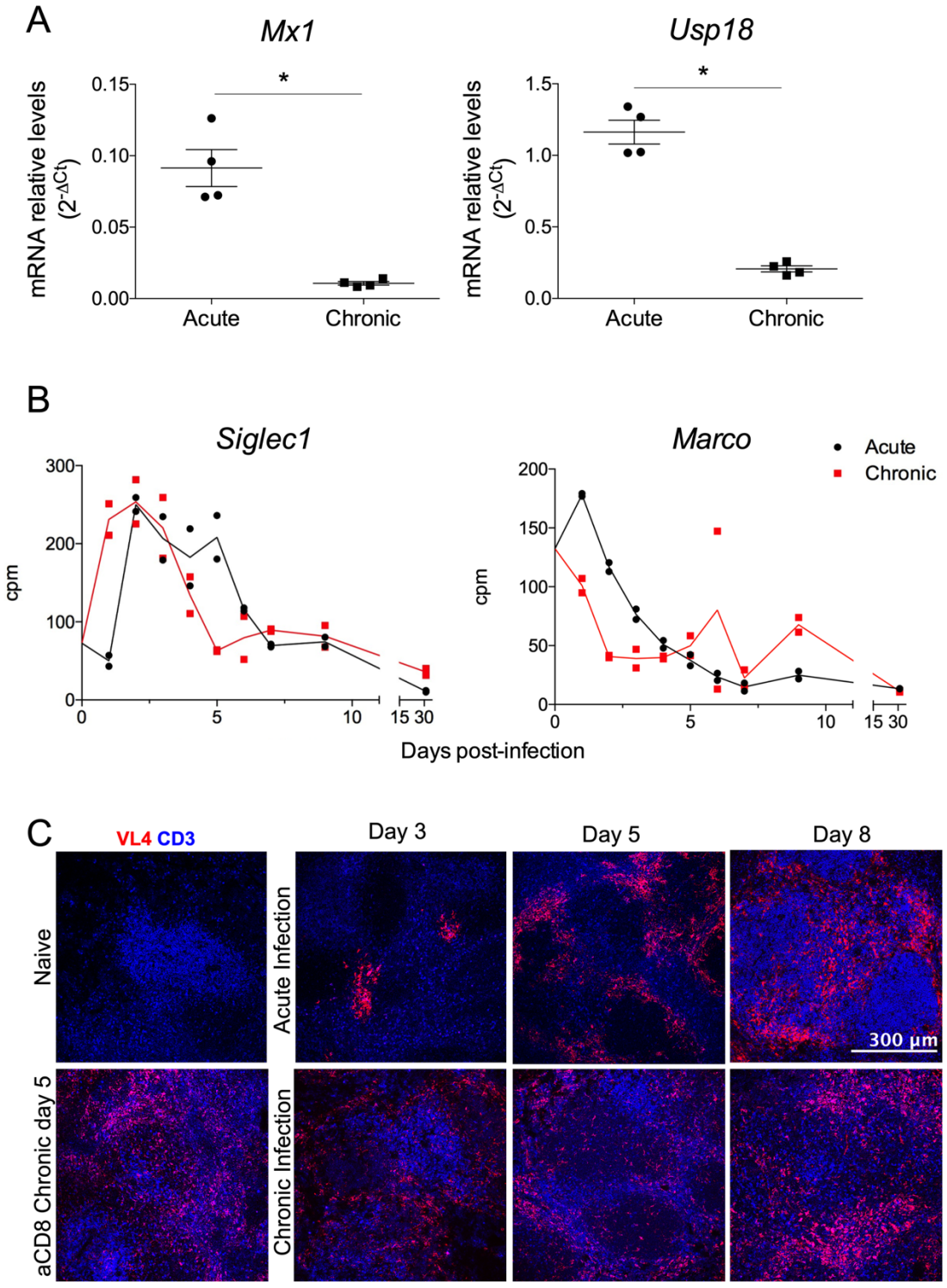

Supplemental Figure S4. (A) Mx1 and Usp18 expression analyzed by qPCR in CD169+ macrophages sorted from spleens from infected mice at day 5 p.i.. Data shown are the mean (± SEM) of n=4 mice; significance determined via unpaired two-tailed t test: * $p \leq 0.05$. (B) RNAseq expression kinetics of Siglec1 (Cd169) and Marco transcripts. (C) Immunofluorescence on spleens from different timepoints (d3, d5 and d8) post-infection and at day 5 post-chronic infection, after CD8 T cell depletion. Spleen sections were stained for CD3 (T cells; blue), VL4

(LCMV-NP; red). One representative section of 3 mice per group is shown. Images were taken at 20X magnification, the scale bar indicates 300 μm.

A manuscript describing the results of this thesis is in preparation:

The spatiotemporal dynamics of the type I IFN response determines viral infection outcomes

Valentina Casella[1]*, Eva Domenjo-Vila[1], Mireia Pedragosa[1], Anna Esteve-Codina[2], Enric Vidal[4], Monica Perez[4], Jordi Argilaguet[1,4]* and Andreas Meyerhans[1,5]*.

[1]Infection Biology Laboratory, Department of Experimental and Health Sciences (DCEXS), Universitat Pompeu Fabra, Barcelona, Spain.

[2]CNAG-CRG, Center for Genomic Regulation (CRG), Barcelona Institute of Science and Technology, Barcelona, Spain.

[3]Universitat Pompeu Fabra, Barcelona, Spain

[4] IRTA, Centre de Recerca en Sanitat Animal (CReSA-IRTA-UAB), Campus de la Universitat Autònoma de Barcelona, Bellaterra, Spain.

[5]Institució Catalana de Recerca i Estudis Avançats (ICREA), Barcelona, Spain.

*Corresponding authors

Correspondence:

Dr. Andreas Meyerhans (andreas.meyerhans@upf.edu)

Dr. Jordi Argilaguet (jordi.argilaguet@irta.cat)

DISCUSSION

In this thesis we analyzed the spatiotemporal events influencing the IFN-I response during early acute and chronic infections and its consequences. To do so, we used the well-established lymphocytic choriomeningitis virus infection mouse model which has been instrumental to detect many fundamental processes in the virus-immune system crosstalk that are also relevant in human virus infections. First, time-resolved spleen-transcriptome analysis revealed that during an acute infection, IFN-I genes were expressed in two waves at days 2 and 5 post-infection. In contrast, in chronically infected mice a single peak of IFN-I gene expression appeared at day 1. Second, we identified metallophilic marginal zone macrophages as an important source of the second peak of IFN-I during acute infection. We consequently demonstrated that lack of production of the second wave of IFN-I in chronic infection is a consequence of the early depletion of these cells by CD8+ cells. Third, we showed a polyfunctional role for the second wave of IFN-I, explained by the induction of pro-inflammatory macrophages and virus-specific CD8 T cells. Finally, we proved that the second wave of IFN-I and the resulting expansion of virus-specific CD8 T cells determine the development of fibrosis in lymphatic tissue after acute LCMV infection. Together our data demonstrate that the tight spatiotemporal regulation of IFN-I response in the early stages of infection is crucial for the induction of IFN-I-dependent sequential immune events that lead to viral infection resolution. Furthermore, our work fills a knowledge gap regarding the mechanisms of induction of lymphoid tissue fibrosis in viral infections and its potential negative consequences for the infected host.

1. Virus expansion kinetics influences IFN-I dynamics

Acute and chronic viral infections differ in their long-term consequences for a virus-infected host. While the infection fate decision is made already during early virus-host interactions, the biological mechanisms underlying this decision point are poorly understood. Early IFN-I response represents a fundamental pillar of antiviral immunity, both restricting viral replication and establishing an efficient adaptive immune response. Despite the broad knowledge acquired regarding IFN-I regulation and functionality during the last decades, its particular role in the fate decision during the early stages of acute and chronic infections remain elusive. In this thesis we characterized spleen transcriptome changes at early time points post-infection to decipher the differential behaviour of IFN-I responses in acute and chronic LCMV infections. The generation of a correlation matrix across all IRG allowed us to have a

global view of the dynamics of IFN-I response in these two infection outcomes. In particular, the identification of defined clusters of coexpressed IRGs in acute infection, compared to the more heterogeneous pattern observed in chronic infection, pointed to a differential regulation of IFN-I responses. Additionally, the number of differentially expressed IRGs over time showed a biphasic behavior in acute infection, in contrast to the constant numbers during chronic infection. This suggested the existence of a fine tuning of the IFN-I response in the early phase of acute infection, that might be lost or altered in the early phase of chronic infection. To further characterize these differences, we used weighted gene coexpression network analysis (WGCNA) of spleen transcriptomes to identify the modules of highly coexpressed genes. This approach was previously used in our group to decompose the complex host response against the invading virus into several modules of highly coexpressed genes (*Argilaguet et al., 2019, Genome Res*). However, early time points in which IFN-I genes are initially expressed were missing in that analysis, and thus we decided to incorporate them to the data set. Despite IFN-I genes were all coexpressed and thus found together in a single module both in acute and chronic infections, their kinetic differed in the two groups, showing two waves of expression at days 2 and 5 post-acute infection, while only one peak of expression was identified at around day 1 post-chronic infection. This suggested the existence of a fine tuning of the IFN-I response in the early phase of acute infection that might be lost or altered in the early phase of chronic infection.

Our results are in concordance with previous studies highlighting the importance of early IFN-I responses on infection outcome. For example, administration of recombinant IFN-I during the first week post LCMV-Cl13 infection can prevent CD8 T cell exhaustion and establishment of chronic infection, while when administered at later time points, it has no impact on the outcome of the infection (*Saprunenko et al., 2019, Viruses; Wang et al., 2012, Cell Host Microbe*). Similarly, early administration of IFNα2 to monkeys infected with the simian immunodeficiency virus (SIV) prevents systemic infection (*Sandler et al., 2014, Nature*). Finally, the current SARS-CoV-2 pandemic has also shown how critical a timely IFN response is for disease progression. The development of severe forms of COVID19 has been linked to an early dysregulation in IFN-I production following SARS-CoV2 infection (*Sa Ribero et al., 2020, PLOs Pathogens*; *Beck et al., 2020, Science*). Altogether, our results highlight the potential of new therapeutic approaches aiming to support innate immune responses at early time points post infection, such as IFNβ administration that gives promising results to

improve disease progression in SARS-CoV-2-infected patients (*Peiffer-Smadja & Yazdanpanah,2021, The Lancet)*.

Our finding that early loss of marginal zone macrophages during chronic LCMV infection is the mechanism underlying the disruption of the IFN-I response, highlights the importance of the race between virus expansion and the subsequent host immune responses. Previous studies already described the critical role of MZ macrophages during acute LCMV infection. Being a target for viral replication, MZ macrophages trigger a potent CTL response. This cytotoxic response then finally leads to the disruption of the highly organized splenic microarchitecture and a concomitant loss of immunosurveillance *(Muller et al., 2002, J Virol; Scandella et al., 2008, Nat Immunol).* Furthermore, *Louten et al.* showed that mice lacking functional splenic architecture exhibited profound reductions in IFN-I during LCMV infection *(Louten et al., 2006, J Immunol)*. In this thesis we gained a deeper understanding of the complex dynamics of this MZ-mediated innate immune response. Indeed, we show a rapid increase of high viral loads in MZ macrophages during chronic infection, which is in concordance with a study from *Duhan et al.,* who showed the presence of LCMV in the MZ as early as 1 day post infection (*Duhan et al., 2016, Sci Reports).* This early viral accumulation accelerates the loss of the marginal zone structure, thereby closing the window of opportunity for MZ macrophages to produce the second wave of IFN-I. It is still to be investigated whether a 'delayed' disruption in secondary lymphoid organ architecture and/or the induction of a second wave of IFN-I in the early phase of a chronic infection would facilitate viral clearance and consequently influence the infection outcome. It is critical for future studies to identify mechanisms that favor the restoration of lymphoid organ structure, as this would help to develop new approaches for clinical intervention.

During chronic LCMV infection, IFN-I functionality eventually shifts from an antiviral to an IFNβ-mediated immunosuppressive role as demonstrated by the recovery of CD8 T cell functionality and tissue architecture after IFNAR blockade at late time points post infection (*Wilson et. al, 2013, Science; Teijaro et al., 2013, Science*; *Ng et al., 2015, Cell Host & Microbe)*. However, the mechanisms underlying this shift are still elusive. Our results identified what could be the first indicator of this differential IFN-I response. Indeed, despite the lack of MZ-mediated production of IFN-I during chronic infection, we observed an ongoing antiviral IFN-I response by macrophages characterized by higher expression of *Mx1* compared to macrophages from acutely infected mice and a

concomitant decreased expression of the IFNAR inhibitor *Usp18*. Further studies are necessary to investigate whether this differential pattern of ISG expression is linked to the shift of IFN-I functionality.

2. Polyfunctional role of the biphasic IFN-I response in acute viral infection

The second peak of the IFN-I response during acute infection was of lower magnitude than the first peak. This fact, together with the involvement of MZ macrophages in its production, suggested that it might have a more immunomodulatory than an antiviral role. Indeed, selective blockage of the second wave of IFN-I via anti-IFNAR antibody treatment and depletion of CD169+ macrophages abolished the induction of pro-inflammatory macrophages and hampered the expansion of virus-specific CD8 T cells. Previous observations from our laboratory identified pro-inflammatory macrophages at day 6 as a specific feature of acute LCMV infection *(Argilaguet et al., 2019, Genome Res)*. However, the regulatory mechanisms underlying this inflammatory response were still unknown. In this thesis we provide an important link between IFN-I-producing MZ macrophages and the induction of inflammatory macrophages. To note, therapeutic injection of recombinant IFNβ at day 5 post-chronic infection was not sufficient to induce these pro-inflammatory macrophages in chronic infection (data not shown), likely due to the extensively disrupted spleen architecture which might be also required to promote this inflammatory response. A hierarchical production of IFNβ and IL1β was previously observed by *Barbet et al.* in a model of vaccination with inactivated bacteria, in which they demonstrate that IFNβ-dependent production of IL1β by CX3CR1hi CCR2- Ly6C- monocytes induced Tfh cell differentiation during the early stages of the innate immune response *(Barbet et al., 2018, Immunity).* In addition, recent work from *De Giovanni et al.,* already identified a link between IFN-I and the Tfh response demonstrating that IFN-I sensing during the first 24 hours post LCMV infection drives Tfh differentiation *(De Giovanni et al., 2020, Nat Immunol).* However, our immunophenotypic analysis of IL1β-producing macrophages showed a dissimilar phenotype from the ones described by *Barbet et al.*, pointing to a possible different function for these cells. This was also confirmed by both liposomal-encapsulated clodronate (LIP-CLOD)-mediated depletion of all macrophages and IFNAR blockage, which only transiently decreased Tfh cell percentages, indicating a minor role of these acute infection-specific events in the induction of the humoral response.

As previously described, IFN-I also profoundly influenced the development of virus-specific CD8 T cell response (see Introduction 2.3.2). Specifically, both the timing and the duration of CD8 T cell exposure to IFN-I significantly influences their differentiation and the magnitude of the response *(Crouse et al., 2015, Nat Rev Immunol)*. However, the cellular sources of IFN-I production involved in this important phenomenon were not properly elucidated. Here we found that when interrupting the second wave of IFN-I signaling, either by IFNAR blockage or CD169+ macrophage depletion, LCMV-specific IFNγ-producing CD8 T cells dropped at days 9 and 15 p.i., with the resulting increase in splenic virus titers. Thus, we demonstrate here that IFN-I production by MZ macrophages is critical in the generation of virus-specific CTLs. It is still to be determined whether this effect is mediated by direct IFNAR signaling in CD8 T cells or indirectly by the coordination of the surrounding immune cells. For instance, pro-inflammatory macrophages are known to stimulate a Th1-biased immune response via production of IL-12 that promotes production of IFNγ by T cells primed in lymph nodes (*Stegelmeier et al., 2019, Viruses*). However, in our study we found that the IFN-I-induced CD8 T cell response was only transiently affected by the blockage of the inflammatory NF-κB pathway at day 8, reaching normal levels by day 15 p.i. Further studies are required to better characterize the direct and/or indirect immune mechanisms underlying the IFN-I mediated expansion of CD8 T cells.

3. Linking early immune events with late consequences

During the previous sections we focused mainly on how the dynamics of early events influenced early immune responses. Additionally, in this project we determined an important link between these early immune events and long-term consequences once the infection is resolved. In a previous work from our laboratory, we identified fibrosis in the spleen after an acute LCMV infection (*Argilaguet et al., 2019, Genome Research*). However, the mechanism behind this process was not elucidated. In this thesis, we have now shown, by blocking IFNAR signaling at days 3 and 4 p.i., that the second wave of IFN-I is the earliest event determining the appearance of fibrosis. Despite having demonstrated that CD169+ macrophages produce the second wave of IFN-I, we could only partially confirm their role in the development of fibrosis because their depletion by DT treatment in CD169DTR mice induced an exacerbated inflammation and death of most animals. This could seem contrary to the fact that the early loss of

CD169+ macrophages in chronic infected mice results in the establishment of a persistent infection. However, the immune context in both experimental models markedly differs, as high levels of virus in the early stages during chronic infection induce an immunosuppressive environment characterized by the expansion of myeloid-derived suppressor cells that might prevent an exacerbated inflammatory response (*Norris et al, 2013, Immunity*).

The main aim of fibrosis is to repair damaged tissue by preserving its architecture. Depending on the context, the mechanisms responsible for fibrosis induction may differ. A dysregulation in innate and adaptive immune responses is known to be one of the major contributors. As an example, tissue fibrosis can be caused by CCL2-mediated recruitment of macrophages to damaged tissues that then produce reactive oxygen and nitrogen species exacerbating the inflammatory response *(Wynn et al., 2013, Nat Med)*. As previously mentioned, our transcriptome analysis revealed a peak of genes related to proinflammatory responses such as *Ccl2, Il1a, Il6* and *Csf1* at day 6 post acute but not post chronic infection, suggesting a possible role for macrophages in fibrosis induction in our model. This hypothesis was further supported by the fact that IL1β is known to exacerbate parenchymal-cell injury and induce myofibroblast activation through TGFβ *(Wynn et al., 2013, Nat Med)*. However, mice treated with NBP2, an inhibitory peptide that blocks the NF-κB pathway, still developed fibrosis indicating the involvement of different players in the process. We finally determined that spleen fibrosis in acute LCMV-infected mice was a consequence of the IFN-I-dependent antiviral CD8 T cell response, as depletion of CD8 T cells at d7 p.i.. abrogated the establishment of spleen fibrosis. Further studies are necessary to determine if this finding applies to any infection by a non cytopathic virus, in which fibrosis in infected organs might be ‘the price’ the host has to pay for a successful clearance of the virus. This viral infection-induced fibrosis of tissues is already well established in the case of chronic SIV and HIV infections (*Schacker et al., 2006, Clin Vacc Immunol*). A recent publication has already suggested that lymph node fibrosis is not limited to HIV infection and may be caused by other infections including those with an attenuated yellow fever vaccine (*Kityo et al., 2018, J Clin Invest*). Importantly, they suggest that it can result in impaired immune responses to vaccines or other subsequent challenges. This issue is currently addressed in our group where one of the main aims is to better define the molecular players involved in this process and to test therapeutic options to reverse it.

In clear contrast with the results presented in this thesis, we previously showed that spleen fibrosis was a specific feature of acute LCMV infection that was not observed in chronically infected mice (*Argilaguet et al., 2019, Genome Research*). In this previous study, fibrosis was analyzed in a few animals at day 48 post-infection, a time point that is slightly delayed compared to the ones analyzed here (days 30, 35 and 42 post-infection). Fibrosis scores observed at these three time points show a tendency to decrease, thus suggesting that it might be resolved over time. We are currently repeating these experiments in order to clarify this issue. In any case, the mechanisms behind fibrosis appearance in acute and chronic infections must differ due to the marked different contexts in which they develop. It is likely that fibrosis in chronic LCMV infection resembles the one observed in SIV and HIV chronic infections, in contrast to the fibrosis induced by the virus-specific CTL response during acute LCMV infection. Finally, considering the great success represented by the use of checkpoint blockade inhibitors for restoring CD8 T cell functionality during chronic viral infections *(Rao et al., 2017, Int J Infect Dis; Wykes et al., 2018, Nat Rev Immunol)*, we investigated whether the prolonged reactivation of T cells during immunotherapy could increase the degree of tissue fibrosis induced. Importantly, we demonstrated anti-PDL1 antibody treatment did not result in an increase of LT fibrosis regardless of the therapy regimen used. This observation has great relevance in the field of immunotherapy for chronic viral infections, as it means that the treatment-mediated reactivation of the exhausted CD8 T cell response is sufficient to facilitate viral clearance but not strong enough to cause CD8-mediated tissue damage.

CONCLUSIONS

The main conclusions of the present study are the following:

In acute LCMV infection:

- IFN-I has a biphasic behaviour, with the second wave of induction at day 5 p.i.
- The second wave of IFN-I produced by CD169+ macrophages has a polyfunctional role bridging innate and adaptive immunity. It induces proinflammatory macrophages at day 6 p.i. and LCMV-specific CD8 T cells at day 8 p.i.
- The IFN-I-mediated CD8 T cell response induces fibrosis in the late phase of infection.

In chronic LCMV infection:

- IFN-I has one early wave of induction at day 1-2 p.i.
- The CD8+ cell-mediated killing of CD169+ macrophages in the early phase of infection dampers the production of the second wave of IFN-I.
- The lack of the second wave of IFN-I is linked to lack of proinflammatory macrophages and spleen fibrosis.

Graphical Summary

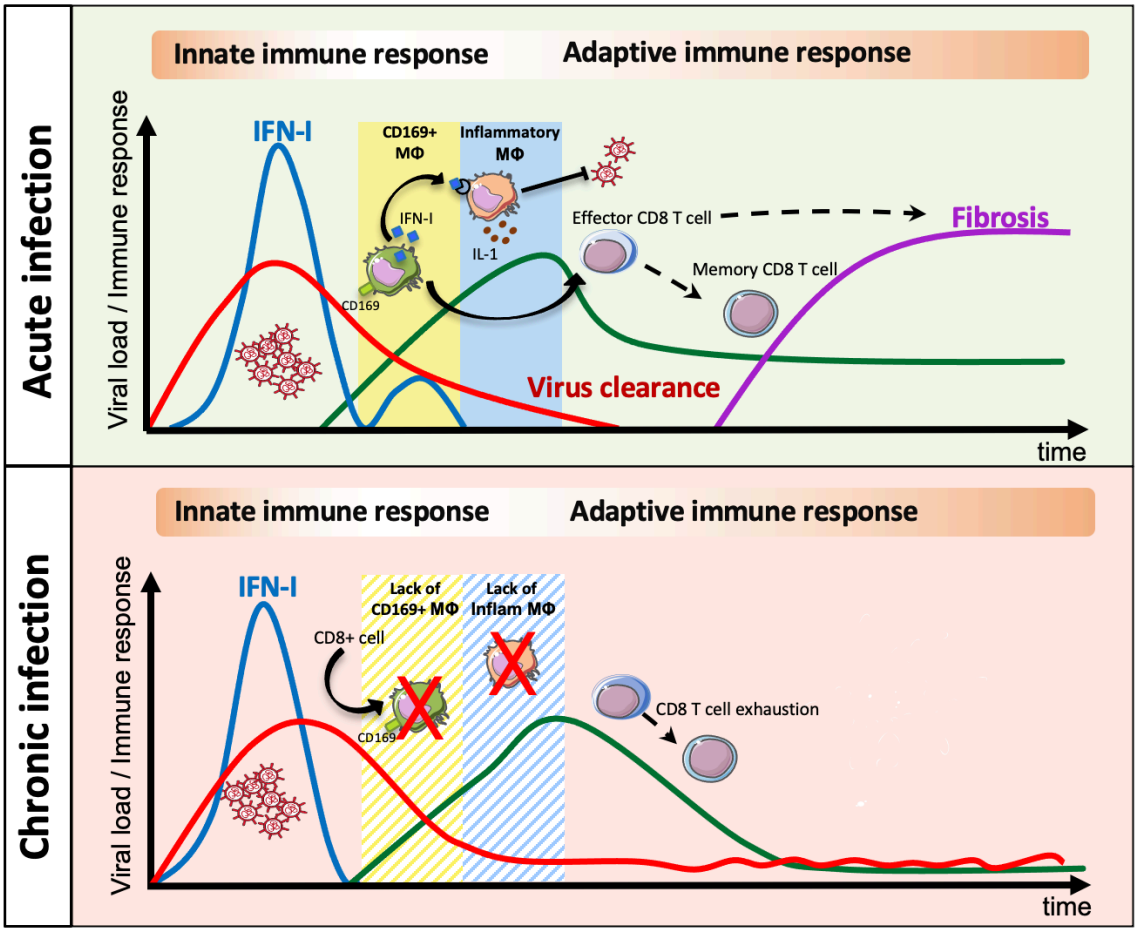

ANNEXES

ANNEX 1

List of abbreviations

aIFNAR	Anti-IFNα/β Receptor Antibody
APC	Antigen Presenting Cell(s)
BSA	Bovine serum albumin
CCR2	CC Chemokine Receptor type 2
CCR5	CC Chemokine Receptor type 5
cDC	Conventional Dendritic cell(s)
CL13	Clone 13
COVID19	Coronavirus Disease 2019
CTL	Cytotoxic T cell
CXCR5	CXC Chemokine Receptor type 5
CX3CR1	CX3C Chemokine Receptor type 1
DC	Dendritic cell(s)
DE	Differentially expressed
Doc	Docile
DT	Diphtheria Toxin
DTR	Diphtheria Toxin Receptor
EDTA	Ethylenediaminetetraacetic acid
FACS	Fluorescence-activated cell sorting
FBS	Fetal Bovine Serum
FC	Fold Change
GO	Gene ontology
HBV	Hepatitis B Virus
HCV	Hepatitis C Virus
HD	High Dose
HIV	Human Immunodeficiency Virus
i.p.	Intraperitoneal
IFN	Interferon(s)
IFN-I	Type I Interferon

IFNAR	IFNα/β receptor
IL	Interleukin
IRG	Interferon-regulated gene(s)
ISG	Interferon-stimulated gene(s)
LCMV	Lymphocytic Choriomeningitis Virus
LD	Low Dose
LIP-CLOD	Liposomal-encapsulated Clodronate
MACS	Magnetic-activated cell sorting
MARCO	Macrophage Receptor with Collagenous structure
MHC	Major Histocompatibility Complex
MMMΦ	Metallophilic Marginal Zone Macrophages
MZMΦ	Marginal Zone Macrophages
MZ	Marginal Zone
NaCl	Sodium Chloride
NBP2	IKK-Gamma NEMO Binding Domain (NBD) inhibitor peptide
NH4Cl	Ammonium Chloride
NK cells	Natural Killer cells
NP	Nucleoprotein
p.i.	Post infection
PBS	Phosphate-buffered saline
PD1	Programmed Cell Death-1
PDL1	Programmed Cell Death-1 ligand
pDC	Plasmacytoid dendritic cell(s)
pfu	Plaque-forming unit
qPCR	Real Time Quantitative Polymerase Chain Reaction
RIN	RNA integrity number
RNA	RiboNucleic Acid
RPMI	Roswell Park Memorial Institute Medium
SARS-CoV-2	Severe acute respiratory syndrome coronavirus 2
SEM	Standard error of the mean
SIGNR1	C-type lectin SIGN-related 1
SIV	Simian immunodeficiency virus
SLO	Secondary Lymphoid Organ(s)
Tex	Exhausted T cell(s)
TGFβ	Transforming growth factor beta

Tfh	Follicular Helper T cell(s)
Th	Helper T cell(s)
TLR7	Toll-like receptor 7
TNF	Tumor Necrosis Factor
Usp18	Ubiquitin Specific Peptidase 18
WGCNA	Weighted Gene Coexpression Network Analysis

ANNEX 2

Table S1. IRGs in acute-brown and chronic-brown modules.

Genes	K_{IM} Acute	K_{IM} Chronic	Genes	K_{IM} Acute	K_{IM} Chronic
March5	0.726444047	0.695477259	Bbx	0.627991805	0.560092164
1600014C10Rik	0.883386037	0.885034775	Bcl3	0.499615008	0.790593401
2810474O19Rik	0.903059064	0.70439518	Bfar	0.171466063	0.434406497
3110001I22Rik	0.312836685	0.611204022	Brd2	0.531488046	0.941324988
4930599N23Rik	0.728055629	0.743130674	Bst2	0.791114285	0.739045656
5430427O19Rik	0.490019436	0.959173681	C130026I21Rik	0.607853403	0.378071554
5730508B09Rik	0.501518819	0.674563382	C1ra	0.378199238	0.479411527
9930111J21Rik1	0.630933336	0.374813387	C2	0.47474933	0.68213187
9930111J21Rik2	0.512608605	0.723677242	Capn5	0.605176979	0.135234541
A230046K03Rik	0.685206776	0.631603508	Car13	0.942630289	0.498350274
A530064D06Rik	0.664066624	0.699893434	Casp4	0.916870104	0.694987699
Abcb1a	0.616925899	0.842826116	Casp8	0.897069099	0.770014152
Abi1	0.268522067	0.19092571	Cass4	0.19670501	0.456245515
Abtb2	0.797410062	0.783013964	Ccdc6	0.522334537	0.429938898

Acap2	0.117447282	0.090997675	Ccnd2	0.879031459	0.495372214
Acvr1	0.243669435	0.228429964	Ccrl2	0.925433772	0.686163203
Adam17	0.516794338	0.054884043	Cd164	0.884036981	0.616419637
Adar	0.610173324	0.905932351	Cd180	0.427294079	0.573467174
Aen	0.711336752	0.666883656	Cd47	0.765674284	0.820355223
Aftph	0.607818693	0.964839437	Cd86	0.711001322	0.946695916
Aida	0.806023989	0.803379654	Cdc42ep2	0.526404136	0.169400237
Aldh1b1	0.710697474	0.667503546	Cenpj	0.853236098	0.184984178
Aldh1l1	0.170706911	0.490510783	Cep350	0.606358296	0.222527604
Amica1	0.585671922	1	Cfap43	0.546924641	0.769483126
Amigo2	0.339334414	0.009239227	Cflar	0.769825755	0.757881578
Ankfy1	0.756082789	0.886431167	Cggbp1	0.516092431	0.536874519
Ankle2	0.468850416	0.889427173	Chd4	0.363922457	0.439647886
Apod	0.571584633	0.881931359	Chic1	0.524432081	0.805490824
Apol9a	0.775688256	0.43025588	Chmp4b	0.866331433	0.629588862
Apol9b	0.766860779	0.530721573	Cmpk2	0.64196458	0.836106434
Arel1	0.773813425	0.382163779	Cngb3	0.735317476	0.575372133
Arf6	0.200074518	0.466228483	Cnot4	0.311306043	0.560499312

Arid5a	0.495375614	0.907670653	Cox18	0.414364266	0.548271646
Asah2	0.608650218	0.282051499	Cpne3	0.581329145	0.405277231
Ascc3	0.795771281	0.400278335	Csf1	0.490863903	0.6423974
Atm	0.586715289	0.465825967	Csrnp1	0.523284829	0.5239369
AW011738	0.483414119	0.887814183	Cul5	0.304559249	0.216267825
Axl	0.443583499	0.443426747	Cxcl11	0.924454671	0.65042312
Azi2	0.863953805	0.825341784	Cxcl9	0.689179286	0.259110784
B2m	0.693380415	0.27584482	D17Wsu92e	0.880650124	0.758642999
Baz1a	0.876734912	0.474336673	Daxx	0.7275781	0.925807202
Dbnl	0.436847207	0.834217213	Gm4759	0.294389779	0.263353296
Dck	0.880401561	0.57109042	Gm4955	0.73580757	0.90084475
Dclre1c	0.20726194	0.460987413	Gm7582	0.461137268	0.310881614
Dcp2	0.645873635	0.426142616	Gm7592	0.591481653	0.443766416
Ddx24	0.772426233	0.791851831	Gm7609	0.506233405	0.402583523
Ddx42	0.087573555	0.176290965	Gm8995	0.842014956	0.827946792
Ddx58	0.564850657	0.963316209	Gmppb	0.934665808	0.205983922
Ddx60	0.746393069	0.83051078	Gnb4	0.729921822	0.648535805
Dennd1b	0.836682158	0.454472748	Grina	0.27045664	0.467297385

Dhx58	0.749801729	0.837231943	Gsdmd	0.651745728	0.64013045
Dopey2	0.500610643	0.769288785	Gvin1	0.848257603	0.37398927
Dtx3l	0.939774289	0.722872647	H2afy	0.118139708	0.248016731
Dtx4	0.0599376	0.209758228	H2-D1	0.734865918	0.453462382
Dusp28	0.524802617	0.875526637	H2-K1	0.682763223	0.420922868
Egr1	0.366124535	0.444344799	H2-M3	0.564351348	0.597041563
Eif2ak2	0.78247593	0.724500645	H2-Q4	0.585956754	0.644196532
Elf1	0.422984365	0.865647843	H2-Q5	0.234908788	0.483039658
Enpp4	0.430446308	0.320560757	H2-T10	0.443636288	0.629622596
Epsti1	0.576516571	0.866809776	H2-T22	0.839093152	0.507536541
Evi2a	0.440956987	0.752845827	H2-T23	0.859037098	0.75214594
Fam111a	0.604286502	0.905915334	H2-T24	0.610454589	0.763068731
Fam175b	0.174787294	0.140313774	H3f3b	0.435687267	0.769982884
Fam46a	0.679968256	0.75830824	Hck	0.811303898	0.856591744
Fam53c	0.417333544	0.658167874	Helz2	0.455096029	0.925882829
Fas	0.350454868	0.401687433	Herc6	0.78502637	0.869791039
Fbxw17	0.716370533	0.777068252	Hhat	0.320628887	0.542530322
Fer	0.380751185	0.447166897	Hmox2	0.670796635	0.762303433

Fez2	0.070791673	0.649264907	Hnrnph2	0.55409953	0.480206364
Fndc3a	0.828409214	0.247622254	Hook2	0.572162026	0.927912402
Foxred1	0.326823104	0.622613827	Hpse	0.734288102	0.472018225
Frmd4a	0.761844283	0.621132754	Hsh2d	0.421822823	0.979054032
Fscn1	0.547121965	0.491370714	Ifi203	0.51108846	0.996029688
Galnt15	0.038447734	0.023870176	Ifi27l2a	0.638526344	0.744358453
Gbp3	0.989210873	0.328801799	Ifi35	0.600881324	0.941484393
Gbp7	0.976554689	0.261765621	Ifi44	0.857683299	0.484322855
Gbp9	0.798023792	0.936028248	Ifih1	0.86112034	0.780331041
Gem	0.733489754	0.812517558	Ifit1	0.749980075	0.770681954
Gm15753	0.36245658	0.795076899	Ifit1bl1	0.738150386	0.894111644
Gm20547	0.568820122	0.508419219	Ifit2	0.884833263	0.73853047
Gm2619	0.216242783	0.140148984	Ifit3	0.670698224	0.829222626
Gm4117	0.407629361	0.559795755	Ifit3b	0.639402934	0.878595976
Ifitm3	0.871408817	0.570504607	Morc3	0.555635909	0.972472101
Ifitm6	0.265354558	0.345194791	Mov10	0.760538881	0.916214803
Igtp	0.998846888	0.277680824	Mrpl30	0.634917781	0.734128026
Il10	0.766217147	0.229650602	Ms4a4c	0.748936187	0.889754815

Il10ra	0.474387514	0.818156484	Ms4a4d	0.680800453	0.702385678
Il15	0.688811099	0.89795143	Ms4a6d	0.788105813	0.147894073
Il1a	0.782069613	0.565659359	Msl3l2	0.27210187	0.672522293
Insl6	0.49019192	0.118773228	Mthfr	0.839302725	0.81880909
Irf7	0.789537194	0.679466464	Mvp	0.954351457	0.702661133
Isg15	0.733867865	0.762480123	Mx1	0.679393622	0.929224819
Isoc1	0.608431764	0.44916131	Mx2	0.509220696	0.948451541
Jak2	0.574063433	0.661851694	Mxd1	0.78871941	0.708740596
Junb	0.606394878	0.773458876	Naa25	0.977834352	0.686855129
Kansl3	0.358393746	0.749328778	Nck2	0.072192706	0.657979048
Kat2b	0.95155262	0.443680803	Ncoa7	0.583984649	0.648168797
Katna1	0.721623012	0.793553408	Nfkbiz	0.208433576	0.409885506
Keap1	0.85357739	0.761079872	Nkiras2	0.309691735	0.655173441
Kpna4	0.671330622	0.474433627	Nlrc5	0.862893516	0.67247746
Lacc1	0.897679242	0.677724459	Nmi	0.805366728	0.827722243
Lgals3bp	0.864493838	0.470391439	Nmral1	0.704700197	0.545010781
Lgals8	0.452193713	0.842039979	Npc2	0.919017141	0.502356583
Lgals9	0.766260864	0.588313994	Npnt	0.076366409	0.050210437

Lhx2	0.743761189	0.717075865	Nt5c3	0.561464897	0.811049492
Lpxn	0.588237965	0.686154614	Nub1	0.518196026	0.982455296
Lrp11	0.500126335	0.610331197	Nudt13	0.089655265	0.403369331
Lrp4	0.802143547	0.653522091	Oas1a	0.849782441	0.703769066
Ly6a	0.825399842	0.153456229	Oas2	0.600796623	0.851425985
Ly6e	0.498245744	0.805435247	Oas3	0.809032989	0.704880064
Ly86	0.3383771	0.893033307	Oasl1	0.824222604	0.758769966
Lyrm1	0.105989877	0.820469916	Oasl2	0.833113159	0.610581326
Mafk	0.464112179	0.796253621	Ogfr	0.766746721	0.835883428
Map2k1	0.424944445	0.99225358	Ogfrl1	0.555350145	0.911316269
Map3k8	0.354279347	0.592101943	Olfr56	0.953294843	0.239180755
Marcksl1	0.592426365	0.859425026	Osm	0.50607996	0.608033537
Max	0.750526962	0.8547643	P2ry13	0.254115988	0.617680057
Mfsd7a	0.483068547	0.588962131	P2ry14	0.737516224	0.67374269
Mgat4a	0.242741591	0.397495484	Papd4	0.509853448	0.20953372
Misp	0.947777999	0.563154806	Papd7	0.763112098	0.831129447
Mitd1	0.534645176	0.974799897	Parp10	0.775355029	0.887089428
Mndal	0.411814497	0.974574303	Parp11	0.743290427	0.918683232

Mob4	0.082224526	0.551647865	Parp12	0.92947527	0.649823202
Parp14	0.850556204	0.827190215	Rgl1	0.180917299	0.456066058
Parp9	0.828936785	0.730770044	Rhcg	0.767038202	0.611110932
Pcgf5	0.925627181	0.622943394	Rilpl1	0.421637923	0.850659264
Pfkfb3	0.793398691	0.743424377	Rin2	0.645192982	0.845544734
Pgap2	0.849829022	0.693873418	Ripk2	0.610504112	0.914028395
Phc2	0.520779294	0.878893134	Rnf114	0.607532739	0.948722249
Phf11a	0.774117067	0.906816538	Rnf135	0.676535491	0.957173102
Phf11d	0.864244968	0.789912247	Rnf213	0.765971743	0.840116615
Phf6	0.84419558	0.30949338	Rnf214	0.877159795	0.439594646
Phyh	0.535353793	0.878561036	Rsad2	0.51362824	0.685332976
Pik3ap1	0.8365078	0.841129346	Rtfdc1	0.302000548	0.742851669
Pira2	0.470747443	0.173843284	Rtp4	0.697271087	0.745539439
Pirb	0.184380892	0.180855188	Rufy3	0.766489254	0.685404591
Piwil4	0.302566548	0.57724285	Samhd1	0.895902474	0.724358124
Pkib	0.677798365	0.947225751	Sat1	0.472398251	0.826191789
Plac8	0.917940495	0.605565718	Sbno2	0.370006469	0.509767693
Plekhf2	0.459111138	0.891800645	Scarb2	0.477342254	0.615359201

Pml	0.596256933	0.961871738	Scimp	0.793939452	0.661045945
Pnpt1	0.802317094	0.740556536	Sco1	0.899937328	0.785024272
Pou3f1	0.741072641	0.77356939	Sct	0.567326608	0.786021562
Ppp4r2	0.543560761	0.42799028	Selt	0.827934126	0.562551028
Prr5l	0.742925267	0.899765401	Sepw1	0.419271295	0.910981602
Prrc2c	0.256448862	0.243445563	Serping 1	0.296311226	0.282265229
Psme1	0.8320526	0.758776825	Sertad1	0.197559385	0.962149923
Pstpip1	0.181328458	0.385542196	Setdb2	0.714299209	0.888339224
Ptges	0.03823249	0.374761535	Sfmbt1	0.624661842	0.43236075
Ptms	0.155257411	0.537818862	Sgcb	0.835241807	0.85988507
Ptpn2	0.970105037	0.400118255	Sh3bp2	0.766537179	0.891817306
Ptpro	0.42722917	0.737369795	Siglec1	0.370066883	0.479411865
Pttg1	0.38484644	0.942997045	Slc2a6	0.772251313	0.903498866
Pvrl4	0.809528033	0.699075954	Slfn1	0.825521945	0.661296663
Pydc3	0.568416925	0.964236151	Slfn2	0.736313639	0.871599643
Pydc4	0.578331604	0.939565963	Slfn4	0.812633044	0.532491999
Pyhin1	0.494619677	0.991574933	Slfn5	0.719854543	0.84308015
Rab22a	0.563858092	0.704256815	Slfn8	0.652361432	0.952197467

Rabepk	0.806817855	0.726414085	Smchd1	0.778395632	0.890786985
Rasa4	0.43787797	0.793512558	Snw1	0.729995252	0.679671358
Rbm18	0.141816272	0.206849798	Snx20	0.453812548	0.516782463
Rbm27	0.731921616	0.255823953	Sos1	0.705947514	0.837708613
Rbm43	0.446038848	0.88423306	Sp100	0.435076078	0.998586528
Rfc3	0.866713873	0.737712491	Sp110	0.458701278	0.978661984
Spats2l	0.472796478	0.899758017	Trim30a	0.695812615	0.912037129
Sppl2a	0.837230867	0.617727055	Trim30d	0.636936906	0.92827477
Spryd7	0.876813752	0.710774872	Triobp	0.843826857	0.759139834
Srsf7	0.216306583	0.143917586	Trip12	0.875995585	0.49721642
Stard3	0.697317757	0.785670517	Tspo	0.873670244	0.664803625
Stat2	0.769752277	0.911144309	Tuba8	0.172203506	0.286963402
Stxbp3	0.772390205	0.766122588	Uaca	0.65968668	0.797401291
Susd6	0.58914693	0.761067134	Ubr4	0.617636689	0.878776197
Synj1	0.694061132	0.351815429	Urgcp	0.188390474	0.648104126
Tagap	0.455574456	0.6373681	Usb1	0.910448482	0.770541596
Tank	0.437649045	0.54997313	Usp18	0.780346054	0.813097405
Taok3	0.698822715	0.387471911	Usp25	0.741756029	0.8078755

Tapbp	0.897717622	0.757790795	Usp42	0.383578989	0.631807583
Tapbpl	0.90720669	0.24999648	Utrn	0.147007094	0.271758611
Tbc1d1	0.606310222	0.820497949	Vcpip1	0.745848657	0.844774953
Tbc1d13	0.344630957	0.60864004	Vps33a	0.31824708	0.209560748
Tcea1	0.39843679	0.443092917	Vps37b	0.732254263	0.850641291
Tcof1	0.667806889	0.925226699	Vps54	0.854589174	0.640393442
Tdrd7	0.72063238	0.932992948	Vwa3b	0.556113559	0.567096791
Themis2	0.883367854	0.642683919	Vwa5a	0.880170591	0.62891637
Tifa	0.155807673	0.693636372	Whsc1l1	0.509851287	0.702315982
Tlk2	0.473514728	0.944181313	Wtap	0.028878895	0.433420148
Tlr3	0.662403435	0.809584863	Xaf1	0.730357715	0.827208765
Tmem140	0.86908125	0.518460838	Xrn1	0.425546383	0.480276922
Tmem184b	0.860662416	0.769261496	Zbp1	0.926164013	0.594013769
Tmem219	0.71740322	0.651425449	Zc3hav1	0.679952854	0.921666571
Tmem67	0.957130157	0.637254752	Zcchc2	0.63182581	0.924944022
Tmem87a	0.312421116	0.651921892	Zfos1	0.412134707	0.531073338
Tnf	0.52654758	0.725529028	Zfp281	0.563593357	0.346639688
Tnfaip3	0.36214515	0.453243568	Zfp36	0.163616904	0.611205912

Tnfsf10	0.826678527	0.56352819
Tomm70a	0.850686871	0.678255922
Tor1aip1	0.748269139	0.865340589
Tor1aip2	0.769415523	0.767334093
Tor3a	0.687704781	0.912072317
Tppp3	0.301261345	0.209105057
Trafd1	0.88673693	0.712301203
Trim12c	0.395066481	0.974553887
Trim14	0.612191171	0.809671714
Trim21	0.716783099	0.94846524
Trim25	0.730900204	0.765136259

Zfp800	0.803332792	0.710590279
Znfx1	0.859873434	0.836836649
Zufsp	0.482160945	0.98633764

ANNEX 3

Other contributions during the thesis:

During the time of my PhD thesis, I also participated in several research projects that led to the following publications with me as co-author. For the manuscript *Beltra et al*., I was performing experiments during my research stay in John Wherry's laboratory, at the University of Pennsylvania (October 2019-December 2019).

Mireia Pedragosa, Graciela Riera, **Valentina Casella**, Anna Esteve-Codina, Yael Steuerman, Celina Seth, Gennady Bocharov, Simon Charles Heath, Irit Gat-Viks, Jordi Argilaguet, Andreas Meyerhans.
Linking cell dynamics with gene coexpression networks to characterize key events in chronic virus infections. **Front. Immunol.** (2019) | doi: 10.3389/fimmu.2019.01002.

Jordi Argilaguet, Mireia Pedragosa, Anna Esteve-Codina, Graciela Riera, Enric Vidal, Cristina Peligero-Cruz, **Valentina Casella**, David Andreu, Tsuneyasu Kaisho, Gennady Bocharov, Burkhard Ludewig, Simon Heath, Andreas Meyerhans.
Systems analysis reveals complex biological processes during virus infection fate decisions. **Genome Research** (2019) | doi: 10.1101/gr.241372.118

Jean-Christophe Beltra, Sasikanth Manne, Mohamed S. Abdel-Hakeem, Makoto Kurachi, Josephine R. Giles, Zeyu Chen, **Valentina Casella**, Shin Foong Ngiow, Omar Khan, Yinghui Jane Huang, Patrick Yan, Kito Nzingha, Wei Xu, Ravi K. Amaravadi, Xiaowei Xu, Giorgos C. Karakousis, Tara C. Mitchell, Lynn M. Schuchter, Alexander C. Huang and E. John Wherry.
Developmental Relationships of Four Exhausted CD8+ T Cell Subsets Reveals Underlying Transcriptional and Epigenetic Landscape Control Mechanisms. **Immunity** (2020) | doi: 10.1016/j.immuni.2020.04.014

Gennady Bocharov, **Valentina Casella**, Jordi Argilaguet, Dmitry Grebennikov, Roberto Guerri-Fernandez, Burkhard Ludewig and Andreas Meyerhans.

Numbers Game and Immune Geography as Determinants of Coronavirus Pathogenicity. **Frontiers in Cellular and Infection Microbiology** (2020) | doi: 10.3389/fcimb.2020.55920

frontiers in Immunology

ORIGINAL RESEARCH
published: 03 May 2019
doi: 10.3389/fimmu.2019.01002

Linking Cell Dynamics With Gene Coexpression Networks to Characterize Key Events in Chronic Virus Infections

Mireia Pedragosa[1†], Graciela Riera[1†], Valentina Casella[1], Anna Esteve-Codina[2,3], Yael Steuerman[4], Celina Seth[1], Gennady Bocharov[5,6], Simon Heath[2,3], Irit Gat-Viks[4], Jordi Argilaguet[1] and Andreas Meyerhans[1,7*]*

[1] Infection Biology Laboratory, Department of Experimental and Health Sciences (DCEXS), Universitat Pompeu Fabra, Barcelona, Spain, [2] CNAG-CRG, Center for Genomic Regulation (CRG), Barcelona Institute of Science and Technology, Barcelona, Spain, [3] Universitat Pompeu Fabra, Barcelona, Spain, [4] Cell Research and Immunology Department, Tel Aviv University, Tel Aviv, Israel, [5] Marchuk Institute of Numerical Mathematics, Russian Academy of Sciences, Moscow, Russia, [6] Institute for Personalized Medicine, Sechenov First Moscow State Medical University, Moscow, Russia, [7] Institució Catalana de Recerca i Estudis Avançats (ICREA), Barcelona, Spain

OPEN ACCESS

Edited by:
Shokrollah Elahi,
University of Alberta, Canada

Reviewed by:
Marina Cella,
Washington University School of Medicine in St. Louis, United States
Aikaterini Alexaki,
United States Food and Drug Administration, United States

***Correspondence:**
Jordi Argilaguet
jordi.argilaguet@upf.edu
Andreas Meyerhans
andreas.meyerhans@upf.edu

† These authors have contributed equally to this work

Specialty section:
This article was submitted to Viral Immunology, a section of the journal Frontiers in Immunology

Received: *30 January 2019*
Accepted: *18 April 2019*
Published: *03 May 2019*

The host immune response against infection requires the coordinated action of many diverse cell subsets that dynamically adapt to a pathogen threat. Due to the complexity of such a response, most immunological studies have focused on a few genes, proteins, or cell types. With the development of "omic"-technologies and computational analysis methods, attempts to analyze and understand complex system dynamics are now feasible. However, the decomposition of transcriptomic data sets generated from complete organs remains a major challenge. Here, we combined Weighted Gene Coexpression Network Analysis (WGCNA) and Digital Cell Quantifier (DCQ) to analyze time-resolved mouse splenic transcriptomes in acute and chronic Lymphocytic Choriomeningitis Virus (LCMV) infections. This enabled us to generate hypotheses about complex immune functioning after a virus-induced perturbation. This strategy was validated by successfully predicting several known immune phenomena, such as effector cytotoxic T lymphocyte (CTL) expansion and exhausticn. Furthermore, we predicted and subsequently verified experimentally macrophage-CD8 T cell cooperativity and the participation of virus-specific $CD8^+$ T cells with an early effector transcriptome profile in the host adaptation to chronic infection. Thus, the linking of gene expression changes with immune cell kinetics provides novel insights into the complex immune processes within infected tissues.

Systems analysis reveals complex biological processes during virus infection fate decisions

Jordi Argilaguet,[1,12] Mireia Pedragosa,[1,12] Anna Esteve-Codina,[2,3,12] Graciela Riera,[1] Enric Vidal,[4] Cristina Peligero-Cruz,[1,13] Valentina Casella,[1] David Andreu,[5] Tsuneyasu Kaisho,[6,7] Gennady Bocharov,[8,9] Burkhard Ludewig,[10] Simon Heath,[2,3] and Andreas Meyerhans[1,11]

[1]*Infection Biology Laboratory, Department of Experimental and Health Sciences (DCEXS), Universitat Pompeu Fabra, Barcelona, Catalonia 08003, Spain;* [2]*CNAG-CRG, Center for Genomic Regulation (CRG), Barcelona Institute of Science and Technology, 08028 Barcelona, Spain;* [3]*Universitat Pompeu Fabra (UPF), Barcelona, Catalonia 08003, Spain;* [4]*IRTA, Centre de Recerca en Sanitat Animal (CReSA-IRTA-UAB), Campus de la Universitat Autònoma de Barcelona, 08193 Bellaterra, Barcelona, Catalonia, Spain;* [5]*Laboratory of Proteomics and Protein Chemistry, DCEXS, Universitat Pompeu Fabra, 08003 Barcelona, Spain;* [6]*Department of Immunology, Institute of Advanced Medicine, Wakayama Medical University, Wakayama 641-8509, Japan;* [7]*Laboratory for Immune Regulation, World Premier International Research Center Initiative, Immunology Frontier Research Center, Osaka University, Osaka 565-0871, Japan;* [8]*Marchuk Institute of Numerical Mathematics, Russian Academy of Sciences, Moscow, 119333, Russia;* [9]*Sechenov First Moscow State Medical University, Moscow, 119991, Russia;* [10]*Institute for Immunobiology, Kantonsspital St. Gallen, 9007 St. Gallen, Switzerland;* [11]*Institució Catalana de Recerca i Estudis Avançats (ICREA), Barcelona, 08003, Spain*

The processes and mechanisms of virus infection fate decisions that are the result of a dynamic virus-immune system interaction with either an efficient effector response and virus elimination or an alleviated immune response and chronic infection are poorly understood. Here, we characterized the host response to acute and chronic lymphocytic choriomeningitis virus (LCMV) infections by gene coexpression network analysis of time-resolved splenic transcriptomes. First, we found an early attenuation of inflammatory monocyte/macrophage prior to the onset of T cell exhaustion, and second, a critical role of the XCL1-XCR1 communication axis during the functional adaptation of the T cell response to the chronic infection state. These findings not only reveal an important feedback mechanism that couples T cell exhaustion with the maintenance of a lower level of effector T cell response but also suggest therapy options to better control virus levels during the chronic infection phase.

[Supplemental material is available for this article.]

Overwhelming infections with noncytopathic viruses can lead to chronic infections. The fate of a virus infection can be fundamentally categorized as acute or chronic according to its temporal relationship with the host organism (Virgin et al. 2009). In humans, acute infections are usually resolved within a few weeks. In contrast, chronic infections are not resolved and, instead, develop when innate and adaptive immune responses are not sufficient to eliminate the invading virus during the primary infection phase. Examples for this latter case are infections with the Human Immunodeficiency Virus (HIV) or the Hepatitis B and C viruses (HBV, HCV) that can establish persistence in their hosts with different probabilities and pathogenic consequences (Rehermann and Nascimbeni 2005; Feinberg and Ahmed 2012).

A hallmark of an overwhelming infection is the down-regulation of immune effector mechanisms to avoid immunopathology. Indeed, the simultaneous presence of a widespread virus infection and strong cytotoxic effector cell responses can induce massive cell and tissue destruction and may directly threaten the life of the infected host (Rouse and Sehrawat 2010). This threat is sensed by incompletely understood mechanisms, and several suppressive immune components are activated that adapt the host response to the viral threat. Among these are T cell exhaustion by deletion (Moskophidis et al. 1993) and functional impairment (Zajac et al. 1998; Wherry et al. 2003; Barber et al. 2006), the generation of monocyte-derived suppressor cells (MDSCs) (Cai et al. 2013; Norris et al. 2013) and regulatory cell subsets (Wilson et al. 2012). They exert their function via distinct processes including interaction with inhibitory ligands, the production of soluble immunosuppressive factors like IL10 and Indoleamine 2,3-dioxygenase, and the delivery of suppressive signals by cell–cell contacts to conventional T cells and to antigen-presenting cells, thus influencing effector functions directly or indirectly (Barber et al. 2006; Day et al. 2006; Doering et al. 2012; Ng et al. 2013).

Despite the various suppressive mechanisms induced during a chronic virus infection, the effector T cell shutdown is only partial and some T cell functionality remains that restrains the expansion of a persisting virus (Schmitz et al. 1999; He et al. 2016;

[12]These authors contributed equally to this work.
[13]Present address: Department of Immunology, Weizmann Institute of Science, Rehovot, 76100, Israel
Corresponding author: andreas.meyerhans@upf.edu
Article published online before print. Article, supplemental material, and publication date are at http://www.genome.org/cgi/doi/10.1101/gr.241372.118.

Immunity

CellPress

Article

Developmental Relationships of Four Exhausted CD8$^+$ T Cell Subsets Reveals Underlying Transcriptional and Epigenetic Landscape Control Mechanisms

Jean-Christophe Beltra,[1,2,3] Sasikanth Manne,[1,2] Mohamed S. Abdel-Hakeem,[1,2,3,4] Makoto Kurachi,[5] Josephine R. Giles,[1,2,3] Zeyu Chen,[1,2] Valentina Casella,[6] Shin Foong Ngiow,[1,2,3] Omar Khan,[1,2,7] Yinghui Jane Huang,[1,2] Patrick Yan,[1,2,7] Kito Nzingha,[1,2] Wei Xu,[8,9] Ravi K. Amaravadi,[8,9] Xiaowei Xu,[9,10] Giorgos C. Karakousis,[9,11] Tara C. Mitchell,[8,9] Lynn M. Schuchter,[8,9] Alexander C. Huang,[2,3,8,9] and E. John Wherry[1,2,3,12,*]

[1]Department of Systems Pharmacology and Translational Therapeutics, Perelman School of Medicine, University of Pennsylvania, Philadelphia, PA, USA
[2]Institute for Immunology, Perelman School of Medicine, University of Pennsylvania, Philadelphia, PA, USA
[3]Parker Institute for Cancer Immunotherapy at University of Pennsylvania, Philadelphia, PA, USA
[4]Department of Microbiology and Immunology, Faculty of Pharmacy, Cairo University, Kasr El-Aini, Cairo, Egypt
[5]Department of Molecular Genetics, Graduate School of Medical Sciences, Kanazawa University, Kanazawa, Japan
[6]Infection Biology Laboratory, Department of Experimental and Health Sciences (DCEXS), Universitat Pompeu Fabra, Barcelona, Spain
[7]Arsenal Biosciences, South San Francisco, CA, USA
[8]Department of Medicine, Perelman School of Medicine, University of Pennsylvania, Philadelphia, PA, USA
[9]Abramson Cancer Center, Perelman School of Medicine, University of Pennsylvania, Philadelphia, PA, USA
[10]Department of Pathology and Laboratory Medicine, Perelman School of Medicine, University of Pennsylvania, Philadelphia, PA, USA
[11]Department of Surgery, Perelman School of Medicine, University of Pennsylvania, Philadelphia, PA, USA
[12]Lead Contact
*Correspondence: wherry@pennmedicine.upenn.edu
https://doi.org/10.1016/j.immuni.2020.04.014

SUMMARY

CD8$^+$ T cell exhaustion is a major barrier to current anti-cancer immunotherapies. Despite this, the developmental biology of exhausted CD8$^+$ T cells (Tex) remains poorly defined, restraining improvement of strategies aimed at "re-invigorating" Tex cells. Here, we defined a four-cell-stage developmental framework for Tex cells. Two TCF1$^+$ progenitor subsets were identified, one tissue restricted and quiescent and one more blood accessible, that gradually lost TCF1 as it divided and converted to a third intermediate Tex subset. This intermediate subset re-engaged some effector biology and increased upon PD-L1 blockade but ultimately converted into a fourth, terminally exhausted subset. By using transcriptional and epigenetic analyses, we identified the control mechanisms underlying subset transitions and defined a key interplay between TCF1, T-bet, and Tox in the process. These data reveal a four-stage developmental hierarchy for Tex cells and define the molecular, transcriptional, and epigenetic mechanisms that could provide opportunities to improve cancer immunotherapy.

frontiers in Cellular and Infection Microbiology

OPINION
published: 23 October 2020
doi: 10.3389/fcimb.2020.559209

Numbers Game and Immune Geography as Determinants of Coronavirus Pathogenicity

Gennady Bocharov[1,2,3]*, *Valentina Casella*[4], *Jordi Argilaguet*[5], *Dmitry Grebennikov*[1,2,3], *Roberto Güerri-Fernandez*[6], *Burkhard Ludewig*[7] and *Andreas Meyerhans*[4,8]*

[1] Marchuk Institute of Numerical Mathematics, Russian Academy of Sciences, Moscow, Russia, [2] Moscow Center for Fundamental and Applied Mathematics at Marchuk Institute of Numerical Mathematics, Russian Academy of Sciences (INM RAS), Moscow, Russia, [3] Institute for Personalized Medicine, Sechenov First Moscow State Medical University, Moscow, Russia, [4] Infection Biology Laboratory, Department of Experimental and Health Sciences, Universitat Pompeu Fabra, Barcelona, Spain, [5] Institut de Recerca i Tecnologia Agroalimentàries (IRTA), Centre de Recerca en Sanitat Animal (CReSA, IRTA-UAB), Campus de la Universitat Autònoma de Barcelona, Bellaterra, Spain, [6] Infectious Diseases Unit, Hospital del Mar-IMIM, Universitat Autònoma de Barcelona, Barcelona, Spain, [7] Institute for Immunobiology, Kantonsspital St.Gallen, St. Gallen, Switzerland, [8] Institució Catalana de Recerca i Estudis Avançats (ICREA), Barcelona, Spain

Keywords: COVID-19, SARS - CoV-2, IFN-I, innate immunity, viral dynamics, pathogenesis

OPEN ACCESS

Edited by:
Heather Shannon Smallwood, University of Tennessee Health Sciences Center, United States

Reviewed by:
Artur Summerfield, Institute of Virology and Immunology (IVI), Switzerland

Correspondence:
Andreas Meyerhans
andreas.meyerhans@upf.edu
Gennady Bocharov
g.bocharov@inm.ras.ru

Specialty section:
This article was submitted to Virus and Host, a section of the journal Frontiers in Cellular and Infection Microbiology

Received: *25 May 2020*
Accepted: *11 September 2020*
Published: *23 October 2020*

Citation:
Bocharov G, Casella V, Argilaguet J, Grebennikov D, Güerri-Fernandez R, Ludewig B and Meyerhans A (2020) Numbers Game and Immune Geography as Determinants of Coronavirus Pathogenicity. Front. Cell. Infect. Microbiol. 10:559209. doi: 10.3389/fcimb.2020.559209

Once again, the new SARS-CoV-2 reminds us about the potential of infectious pathogens to fiercely spread worldwide and puts our well-being in danger. With respect to its pathogenicity, one may be reminded of two simple principles that underlie our constant fight with viruses of our surrounding, the "numbers game" and "immune geography" (Zinkernagel et al., 1985). These conceptual terms refer to the kinetics of virus growth and immune reactions, and the spatial organization of immune responses in relation to viral entry sites and tissue tropism which determines cytokine gradients and immune cell homing patterns across tissues, respectively. Jointly, both concepts provide a rationale for a dynamic view on the balance between virus expansion and development of antiviral immune responses that will ultimately help to understand virus pathogenicity and how to gain immune control (**Figure 1A**).

Coronaviruses are a family of enveloped plus-strand RNA viruses that infect mammals and birds. In humans, there are four endemic, usually mildly pathogenic viruses 229E, OC43, NL63 and HKU1, and the newly emerged viruses SARS-CoV, MERS-CoV, and SARS-CoV-2 that cause lethal infections in around 10, 30, and 1% of cases, respectively (Gaunt et al., 2010; Raoult et al., 2020). All these viruses can be transmitted by aerosols and infect the upper respiratory tract and the lung. However, since human infections only allow for very limited experimental manipulations, much of our fundamental knowledge of virus infections are derived from animal studies. To understand the containment of the initial virus spread, which subsequently determines virus pathogenicity, the murine coronavirus (M-CoV, also known as mouse hepatitis virus, MHV) model system is most instructive. M-CoV is a rapidly replicating, highly cytopathic virus that leads to severe inflammation in several organs and can disseminate via the bloodstream. In particular, the liver, a peripheral organ and the spleen, a secondary lymphoid organ, are the major target organs of this virus, and hematopoietic cell-derived type I interferon (IFN) primarily controls viral replication and virus-induced liver disease. Three clinical outcomes are observable that depend on the balance of infection spreading and the innate immune response (**Figure 1B**). With an optimal innate response, the infection is well controlled and generates only mild symptoms, whereas, a delayed and weak innate response results in severe infection spread and fatal outcome. Between these extremes, tissue damage of various severity is observed but the host ultimately survives.

How can this qualitative description of virus-induced pathogenicity be transformed into a more quantitative characterization of host protection and its limits? A systems biology-based analysis combining experimental data of murine coronavirus infection and mathematical modeling has

REFERENCES

A

Aiuti, F. & Mezzaroma, I., 2006. Failure to reconstitute CD4+ T-cells despite suppression of HIV replication under HAART. AIDS Rev; 8(2), pp.88-97.

Alcami, A. et al., 2000. Viral mechanisms of immune evasion. Trends in Microbiology; 8(9), pp.410-418.

Ali, S. et al., 2019. Sources of Type I Interferons in Infectious Immunity: Plasmacytoid Dendritic Cells Not Always in the Driver's Seat. Frontiers Immunology; 778(10)

B

Barber, D.L. et al., 2006. Restoring function in exhausted CD8 T cells during chronic viral infection. Nature, 439(7077), pp.682–687.

Barbet, G. et al., 2018. Sensing Microbial Viability through Bacterial RNA Augments T Follicular Helper Cell and Antibody Responses. Immunity; 48, pp.584–598

Battegay, M. et al., 1991. Quantification of lymphocytic choriomeningitis virus with an immunological focus assay in 24- or 96-well plates. Journal of virological methods, 33(1-2), pp.191–198.

Battegay, M. et al., 1994. Enhanced establishment of a virus carrier state in adult CD4+ T-cell-deficient mice. Journal of virology, 68(7), pp.4700–4704.

Beck, D.B. et al., 2020. Susceptibility to severe COVID-19. Science Perspectives; 370(6515)

Beltra, J.C. et al., 2020. Developmental Relationships of Four Exhausted CD8+ T Cell Subsets Reveals Underlying Transcriptional and Epigenetic Landscape Control Mechanisms. 52, pp.1–17. doi: 10.1016/j.immuni.2020.04.014

Bergthaler, A. et al., 2010. Viral replicative capacity is the primary determinant of lymphocytic choriomeningitis virus persistence and immunosuppression. Proceedings of the National Academy of Sciences of the United States of America, 107(50), pp.21641–21646.

Blackburn, S.D. et al., 2008. Selective expansion of a subset of exhausted CD8 T cells by αPD-L1 blockade. Proceedings of the National Academy of Sciences, 105(39), pp.15016–15021.

Bocharov, G. et al., 2015. Understanding Experimental LCMV Infection of Mice: The Role of Mathematical Models. Journal of Immunology Research; 2015(739706)

Bocharov et al., 2016. Spatiotemporal Dynamics of Virus Infection Spreading in Tissues. PLoS ONE; 11(12)

Bocharov, G. et al., 2020. Game and Immune Geography as Determinants of Coronavirus Pathogenicity. Frontiers in Cellular and Infection Microbiology; 10(559209)

Borges de Silva et al., 2015. Splenic macrophage subsets and their function during blood-borne infections, Frontiers Immunology; 6(480). doi: 10.3389/fimmu.2015.00480

Brooks, D.G. et al., 2006. Interleukin-10 determines viral clearance or persistence in vivo.Nature Medicine, 12(11) pp.1301–1309. doi: 10.1038/nm1492.

Brown, F.D. et al., 2015. Fibroblastic Reticular Cells: Organization and Regulation of the T Lymphocyte Life Cycle,Journal of Immunology; 194 (4), pp.1389-1394

C

Cao, W., 1998. Identification of -Dystroglycan as a Receptor for Lymphocytic Choriomeningitis Virus and Lassa Fever Virus. Science, 282(5396), pp.2079–2081.

Cheng, L. et al., 2017. Blocking type I interferon signaling enhances T cell recovery and reduces HIV-1 reservoirs. The Journal of clinical investigation, 127(1), pp.269–279.

Clerici, M. et al., 1994. Role of interleukin-10 in T helper cell dysfunction in asymptomatic individuals infected with the human immunodeficiency virus. The Journal of clinical investigation, 93(2), pp.768–775.

Cole, G.A., Nathanson, N. & Prendergast, R.A., 1972. Requirement for Θ-Bearing Cells in Lymphocytic Choriomeningitis Virus-induced Central Nervous System Disease. Nature, 238(5363), pp.335–337.

Cornberg, M. et al., 2013a. Clonal Exhaustion as a Mechanism to Protect Against Severe Immunopathology and Death from an Overwhelming CD8 T Cell Response. Frontiers in immunology, 4. doi: 10.3389/fimmu.2013.00475.

Crawford, A. & Wherry, E.J., 2009. The diversity of costimulatory and inhibitory receptor pathways and the regulation of antiviral T cell responses. Current opinion in immunology, 21(2), pp.179–186.

Crawford, A. et al., 2014. Molecular and transcriptional basis of CD4+ T cell dysfunction during chronic infection. Immunity, 40(2), pp.289–302.

Crouse, J. et al., 2014. Type I Interferons Protect T Cells against NK Cell Attack Mediated by the Activating Receptor NCR1. Immunity, 40(6), pp.961-973.

Crouse, J. et al., 2015. Regulation of antiviral T cell responses by type I interferons. Nature reviews Immunology. 15 pp. 231-242. doi: 10.1038/nri3806

D

Davies, L.C. et al., 2013. Tissue resident macrophages. Nat Immunol,14(10) pp.986–95.

Day, C.L. et al., 2006. PD-1 expression on HIV-specific T cells is associated with T-cell exhaustion and disease progression. Nature, 443(7109), pp.350–354.

De Giovanni, M. et al., 2020. Spatiotemporal regulation of type I interferon expression determines the antiviral polarization of CD4+ T cells. Nature Immunology, 21 pp.321-330. doi: 10.1038/s41590-020-0596-6

De la Torre, J.C., 2009. Molecular and cell biology of the prototypic arenavirus LCMV: implications for understanding and combating hemorrhagic fever arenaviruses. Annals of the New York Academy of Sciences, 1171 Suppl 1, pp. E57–64.

Duhan, V. et al., 2016. Virus-specific antibodies allow viral replication in the marginal zone, thereby promoting CD8+ T-cell priming and viral control. Nature Scientific Reports, 6(19191). doi 10.1038/srep19191

F

Farmer, T.W. & Janeway, C.A., 1942. INFECTIONS WITH THE VIRUS OF LYMPHOCYTIC CHORIOMENINGITIS. Medicine, 21(1), pp.65–94.

Feinberg, M.B. & Ahmed, R., 2012. Born this way? Understanding the immunological basis of effective HIV control. Nature immunology, 13(7), pp.632–634.

Fröhlich, A. et al., 2009. IL-21R on T cells is critical for sustained functionality and control of chronic viral infection. Science, 324(5934), pp.1576–1580.

Fukuyama, S. & Kawaoka, Y., 2011. The pathogenesis of influenza virus infections: the contributions of virus and host factors. Current opinion in immunology, 23(4), pp.481–486.

G

Gallaher, W.R., DiSimone, C. & Buchmeier, M.J., 2001. The viral transmembrane superfamily: possible divergence of Arenavirus and Filovirus glycoproteins from a common RNA virus ancestor. BMC microbiology, 1, p.1.

Gangaplara, A. et al., 2018. Type I interferon signaling attenuates regulatory T cell function in viral infection and in the tumor microenvironment. PLOS Pathogens. doi: 10.1371/journal.ppat.1006985

Garcia-Revilla, J. et al., 2020. Hyperinflammation and Fibrosis in Severe COVID-19 Patients: Galectin-3, a Target Molecule to Consider. Frontiers Immunology. doi: 10.3389/fimmu.2020.02069

Glass, W. G. et al., 2006. CCR5 deficiency increases risk of symptomatic West Nile virus infection. Journal of Experimental Medicine, 203(1), pp.35-40. doi: 10.1084/jem.20051970

Gonzalez-Navajas, J.M. et al., 2012. Immunomodulatory functions of type I

Interferon.Nature Rev, 12 pp.125-135. doi:10.1038/nri3133

Grabowska, J. et al., 2018. CD169+ Macrophages Capture and Dendritic Cells Instruct: The Interplay of the Gatekeeper and the General of the Immune System. Frontiers in Immunology, 9(2472). doi: 10.3389/fimmu.2018.02472

Greczmiel, U. et al., 2017. Sustained T follicular helper cell response is essential for control of chronic viral infection. Science Immunology, 2, eaam8686

H

Hadjadj, J. et al., 2020. Impaired type I interferon activity and inflammatory responses in severe COVID-19 patients. Science, 369(6504) pp. 718-724. doi: 10.1126/science.abc6027.

Hervas-Stubbs, S. et al., 2014. Conventional but Not Plasmacytoid Dendritic Cells Foster the Systemic Virus −Induced Type I IFN Response Needed for Efficient CD8 T Cell Priming.The Journal of Immunology, 193 pp.1151-1161.

Hervas-Stubbs, S. et al., 2011. Direct Effects of Type I Interferons on Cells of the Immune System. Clinical Cancer Research, 17(9), pp.2619–27. doi:10.1158/1078-0432.CCR-10-1114

Honke, N. et al., 2011. Enforced viral replication activates adaptive immunity and is essential for the control of a cytopathic virus. Nature Immunology, 13(1) pp.51-58. doi:10.1038/ni.2169.

Huang, E. et al., 2020. The Roles of Immune Cells in the Pathogenesis of Fibrosis. International Journal of Molecular Sciences, 21(5203). doi:10.3390/ijms21155203.

Huang, D.W., Sherman, B.T. & Lempicki, R.A., 2009. Systematic and integrative analysis of large gene lists using DAVID bioinformatics resources. Nature protocols, 4(1), pp.44–57.

I

Isaacs, A. & Lindenmann, J., 1957. Virus interference. I. The interferon. Proceedings of the Royal Society B, 147(927). doi: 10.1098/rspb.1957.0048.

Isaacs, A. et al., 1957. Virus interference. II. Some properties of interferon. Proceedings of the Royal Society B, 147(927), pp.268-73. doi: 10.1098/rspb.1957.0049.

Ivashkiv, L.B. et al., 2014. Regulation of type I interferon responses. Nature Reviews, 14. doi:10.1038/nri3581.

K

Kägi, D. et al., 1994. Cytotoxicity mediated by T cells and natural killer cells is greatly impaired in perforin-deficient mice. Nature, 369(6475) pp.31-7. doi: 10.1038/369031a0.

Karrer, U. et al, 1997. On the Key Role of Secondary Lymphoid Organs in Antiviral Immune Responses Studied in Alymphoplastic (aly/aly) and Spleenless (Hox11− /−) Mutant Mice. J Exp Med. 185(12), pp.2157–2170. doi: 10.1084/jem.185.12.2157

Kim, J.V. et al., 2009. Myelomonocytic cell recruitment causes fatal CNS vascular injury during acute viral meningitis. Nature, 457(7226), pp.191–195.

Klenerman, P. & Hill, A., 2005. T cells and viral persistence: lessons from diverse infections. Nature immunology, 6(9), pp.873–879.

Kunz, S. et al., 2003. Mechanisms for lymphocytic choriomeningitis virus glycoprotein cleavage, transport, and incorporation into virions. Virology, 314(1), pp.168–178.

Kunz, S., Borrow, P. & Oldstone, M.B.A., 2002. Receptor structure, binding, and cell entry of arenaviruses. Current topics in microbiology and immunology, 262, pp.111–137.

Kityo, C. et al., 2018. Lymphoid tissue fibrosis is associated with impaired vaccine responses. Journal of Clinical Investigation, 128(7) pp.2763-2773. doi: 10.1172/JCI97377

L

Landay, A.L. et al., 1996. In vitro restoration of T cell immune function in human immunodeficiency virus-positive persons: effects of interleukin (IL)-12 and anti-IL-10. The Journal of infectious diseases, 173(5), pp.1085–1091.

Langfelder, P. & Horvath, S., 2008. WGCNA: an R package for weighted correlation network analysis. BMC bioinformatics, 9, p.559.

Li, Q. et al., 2009. Visualizing antigen-specific and infected cells in situ predicts outcomes in early viral infection. Science, 323(5922), pp.1726–1729.

Louten, J. et al., 2006. Journal of Imm.Type 1 IFN Deficiency in the Absence of Normal Splenic Architecture during Lymphocytic Choriomeningitis Virus Infection. 177, pp.3266-3272. doi: 10.4049/jimmunol.177.5.3266.

M

Masson, D. & Tschopp, J., 1985. Isolation of a lytic, pore-forming protein (perforin) from

cytolytic T-lymphocytes. The Journal of biological chemistry, 260(16), pp.9069–9072.

Martínez-Sobrido, L. et al., 2007. Differential Inhibition of Type I Interferon Induction by Arenavirus Nucleoproteins. Journal of Virology, 81(22) pp.12696–12703. doi: 10.1128/JVI.00882-07

Matloubian, M., Concepcion, R.J. & Ahmed, R., 1994. CD4+ T cells are required to sustain CD8+ cytotoxic T-cell responses during chronic viral infection. Journal of virology, 68(12), pp.8056–8063.

McNab, F. et al., 2015. Type I Interferons in infectipus diseases. Nature Rev Immunol,15. doi:10.1038/nri3787.

Moskophidis, D. et al., 1993. Virus persistence in acutely infected immunocompetent mice by exhaustion of antiviral cytotoxic effector T cells. Nature, 362(6422), pp.758–761.

Muller, S. et al., 2002. Role of an Intact Splenic Microarchitecture in Early Lymphocytic Choriomeningitis Virus Production. J Virolology, 76(5), pp. 2375–2383.

Murali-Krishna, K. et al., 1998. Counting antigen-specific CD8 T cells: a reevaluation of bystander activation during viral infection. Immunity, 8(2), pp.177–187.

Murira, A. & Lamarre, A., 2016. Type-I interferon Responses: From Friend to Foe in the Battle against Chronic viral infection. Front Immunol, 7(609). doi: 10.3389/fimmu.2016.00609.

N

Ng, C.T. et al., 2013. Networking at the level of host immunity: immune cell interactions during persistent viral infections. Cell Host & Microbe, 13(6), pp.652–664.

Nguyen, L.T. & Ohashi, P.S., 2014. Clinical blockade of PD1 and LAG3 — potential mechanisms of action. Nature Reviews. Immunology, 15(1), pp.45–56.

Norris, B.A. et al., 2013. Chronic but Not Acute Virus Infection Induces Sustained Expansion of Myeloid Suppressor Cell Numbers that Inhibit Viral-Specific T Cell Immunity. Immunity 38, pp.309–321. doi: 10.1016/j.immuni.2012.10.022

O

Okoye, I.S. et al., 2017. Coinhibitory Receptor Expression and Immune Checkpoint Blockade: Maintaining a Balance in CD8+ T Cell Responses to Chronic Viral Infections and Cancer. Frontiers in immunology, 8, p.1215.

Oldstone, M.B.A., 2013. Lessons learned and concepts formed from study of the pathogenesis of the two negative-strand viruses lymphocytic choriomeningitis and influenza. Proceedings of the National Academy of Sciences of the United States of America, 110(11), pp.4180–4183.

Oldstone, M.B.A. & Campbell, K.P., 2011. Decoding arenavirus pathogenesis: essential roles for alpha-dystroglycan-virus interactions and the immune response. Virology, 411(2), pp.170–179.

P

Peiffer-Smadja, N. & Yazdanpanah, Y., 2021. Nebulised interferon beta-1a for patients with COVID-19. The Lancet, 9(2), pp.122-123. doi:10.1016/S2213-2600(20)30523-3

Perez, M. & de la Torre, J.C., 2003. Characterization of the Genomic Promoter of the Prototypic Arenavirus Lymphocytic Choriomeningitis Virus. Journal of Virology. 10.1128/JVI.77.2.1184-1194.2003

Petrovas, C. et al., 2006. PD-1 is a regulator of virus-specific CD8 T cell survival in HIV infection. The Journal of experimental medicine, 203(10), pp.2281–2292.

Pipkin, M.E. et al., 2010. Interleukin-2 and inflammation induce distinct transcriptional programs that promote the differentiation of effector cytolytic T cells. Immunity, 32(1), pp.79–90.

Pitha, P.M. ,2007. Interferon: the 50th Anniversary. Current Topics in Microbiology and Immunology,316. Springer, ISBN 978-3-540-71329-6

Pirgova, G. et al., 2020. Marginal zone SIGN-R1+ macrophages are essential for the maturation of germinal center B cells in the spleen. PNAS, 117 (22) pp.12295-12305. doi: 10.1073/pnas.1921673117

R

Rehermann, B. & Nascimbeni, M., 2005. Immunology of hepatitis B virus and hepatitis C virus infection. Nature Reviews. Immunology, 5(3), pp.215–229.

Riviere, Y. et al., 1977. Inhibition by anti-interferon serum of lymphocytic choriomeningitis virus disease in suckling mice. Proceedings of the National Academy of Sciences, 74(5), pp.2135–2139.

Robinson, M.D. & Oshlack, A., 2010. A scaling normalization method for differential expression analysis of RNA-seq data. Genome biology, 11(3), p. R25.

Rosenbloom, J. at al., 2013. Strategies for anti-fibrotic therapies. Biochimica et Biophysica Acta, 1832 pp.1088–1103. doi: 10.1016/j.bbadis.2012.12.007

Rouse, B.T. & Sehrawat, S., 2010. Immunity and immunopathology to viruses: what decides the outcome? Nature Reviews. Immunology, 10(7), pp.514–526.

S

Sa Ribero, M. et al., 2020. Interplay between SARS-CoV-2 and the type I interferon response. PLOS Pathogens, doi: 10.1371/journal.ppat.1008737

Sandler, N.G. et al., 2014. Type I interferon responses in rhesus macaques prevent SIV infection and slow disease progression. Nature Letter. doi:10.1038/nature13554

Saprunenko, T. et al., 2019. Complexities of Type I Interferon Biology: Lessons from LCMV. Viruses, 11(72). doi:10.3390/v11020172

Scandella, E. et al., 2008. Restoration of lymphoid organ integrity through the interaction of lymphoid tissue–inducer cells with stroma of the T cell zone. Nature Immunology, 9(6). doi:10.1038/ni.1605

Seiler, P. et al., 1997. Crucial role of marginal zone macrophages and marginal zone metallophils in the clearance of lymphocytic choriomeningitis virus infection. Eur J Immunol,27: 2626-2633.

Shaabani, L. et al., 2016. CD169+ macrophages regulate PD-L1 expression via type I interferon and thereby prevent severe immunopathology after LCMV infection. Cell death & disease, 7, e2446; doi:10.1038/cddis.2016.350

Schacker, T.W. et al., 2006. Lymphatic tissue fibrosis is associated with reduced numbers of naive CD4+ T cells in human immunodeficiency virus type 1 infection. Clinical and vaccine immunology: CVI, 13(5), pp.556–560.

Snell, L.M. et al., 2015. New insights into type I interferon and the immunopathogenesis of persistent viral infections. Curr Opinion Imm, 34 pp.91–98.

Snell, L.M. et.al, 2017.Type I Interferon in Chronic Virus Infection and Cancer. Trends in Immunology. 1391.doi: 10.1016/j.it.2017.05.005.

Spiropoulou, C.F. et al., 2002. New World arenavirus clade C, but not clade A and B viruses, utilizes alpha-dystroglycan as its major receptor. Journal of virology, 76(10), pp.5140–5146.

Stegelmeier, A.A. et al., 2019. Myeloid Cells during Viral Infections and Inflammation. Viruses, 1(2) 168. doi:10.3390/v11020168

Sumbria, D., 2019. Factors Affecting the Tissue Damaging Consequences of Viral Infections. Frontiers in Microbiology, 10(2314). doi: 10.3389/fmicb.2019.02314

Suthahar, N. et al., 2017. From Inflammation to Fibrosis—Molecular and Cellular Mechanisms of Myocardial Tissue Remodelling and Perspectives on Differential Treatment Opportunities. Curr Heart Failure Reports, 14 pp.235–250. doi: 10.1007/s11897-017-0343-y

Swiecki M. & Colonna, M., 2011. Type I interferons: diversity of sources, production pathways and effects on immune responses. Current Opinions in Virology. 1, pp.463-475. doi: 10.1016/j.coviro.2011.10.026

T

Teijaro, J.R. et al., 2013. Persistent LCMV infection is controlled by blockade of type I interferon signaling. Science, 340(6129), pp.207–211.

Teijaro, J.R. et al., 2016. Pleiotropic Roles of Type 1 Interferons in Antiviral Immune Responses. Advances in Immunology, 132. doi: 10.1016/bs.ai.2016.08.001

Traub, E., 1936a. AN EPIDEMIC IN A MOUSE COLONY DUE TO THE VIRUS OF ACUTE LYMPHOCYTIC CHORIOMENINGITIS. The Journal of experimental medicine, 63(4), pp.533–546.

Traub, E., 1936b. PERSISTENCE OF LYMPHOCYTIC CHORIOMENINGITIS VIRUS IN IMMUNE ANIMALS AND ITS RELATION TO IMMUNITY. The Journal of experimental medicine, 63(6), pp.847–861.

Trinchieri, G., 2012. Lymphocyte Choriomeningitis Virus Plays Hide-and-Seek with Type 1 Interferon. Cell Host & Microbe,11. doi: 10.1016/j.chom.2012.05.007

V

Virgin, H.W., Wherry, E.J. & Ahmed, R., 2009. Redefining chronic viral infection. Cell, 138(1), pp.30–50.

W

Waggoner, S.N. et al., 2011. Natural killer cells act as rheostats modulating antiviral T cells. Nature, 481(7381), pp.394–398.

Wang, Y. et al., 2012. Timing and Magnitude of Type I Interferon Responses by Distinct Sensors Impact CD8 T Cell Exhaustion and Chronic Viral Infection. Cell Host & Microbe, 11, 631–642 doi: 10.1016/j.chom.2012.05.003

Welsh, R.M. and Seedhom, M.O. 2008. Lymphocytic choriomeningitis virus (LCMV): propagation, quantitation, and storage. Current Protocols in Microbiology. doi: 10.1002/9780471729259.mc15a01s8.

Wherry, E.J. et al., 2007. Molecular signature of CD8+ T cell exhaustion during chronic viral infection. Immunity, 27(4), pp.670–684.

Wilson, E.B. et al., 2013. Blockade of chronic type I interferon signaling to control persistent LCMV infection. Science, 340(6129), pp.202–207.

Wilson, E.B. & Brooks, D.G., 2010. Translating insights from persistent LCMV infection into anti-HIV immunity. Immunologic research, 48(1-3), pp.3–13.

Wynn, T.A. & Vannella, K.M., 2016. Macrophages in Tissue Repair, Regeneration, and

Fibrosis. Immunity, 44(3), pp.450–462.

Wynn, T.A., 2004. FIBROTIC DISEASE AND THE TH1/TH2 PARADIGM. Nature Review Immunology, 4(8), pp.583–594. doi: 10.1038/nri1412

Wynn, T.A. et al., 2013. Myeloid-cell differentiation redefined in cancer. Nature Immunology, 14(3), pp.197–199. doi: 10.1038/ni.2539

Y

Yi, J.S., Du, M. & Zajac, A.J., 2009. A vital role for interleukin-21 in the control of a chronic viral infection. Science, 324(5934), pp.1572–1576.

Yue, F.Y. et al., 2010. HIV-specific IL-21 producing CD4+ T cells are induced in acute and chronic progressive HIV infection and are associated with relative viral control. Journal of immunology, 185(1), pp.498–506.

Z

Zhang, B. & Horvath, S., 2005. A general framework for weighted gene co-expression network analysis. Statistical applications in genetics and molecular biology, 4, p.Article17.

Zhen, A. et al., 2017. Targeting type I interferon-mediated activation restores immune function in chronic HIV infection. The Journal of clinical investigation, 127(1), pp.260–268.

Zhou, X., Lindsay, H. & Robinson, M.D., 2014. Robustly detecting differential expression in RNA sequencing data using observation weights. Nucleic acids research, 42(11), p.e91.

Zinkernagel, R.M., 2002. Lymphocytic choriomeningitis virus and immunology. Current topics in microbiology and immunology, 263, pp.1–5.

Zinkernagel, R.M., & Doherty, P.C., 1975. Enhanced immunological surveillance in mice heterozygous at the H-2 gene complex. Nature, 256, pp.50-52. doi: 10.1038/256050a0.

Zhang, M. & Zhang, S., 2020. T Cells in Fibrosis and Fibrotic Diseases. Frontiers Immunology. doi: 10.3389/fimmu.2020.01142

Zhang et al., 2019. Demystifying the manipulation of host immunity, metabolism, and extraintestinal tumors by the gut microbiome. Signal Transduction and Targeted Therapy, 4(41). doi:10.1038/s41392-019-0074-5

Nothing in life is to be feared, it is only to be understood.
Now is the time to understand more, so that we may fear less.

– Marie Curie